

Weierstraß–Institut für Angewandte Analysis und Stochastik

im Forschungsverbund Berlin e.V.

Report

ISSN 0946 – 8838

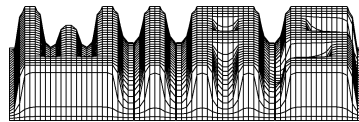
Longitudinal Dynamics of Semiconductor Lasers

Jan Sieber¹

submitted: 11th October 2001

¹ Weierstraß Institute
for Applied Analysis
and Stochastics
Mohrenstr. 39
D-10117 Berlin
E-Mail: sieber@wias-berlin.de

Report No. 20
Berlin 2001



2000 *Mathematics Subject Classification.* 78A60, 35B25, 37D10, 34C60.

Key words and phrases. semiconductor lasers, infinite-dimensional dynamical systems, invariant manifolds, bifurcation analysis.

PhD thesis submitted to the Mathematisch-naturwissenschaftliche Fakultät II of the Humboldt University of Berlin, accepted 23rd July 2001.

Edited by
Weierstraß-Institut für Angewandte Analysis und Stochastik (WIAS)
Mohrenstraße 39
D — 10117 Berlin
Germany

Fax: + 49 30 2044975
E-Mail (X.400): c=de;a=d400-gw;p=WIAS-BERLIN;s=preprint
E-Mail (Internet): preprint@wias-berlin.de
World Wide Web: <http://www.wias-berlin.de/>

Abstract

We investigate the longitudinal dynamics of semiconductor lasers using a model which couples a hyperbolic linear system of partial differential equations nonlinearly with ordinary differential equations. We prove the global existence and uniqueness of solutions using the theory of strongly continuous semigroups. Subsequently, we analyse the long-time behavior of the solutions in two steps. First, we find attracting invariant manifolds of low dimension benefitting from the fact that the system is singularly perturbed, i. e., the optical and the electronic variables operate on different time-scales. The flow on these manifolds can be approximated by the so-called mode approximations. The dimension of these mode approximations depends on the number of critical eigenvalues of the linear hyperbolic operator. Next, we perform a detailed numerical and analytic bifurcation analysis for the two most common constellations. Starting from known results for the single-mode approximation, we investigate the two-mode approximation in the special case of a rapidly rotating phase difference between the two optical components. In this case, the first-order averaged model unveils the mechanisms for various phenomena observed in simulations of the complete system. Moreover, it predicts the existence of a more complex spatio-temporal behavior. In the scope of the averaged model, this is a bursting regime.

Acknowledgment

I wish to thank my colleagues at the WEIERSTRASS-INSTITUT FÜR ANGEWANDTE ANALYSIS UND STOCHASTIK and in particular the members of the group of Klaus Schneider for continuous support, fruitful discussions, and the opportunity to experience the highly interdisciplinary spirit of our project on laser dynamics.

Jan Sieber.

Contents

1	Introduction	2
2	Traveling Wave Model with Nonlinear Gain Dispersion — Existence Theory	5
2.1	The Initial-Boundary Value Problem	5
2.2	Existence and Uniqueness of Classical and Mild Solutions	7
3	Model reduction — Mode Approximations	13
3.1	Introduction of the Singular Perturbation Parameter	13
3.2	Spectral Properties of $H(n)$	14
3.3	Existence and Properties of the Finite-dimensional Center-unstable Manifold	22
4	Bifurcation Analysis of the Mode Approximations	29
4.1	The Single Mode Case	29
4.2	Two modes with different frequencies	39
A	Physical Interpretation of the Traveling-Wave Equations — Discussion of Typical Parameter Ranges	60
A.1	Physical Interpretation of the Model	60
A.2	Scaling of the Variables	60
B	Normally Hyperbolic Invariant Manifolds	62
	Bibliography	65
	List of Figures	68
	List of Tables	68

1 Introduction

The dynamics of semiconductor lasers can be described by the interaction of two physical variables: the complex electromagnetic field E , roughly speaking the light amplitude, and the inversion (carrier density) n within the active zone of the device. These variables are governed by a system of equations which fits for most models of moderate complexity into the form

$$\begin{aligned}\dot{E} &= H(n)E \\ \dot{n} &= \varepsilon f(n) - g(n)[E, E]\end{aligned}\tag{1.1}$$

if we neglect noise, and if the magnitude of E is moderate. System (1.1) is nonlinear due to the n -dependence of the linear operator H . A characteristic feature of semiconductor lasers is the large ratio between the average lifetime of carriers and the average lifetime of photons expressed in the small parameter ε in (1.1). Another remarkable property of (1.1) is its symmetry with respect to rotation $E \rightarrow Ee^{i\varphi}$ for $\varphi \in [0, 2\pi)$ since g is a hermitian form. This implies the existence of rotating-wave solutions ($E = E_0e^{i\omega t}$, $n = \text{const}$) which are referred to as *stationary lasing states* or *on-states*. The properties of these stationary states are obviously important from the point of view of applications: their stability, domain of attraction, bifurcation scenarios, whether they are excitable, etc. Another object of interest are modulated waves, i. e., quasi-periodic solutions, branching from the stationary states. Lasers exhibiting *self-pulsations* are potentially useful for, e. g., clock-recovery in optical communication networks [9].

The particular form of the coefficients H , f , and g depends on the complexity level of the model. In the introduction, we start with a short survey about some laser models and integrate the model considered in our paper into this hierarchy. Then, we give an overview about the contents of this paper.

Laser Modeling

In the simplest case, one may consider the laser as a solitary point-like light source with a given (n -dependent) frequency. This reduces E to a complex number and H to a complex function of one real variable n . The resulting system of ordinary differential equations is typically referred to as *amplitude equations* and exhibits weakly damped oscillations. Hence, it is highly susceptible to external injection, feedback or other perturbations. E. g., the addition of a saturable absorber (a second component for n) leads to self-sustained oscillations and excitable behavior [17]. System (1.1) subject to optical injection is studied in [48] and exhibits very complex dynamical behavior including chaos.

A popular subject of research are laser diodes subject to *delayed optical feedback*. The most popular models, e. g., the Lang-Kobayashi equations [26], still consider the laser as a point-like light source but $H(n)$ is now a delay operator, and E is a continuous space dependent function. Then, system (1.1) is a delay-differential equation and has an infinite-dimensional phase space. The long-time behavior of

this kind of systems can become arbitrarily complex [30]. However, the bifurcations of the stationary states and the appearance and properties of modulated waves have been investigated extensively numerically [40], and analytically in, e. g., [18], [43]. The model considered in our paper resolves the laser spatially in longitudinal direction. In this case, the amplitude E is in \mathbb{L}^2 , and the linear operator H is a hyperbolic differential operator describing the wave propagation, its amplification and the internal refraction. We investigate an extension of the model proposed in [6] by taking the nonlinear material gain dispersion into account [50]. On the other hand, we treat the carrier density n as a piecewise spatially homogeneous quantity such that $n \in \mathbb{R}^m$, and $g(n)$ is a hermitian form. This treatment is particularly well adapted to *multi-section lasers* which are composed of several sections with different parameters. Then, system (1.1) is a linear system of partial differential equations for E which is nonlinearly coupled to a system of ordinary differential equations for n . This system is not essentially more complicated than the delay-differential equations considered by the external feedback models from the functional analytic point of view. Indeed, multi-section lasers are often constructed in a way such that one section acts as a laser and the other sections give a finely tuned delayed feedback. However, the longitudinally resolved model allows us to study how the geometry of the device influences the dominant eigenvalues and corresponding eigenspaces (*modes*) of H and how these modes interact or compete.

Non-technical Overview

In chapter 2, we introduce the solution concepts for the hyperbolic system (1.1) and prove the global existence and uniqueness of solutions. Uniqueness and existence results for short time intervals are covered by the theory of C_0 semigroups. An a-priori estimate ensures the global existence of solutions. We permit discontinuous inhomogeneous boundary conditions (optical inputs which are \mathbb{L}^∞ in time) only in this chapter.

In chapter 3, we reduce the infinite-dimensional system (1.1) to a low-dimensional system of ordinary differential equations. To this end, we treat (1.1) as a singularly perturbed system by exploiting the smallness of ε . The spectral properties of H allow for the application of theorems on the existence of invariant manifolds in the spirit of [19]. Truncation of the higher order terms in the expansion of the center manifold leads to the *mode approximations*. The dimension of these mode approximations may depend on the number of critical modes of H (i. e., the number of components of E we have to take into account). Each particular reduced model is valid only within a finite region of the phase space and the parameter space.

In chapter 4, we investigate the previously obtained mode approximations in the two simplest and most generic situations. Firstly, we revisit the two-dimensional single mode model introduced and studied numerically in [44]. It resembles the amplitude equations but the coefficient functions may be modified due to the geometry of the dominating mode. We consider the single mode system as a $O(\sqrt{\varepsilon})$ -perturbation of a conservative oscillator, and obtain conditions implying that the stable periodic solutions (*self-pulsations*) found in [44] are uniformly bounded for small ε . Moreover,

we provide an analytic formula for the location of the self-pulsation which is a good approximation for small ε .

Secondly, we analyse the situation where two modes of H are critical but have very different frequencies. In this case, the phase difference between the two components of E rotates very fast. Hence, we can average the system with respect to this rotation simplifying the system to a three-dimensional system. This system contains two invariant planes governed by the single-mode dynamics. Moreover it is singularly perturbed since the drift between these invariant planes is slow. We use this time-scale difference and the knowledge about the single-mode equations to reduce the model further and give a concise overview over the mechanisms behind various phenomena observed in numerical simulations of system (1.1). In particular, we locate the stability boundaries of the single-mode self-pulsations, and detect a regime of more complex spatio-temporal behavior. In the scope of the averaged model, this is a bursting regime. This kind of solutions is observed frequently in the dynamics of neurons (see [24] for a classification of these phenomena).

2 Traveling Wave Model with Nonlinear Gain Dispersion — Existence Theory

A well known model describing the longitudinal effects in narrow laser diodes is the *traveling wave model*, a hyperbolic system of partial differential equations and of ordinary differential equations [6], [29], [42]. This model has been extended by adding polarization equations to include the nonlinear gain dispersion effects [2], [6], [39], [50]. In this chapter, we introduce the corresponding system of differential equations and prove global existence and uniqueness of mild and classical solutions for the initial-boundary value problem. This extends the results for the traveling wave equations of [20], [25]. In this chapter, we treat also inhomogeneous boundary conditions whereas the other chapters will restrict to the autonomous system.

2.1 The Initial-Boundary Value Problem

Let $\psi(t, z) \in \mathbb{C}^2$ describe the complex amplitude of the optical field split into a forward and a backward traveling wave. Let $p(t, z) \in \mathbb{C}^2$ be the corresponding nonlinear polarization (see appendix A). Both quantities depend on time and the one-dimensional spatial variable $z \in [0, L]$ (the longitudinal direction within the laser). The vector $n(t) \in \mathbb{R}^m$ represents the spatially averaged carrier densities within the active sections of the laser (see Fig. 2.1). The initial-boundary value

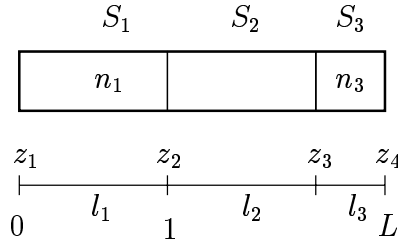


Figure 2.1: Typical geometric configuration of the domain in a laser with 3 sections. Two of them are active ($\mathcal{A} = \{1, 3\}$)

problem reads as follows:

$$\partial_t \psi(t, z) = \sigma \partial_z \psi(t, z) + \beta(n(t), z) \psi(t, z) - i\kappa(z) \sigma_c \psi(t, z) + \rho(n(t), z) p(t, z) \quad (2.1)$$

$$\partial_t p(t, z) = (i\Omega_r(n(t), z) - \Gamma(z)) \cdot p(t, z) + \Gamma(z) \psi(t, z) \quad (2.2)$$

$$\begin{aligned} \frac{d}{dt} n_k(t) &= I_k - \frac{n_k(t)}{\tau_k} - \frac{P}{l_k} (G_k(n_k(t)) - \rho_k(n_k(t))) \int_{S_k} \psi(t, z)^* \psi(t, z) dz \\ &\quad - \frac{P}{l_k} \rho_k(n_k(t)) \operatorname{Re} \left(\int_{S_k} \psi(t, z)^* p(t, z) dz \right) \text{ for } k \in \mathcal{S}_a \end{aligned} \quad (2.3)$$

accompanied by the inhomogeneous boundary conditions

$$\psi_1(t, 0) = r_0 \psi_2(t, 0) + \alpha(t), \quad \psi_2(t, L) = r_L \psi_1(t, L) \quad (2.4)$$

and the initial conditions

$$\psi(0, z) = \psi^0(z), p(0, z) = p^0(z), n(0) = n^0. \quad (2.5)$$

The Hermitian transpose of a \mathbb{C}^2 -vector ψ is denoted by ψ^* in (2.3). We will define the appropriate function spaces and discuss the possible solution concepts in section 2.2. The quantities and coefficients appearing above have the following sense (see also table A.1):

- L is the length of the laser. The laser is subdivided into m sections S_k having length l_k and starting points z_k for $k = 1 \dots m$. We scale the system such that $l_1 = 1$ and define $z_{m+1} = L$. Thus, $S_k = [z_k, z_{k+1}]$. All coefficients are supposed to be spatially constant in each section, i. e. if $z \in S_k$, $\kappa(z) = \kappa_k$, $\Gamma(z) = \Gamma_k$, $\beta(n, z) = \beta_k(n_k)$, $\rho(n, z) = \rho_k(n_k)$. Moreover, we define a subset of *active* sections $\mathcal{A} \subseteq \{1, \dots, m\}$ and consider (2.3) and the dynamic variable n_k only for active sections ($k \in \mathcal{A}$). Let $m_a := \#\mathcal{A}$ be the number of active sections.

- $\sigma = \begin{pmatrix} -1 & 0 \\ 0 & 1 \end{pmatrix}$, $\sigma_c = \begin{pmatrix} 0 & 1 \\ 1 & 0 \end{pmatrix}$

- $\beta(n, z) = \beta_k(n_k) \in \mathbb{C}$ for $z \in S_k$. The model we use throughout the work reads

$$\beta_k(\nu) = d_k + (1 + i\alpha_{H,k})G_k(\nu) - \rho_k(\nu) \quad (2.6)$$

where $d_k \in \mathbb{C}$, $\alpha_{H,k} \in \mathbb{R}$. For $k \in \mathcal{A}$, $G_k : (\underline{n}, \infty) \rightarrow \mathbb{R}$ is a smooth strictly monotone increasing function satisfying $G_k(1) = 0$, $G'_k(1) > 0$. Its limits are $\lim_{\nu \searrow \underline{n}} G_k(\nu) = -\infty$, $\lim_{\nu \rightarrow \infty} G_k(\nu) = \infty$ where $\underline{n} \leq 0$. Typical models for G_k in active sections are

$$G_k(\nu) = g_k \log \nu, \quad (\underline{n} = 0) \text{ or} \quad (2.7)$$

$$G_k(\nu) = g_k \cdot (\nu - 1), \quad (\underline{n} = -\infty). \quad (2.8)$$

G_k is identically zero for $k \notin \mathcal{A}$. These sections are called *passive*.

- $\rho(n, z) = \rho_k(n_k)$, $\Omega_r(n, z) = \Omega_{r,k}(n_k)$ for $z \in S_k$, $k \in \{1 \dots m\}$. For $k \notin \mathcal{A}$, we suppose $\rho_k = 0$. Moreover, we suppose $\rho_k, \Omega_{r,k} : (\underline{n}, \infty) \rightarrow \mathbb{R}$ to be smooth and Lipschitz continuous. Let $|\rho_k(\nu)|$ be bounded for $\nu < 1$, and $\rho_k(1) = 0$.

The variables and coefficients, their physical meanings, and their typical ranges are shown in Table A.1. The traveling wave model described in [6], [9], [8], [20], [37], [51] can be obtained formally by ‘‘adiabatic elimination’’ of $p(t, z)$, i. e. by replacing $\partial_t p(t, z)$ by 0 in (2.2).

For convenience, we introduce the hermitian form

$$g_k(\nu) \left[\begin{pmatrix} \psi \\ p \end{pmatrix}, \begin{pmatrix} \varphi \\ q \end{pmatrix} \right] = \frac{1}{l_k} \int_{S_k} (\psi^*(z), p^*(z)) \begin{pmatrix} G_k(\nu) - \rho_k(\nu) & \frac{1}{2}\rho_k(\nu) \\ \frac{1}{2}\rho_k(\nu) & 0 \end{pmatrix} \begin{pmatrix} \varphi(z) \\ q(z) \end{pmatrix} dz \quad (2.9)$$

and the notations

$$\begin{aligned}
\|\psi\|_k^2 &= \int_{S_k} \psi^*(z)\psi(z)dz \\
(\psi, \varphi)_k &= \int_{S_k} \psi^*(z)\varphi(z)dz \\
f_k(\nu, (\psi, p)) &= I_k - \frac{\nu}{\tau_k} - P g_k(\nu) \left[\begin{pmatrix} \psi \\ p \end{pmatrix}, \begin{pmatrix} \psi \\ p \end{pmatrix} \right]
\end{aligned} \tag{2.10}$$

for $\nu \in [\underline{n}, \infty)$ and $\psi, p \in \mathbb{L}^2([0, L]; \mathbb{C}^2)$. Using these notations, (2.3) reads

$$\frac{d}{dt}n_k = f_k(n_k, (\psi, p)) \text{ for } k \in \mathcal{A}. \tag{2.11}$$

2.2 Existence and Uniqueness of Classical and Mild Solutions

In this section, we treat the inhomogeneous initial-boundary value problem (2.1)-(2.4) as an autonomous nonlinear evolution system

$$\frac{d}{dt}u(t) = Au(t) + g(u(t)), \quad u(0) = u_0 \tag{2.12}$$

where $u(t)$ is an element of a Hilbert space V , A is a generator of a C_0 semigroup $S(t)$, and $g : U \subseteq V \rightarrow V$ is locally Lipschitz continuous in the open set $U \subseteq V$. The inhomogeneity is included in (2.12) as a component of u . We will define V , A and g appropriately and prove the global existence of mild and classical solutions of (2.12).

2.2.1 Notation

The Hilbert space V is defined as

$$V := \mathbb{L}^2([0, L]; \mathbb{C}^4) \times \mathbb{R}^{m_a} \times \mathbb{L}_\eta^2([0, \infty); \mathbb{C}) \tag{2.13}$$

where $\mathbb{L}_\eta^2([0, \infty); \mathbb{C})$ is the space of weighted square integrable functions. The scalar product of $\mathbb{L}_\eta^2([0, \infty); \mathbb{C})$ is defined by

$$(v, w)_\eta := \operatorname{Re} \int_0^\infty \bar{v}(x) \cdot w(x)(1+x^2)^\eta dx.$$

We choose the exponent $\eta < -1/2$ such that $\mathbb{L}^\infty([0, \infty); \mathbb{C})$ is continuously embedded in $\mathbb{L}_\eta^2([0, \infty); \mathbb{C})$. The complex plane is treated as two-dimensional real plane in the definition of the vector space V such that the standard \mathbb{L}^2 scalar product $(\cdot, \cdot)_V$ of V is differentiable. The corresponding components of $v \in V$ are denoted by

$$v = (\psi_1, \psi_2, p_1, p_2, n, a)^T.$$

The spatial variable in ψ and p is denoted by $z \in [0, L]$ whereas the spatial variable in a is denoted by $x \in [0, \infty)$. The Hilbert space $\mathbb{H}_\eta^1([0, \infty); \mathbb{C})$ equipped with the scalar product

$$(v, w)_{1, \eta} := (v, w)_\eta + (\partial_x v, \partial_x w)_\eta$$

is densely and continuously embedded into $\mathbb{L}_\eta^2([0, \infty); \mathbb{C})$. Moreover, its elements are continuous [41]. Consequently, the Hilbert spaces

$$\begin{aligned} W &:= \mathbb{H}^1([0, L]; \mathbb{C}^2) \times \mathbb{L}^2([0, L]; \mathbb{C}^2) \times \mathbb{R}^{m_a} \times \mathbb{H}_\eta^1([0, \infty); \mathbb{C}) \\ W_{\text{BC}} &:= \{(\psi, p, n, a) \in W : \psi_1(0) = r_0 \psi_2(0) + a(0), \psi_2(L) = r_L \psi_1(L)\} \end{aligned}$$

are densely and continuously embedded in V . The linear functionals $\psi_1(0) - r_0 \psi_2(0) - a(0)$ and $\psi_2(L) - r_L \psi_1(L)$ are continuous from $W \rightarrow \mathbb{R}$. We define the linear operator $A : W_{\text{BC}} \rightarrow V$ by

$$A \begin{pmatrix} \psi_1 \\ \psi_2 \\ p \\ n \\ a \end{pmatrix} := \begin{pmatrix} -\partial_z \psi_1 \\ \partial_z \psi_2 \\ 0 \\ 0 \\ \partial_x a \end{pmatrix}. \quad (2.14)$$

The definition of A and W_{BC} treat the inhomogeneity α in the boundary conditions as the boundary value at 0 of the variable a . We define the open set $U \subseteq V$ by

$$U := \{(\psi, p, n, a) \in V : n_k > \underline{n} \text{ for } k \in \mathcal{A}\},$$

and the nonlinear function $g : U \rightarrow V$ by

$$g(\psi, p, n, a) = \begin{pmatrix} \beta(n)\psi - i\kappa\sigma_c\psi + \rho(n)p \\ (i\Omega_r(n) - \Gamma)p + \Gamma\psi \\ (f_k(n_k, (\psi, p)))_{k \in \mathcal{A}} \\ 0 \end{pmatrix}. \quad (2.15)$$

The function g is continuously differentiable to any order with respect to all arguments and its Frechet derivative is bounded in any closed bounded ball $B \subset U$ [20].

According to the theory of C_0 semigroups we have two solution concepts [34]:

Definition 2.1 *Let $T > 0$. A solution $u : [0, T] \rightarrow V$ is a classical solution of (2.12) if $u(t) \in W_{\text{BC}} \cap U$ for all $t \in [0, T]$, $u \in C^1([0, T]; V)$, $u(0) = u_0$, and equation (2.12) is valid in V for all $t \in (0, T)$.*

The inhomogeneous initial-boundary value problem (2.1)-(2.5) and the autonomous evolution system (2.12) are equivalent in the following sense: Suppose the inhomogeneity $\alpha \in \mathbb{H}^1([0, T]; \mathbb{C})$ in (2.4).

Let $u = (\psi, p, n, a)$ be a classical solution of (2.12). Then, u satisfies (2.1)-(2.2), and (2.5) in \mathbb{L}^2 and (2.3), (2.4) for each $t \in [0, T]$ if and only if $a^0|_{[0, T]} = \alpha$.

On the other hand, assume that (ψ, p, n) satisfies (2.1)-(2.2), and (2.5) in \mathbb{L}^2 and (2.3), (2.4) for each $t \in [0, T]$. Then, we can choose a $a^0 \in \mathbb{H}_\eta^1([0, \infty); \mathbb{C})$ such that $a^0|_{[0, T]} = \alpha$ and obtain that $u(t) = (\psi(t), p(t), n(t), a^0(t + \cdot))$ is a classical solution of (2.12) in $[0, T]$.

Definition 2.2 Let $T > 0$, A a generator of a C_0 semigroup $S(t)$ of bounded operators in V . A solution $u : [0, T] \rightarrow V$ is a mild solution of (2.12) if $u(t) \in U$ for all $t \in [0, T]$, and $u(t)$ satisfies the variation of constants formula in V

$$u(t) = S(t)u_0 + \int_0^t S(t-s)g(u(s))ds. \quad (2.16)$$

We prove in Lemma 2.3 that A generates a C_0 semigroup in V . Mild solutions of (2.12) are a reasonable generalization of the classical solution concept of (2.1)-(2.4) to boundary conditions including discontinuous inputs $\alpha \in \mathbb{L}_\eta^2([0, \infty); \mathbb{C})$.

2.2.2 Global Existence and Uniqueness of Solutions for the Truncated Problem

In order to prove uniqueness and global existence of solutions of (2.12), we apply the theory of strongly continuous semigroups (see [34]).

Lemma 2.3 $A : W_{\text{BC}} \subset V \rightarrow V$ generates a C_0 semigroup $S(t)$ of bounded operators in V .

Proof:

We specify $S(t)$ explicitly. Denote the components of $S(t)(\psi_1^0, \psi_2^0, p^0, n^0, a^0)$ by $(\psi_1(t, z), \psi_2(t, z), p(t, z), n(t), a(t, x))$ and let $t \leq L$.

$$\begin{aligned} \psi_1(t, z) &= \begin{cases} \psi_1^0(z-t) & \text{for } z > t \\ r_0\psi_2^0(t-z) + a^0(t-z) & \text{for } z \leq t \end{cases} \\ \psi_2(t, z) &= \begin{cases} \psi_2^0(z+t) & \text{for } z < L-t \\ r_L\psi_1^0(2L-t-z) & \text{for } z \geq L-t \end{cases} \\ p(t, z) &= 0 \\ n(t) &= 0 \\ a(t, x) &= a^0(x+t). \end{aligned}$$

For $t > L$ we define inductively $S(t)u = S(L)S(t-L)u$. This procedure defines a semigroup of bounded operators in V properly since

$$\|\psi_1(t, \cdot)\|^2 + \|\psi_2(t, \cdot)\|^2 + \|a(t, \cdot)\|^2 \leq 2(1+t^2)^{-\eta} (\|\psi_1^0\| + \|\psi_2^0\| + \|a^0\|)$$

for $t \leq L$. The strong continuity of S is a direct consequence of the continuity in the mean in \mathbb{L}^2 . It remains to be shown that S is generated by A .

Let $u = (\psi_1^0, \psi_2^0, p^0, n^0, a^0)$ satisfy $\lim_{t \rightarrow 0} \frac{1}{t}(S(t)u - u) \in V$, define $\varphi_t(z) := \frac{1}{t}(\psi_1(t, z) - \psi_1^0(z))$, $\varphi_0 = \lim_{t \rightarrow 0} \varphi_t$, and $\delta > 0$ small. Firstly, we prove that $u \in W_{\text{BC}}$. φ_t coincides with the difference quotient $\frac{1}{t}(\psi_1^0(z-t) - \psi_1^0(z))$ for $t < \delta$ in the interval $[\delta, L]$. Thus, $\partial_z \psi_1^0 \in \mathbb{L}^2([\delta, L]; \mathbb{C})$ exists. Furthermore, $\varphi_t(\cdot + t) \rightarrow \varphi_0$ in $\mathbb{L}^2([0, L-\delta]; \mathbb{C})$. Since $\varphi_t(\cdot + t) = \frac{1}{t}(\psi_1^0(z) - \psi_1^0(z+t))$, $\partial_z \psi_1^0$ exists also in $\mathbb{L}^2([0, L-\delta]; \mathbb{C})$. Consequently $\psi_1^0 \in \mathbb{H}^1([0, L]; \mathbb{C})$. The same argument holds for $\psi_2^0 \in \mathbb{H}^1([0, L]; \mathbb{C})$ and for $a^0 \in \mathbb{H}_\eta^1([0, \infty); \mathbb{C})$.

In order to verify that u satisfies the boundary conditions we write

$$\varphi_t(z) = \begin{cases} z \in [t, L] : & -\frac{1}{t} \int_{z-t}^z \partial_z \psi_1^0(\zeta) d\zeta \\ z \in [0, t] : & \frac{1}{t} \left(r_0 \int_0^{t-z} \partial_z \psi_2^0(\zeta) + \partial_z a^0(\zeta) d\zeta - \int_0^z \partial_z \psi_1^0(\zeta) d\zeta \right) + \\ & + \frac{1}{t} (r_0 \psi_2^0(0) + a^0(0) - \psi_1^0(0)) \end{cases} \quad (2.17)$$

Consequently, the limit φ_0 is in $\mathbb{L}^2([0, L]; \mathbb{C})$ if and only if $r_0 \psi_2^0(0) + a^0(0) - \psi_1^0(0) = 0$. The same argument using $\frac{1}{t}(\psi_2(t, z) - \psi_2^0(z))$ leads to the boundary condition $r_L \psi_1^0(L) - \psi_2^0(L) = 0$.

Finally, we prove that $\frac{1}{t}(S(t)u - u) = Au$ for any $u \in W_{\text{BC}}$. Using the notation φ_t introduced above, we have $\int_0^t |\varphi_t(z)|^2 dz \rightarrow 0$ due to (2.17). Hence, $\varphi_t \rightarrow -\partial_z \psi_1^0$ on $[0, L]$. Again, we can use the same arguments to obtain the limits $\partial_z \psi_2^0$ and $\partial_x a^0$. \square The operators $S(t)$ have a uniform upper bound

$$\|S(t)\| \leq C e^{\gamma t} \quad (2.18)$$

within finite intervals $[0, T]$. In order to apply the results of the C_0 semigroup theory [34], we truncate the nonlinearity g smoothly: For any bounded ball $B \subset U$ which is closed w. r. t. V , we choose $g_B : V \rightarrow V$ such that $g_B(u) = g(u)$ for all $u \in B$, g_B is continuously differentiable and globally Lipschitz continuous. This is possible because the Frechet derivative of g is bounded in B and the scalar product in V is differentiable with respect to its arguments. We call

$$\frac{d}{dt} u(t) = Au(t) + g_B(u(t)), \quad u(0) = u_0 \quad (2.19)$$

the truncated problem (2.12). The following Lemma 2.4 is a consequence of the results in [34].

Lemma 2.4 (global existence for the truncated problem)

The truncated problem (2.19) has a unique global mild solution $u(t)$ for any $u_0 \in V$. If $u_0 \in W_{\text{BC}}$, $u(t)$ is a classical solution of (2.19).

Corollary 2.5 (local existence) *Let $u_0 \in U$. There exists a $t_{\text{loc}} > 0$ such that the evolution problem (2.12) has a unique mild solution $u(t)$ on the interval $[0, t_{\text{loc}}]$. If $u_0 \in W_{\text{BC}} \cap U$, $u(t)$ is a classical solution.*

2.2.3 A-priori Estimates — Existence of Semiflow

In order to state the result of Lemma 2.4 for (2.12), we need the following a-priori estimate for the solutions of the truncated problem (2.19).

Lemma 2.6 *Let $T > 0$, $u_0 \in W_{\text{BC}} \cap U$. If $\underline{n} > -\infty$, suppose $I_k \tau_k > \underline{n}$ for all $k \in \mathcal{A}$. There exists a closed bounded ball B such that $B \subset U$ and the solution $u(t)$ of the B -truncated problem (2.19) starting at u_0 stays in B for all $t \in [0, T]$.*

Proof: Let $u_0 = (\psi^0, p^0, n^0, a^0) \in W_{\text{BC}} \cap U$. We choose $n_{\text{low}} > \underline{n}$ such that $n_{\text{low}} < n_k^0$ and $G_k(n_{\text{low}}) - \rho_k(n_{\text{low}}) < 0$ for all $k \in \mathcal{A}$ and define the function

$$h(t) := \frac{P}{2} \|\psi(t)\|^2 + \sum_{k \in \mathcal{A}} l_k (n_k(t) - n_{\text{low}}).$$

Let $t_1 > 0$ such that the solution $u(t)$ of (2.12) exists on $[0, t_1]$ and $n_k(t) \geq n_{\text{low}}$. Because of the structure of the nonlinearity g , $u(t)$ is classical in $[0, t_1]$. Hence, $h(t)$ is differentiable and

$$\begin{aligned} \frac{d}{dt} h(t) &\leq J - \sum_{k \in \mathcal{A}} l_k \tau_k^{-1} n_k + \frac{P}{2} \sum_{k=1}^m \text{Re } d_k \|\psi\|_k^2 \\ &\leq J - \tilde{\tau}^{-1} n_{\text{low}} - \gamma h(t), \end{aligned}$$

due to (2.1), (2.3) and the supposition $\rho_k = 0$ for $k \notin \mathcal{A}$ where

$$\begin{aligned} \gamma &:= \min \left\{ \tau_k^{-1}, -\frac{P}{2} \text{Re } d_j : k \in \mathcal{A}, j \leq m \right\} > 0 \\ J &:= \sum_{k \in \mathcal{A}} l_k I_k + \sup \{ |r_0 z + a^0(x)|^2 - |z|^2 : z \in \mathbb{C}, x \in [0, T] \} < \infty \\ \tilde{\tau}^{-1} &:= \sum_{k \in \mathcal{A}} l_k \tau_k^{-1}. \end{aligned}$$

Consequently, $h(t) \leq \max\{h(0), \gamma^{-1} J - \gamma^{-1} \tilde{\tau}^{-1} n_{\text{low}}\}$. Since $h(0) = \frac{P}{2} \|\psi^0\|^2 + \sum_{k \in \mathcal{A}} l_k n_k^0 - L n_{\text{low}}$, we obtain the estimate

$$0 \leq h(t) \leq M - \xi \cdot n_{\text{low}} \tag{2.20}$$

where

$$\begin{aligned} M &:= \max \left\{ \gamma^{-1} J, \frac{P}{2} \|\psi^0\|^2 + \sum_{k \in \mathcal{A}} l_k n_k^0 \right\} \\ \xi &:= \min \{ \gamma^{-1} \tilde{\tau}^{-1}, L \}. \end{aligned}$$

Since $n_k(t) \geq n_{\text{low}}$ in $[0, t_1]$, the estimate (2.20) for $h(t)$ and the differential equation (2.2) for p lead to bounds for ψ , p and n in $[0, t_1]$:

$$\begin{aligned} \|\psi(t)\|^2 &\leq \psi_{\text{max}}^2 := 2P^{-1}(M - \xi \cdot n_{\text{low}}) \\ \|p(t)\| &\leq \|p^0\| + \sqrt{2P^{-1}(M - \xi n_{\text{low}})} \\ n_k &\in [n_{\text{low}}, n_{\text{low}} + l_k^{-1} M - l_k^{-1} \xi n_{\text{low}}]. \end{aligned} \tag{2.21}$$

The bounds (2.21) are valid for arbitrary $n_{\text{low}} \in (\underline{n}, \min\{1, n_k^0 : k \in \mathcal{A}\})$ if $n_k(t) \geq n_{\text{low}}$ for all $k \in \mathcal{A}$ and $t \in [0, t_1]$. Due to the properties of G_k and ρ_k (see section 2.1) and the supposition $I_k \tau_k > \underline{n}$, we find some n_{low} (sufficiently close to \underline{n}) such that

$$\begin{aligned} I_k &> \frac{n_{\text{low}}}{\tau_k} + \frac{P \rho_k(n_{\text{low}})}{l_k} \left(\sqrt{2P^{-1}(M - \xi n_{\text{low}})} + \|p^0\| \right) S + \\ &+ \frac{G_k(n_{\text{low}}) - \rho_k(n_{\text{low}})}{l_k} P S^2 \end{aligned} \tag{2.22}$$

holds for all $S \geq 0$ and $k \in \mathcal{A}$. By choosing n_{low} according to (2.22), we ensure that $\frac{d}{dt}n_k(t) > 0$ if $n_k(t) = n_{\text{low}}$. Consequently, $n_k(t)$ can never cross n_{low} and the bounds (2.21) are valid on the whole interval $[0, T]$ for n_{low} meeting (2.22). Therefore, we can choose the ball B such that the bounds (2.21) are met by all $u \in B$. \square

Moreover, a solution $u(t)$ starting at $u_0 \in W_{\text{BC}} \cap U$ and staying in a bounded closed ball $B \subset U$ in $[0, T]$ is a classical solution in the whole interval $[0, T]$ because of the structure of the nonlinearity g .

The bounds (2.21) do not depend on the complete W_{BC} -norm of u_0 but on its V -norm and the \mathbb{L}^∞ -norm of $a^0|_{[0, T]}$. Hence, we can state the global existence theorem also for mild solutions:

Theorem 2.7 (global existence and uniqueness)

Let $T > 0$, $u_0 = (\psi^0, p^0, n^0, a^0) \in U$ and $\|a^0|_{[0, T]}\|_\infty < \infty$. If $\underline{n} > -\infty$, let $I_k \tau_k > \underline{n}$ for all $k \in \mathcal{A}$. There exists a unique mild solution $u(t)$ of (2.12) in $[0, T]$. Furthermore, if $u_0 \in W_{\text{BC}} \cap U$, $u(t)$ is a classical solution of (2.12).

Corollary 2.8 (global boundedness) Let $u_0 = (\psi^0, p^0, n^0, a^0) \in U$ and $\|a^0\|_\infty < \infty$. There exists a constant C such that $\|u(t)\|_V \leq C$.

Corollary 2.9 (continuous dependence on initial values)

Let $T > 0$, $u_j^0 = (\psi^j, p^j, n^j, a^j) \in U$, $\|a^j|_{[0, T]}\|_\infty < \infty$ for $j = 1, 2$. There exists a constant $C(\|u_1^0\|_V, \|u_2^0\|_V, \|a^1|_{[0, T]}\|_\infty, \|a^2|_{[0, T]}\|_\infty, T)$ such that $\|u_1(t) - u_2(t)\|_V \leq C \cdot \|u_1^0 - u_2^0\|_V$.

Therefore, the nonlinear equation defines a semiflow $S(t; u_0)$ for $t > 0$. S is even continuously differentiable with respect to its second argument in the following sense:

Corollary 2.10 (continuous differentiability of the semiflow)

Let $T > 0$, $u^0 = (\psi^0, p^0, n^0, a^0) \in U$, $\|a^0|_{[0, T]}\|_\infty < \infty$. Let

$$\mathcal{M}_{C, \varepsilon} := \{(\psi, p, n, a) \in V : \|a|_{[0, T]}\|_\infty \leq C, \|(\psi, p, n, a)\|_V < \varepsilon\}.$$

Then,

$$S(t; u_0 + h_0) - S(t; u_0) = S_L(t, 0)h_0 + o_C(\|h_0\|_V)$$

for all $h_0 \in \mathcal{M}_{C, \varepsilon}$ for arbitrary C and sufficiently small ε . $S_L(t, s)$ is the evolution operator of the linear evolution equation in V

$$\frac{d}{dt}v(t) = Av(t) + \frac{\partial}{\partial u}g(u(t))v(t), \quad v(s) = v_0.$$

This follows from the C_0 semigroup theory [34] since we can choose a common ball B for all $u_0 + h_0$, $h_0 \in \mathcal{M}_{C, \varepsilon}$. This result extends to C^k smoothness ($k > 1$) since the nonlinearity g is C^∞ with respect to all arguments.

The continuous dependence of the solution on all parameters within a bounded parameter region is also a direct consequence of the C_0 semigroup theory. In order to obtain a uniform a-priori estimate, we impose additional restrictions on the parameters: $1 - |r_0| > c > 0$, $I_k \tau_k - \underline{n} > c > 0$, $\text{Re } d_k < -c < 0$, $g_k > c > 0$ for $k \in \mathcal{A}$ and a uniform constant c .

3 Model reduction — Mode Approximations

After showing that the initial-boundary-value problem has a smooth global semiflow $S(t; u_0)$, we focus on the long-time behavior of S . The goal of this chapter is to construct low-dimensional ODE models approximating $S(t; u_0)$ for large t . These *mode approximations* are often used to describe the long-time behavior of S [6], [8], [9], [44]. A heuristic justification for mode approximations was given in [9] for the traveling wave equations without gain dispersion by exploiting the property that the variables $\psi(t, z)$ and $n(t)$ operate on different time scales. We show how these models approximate the semiflow on invariant manifolds of the system of partial differential equations using singular perturbation theory. The basic idea for this reduction was outlined already in [45] assuming a-priori that the phase space is finite-dimensional and the spectrum of H has a gap.

3.1 Introduction of the Singular Perturbation Parameter

This and the following chapter treat the autonomous system (2.1)-(2.3). Its boundary conditions are

$$\psi_1(t, 0) = r_0 \psi_2(t, 0), \quad \psi_2(t, L) = r_L \psi_1(t, L) \quad \text{where } r_0 r_L \neq 0. \quad (3.1)$$

The condition on the facette reflectivities $r_0 r_L \neq 0$ converts the semiflow $S(t, \cdot)$ locally into a flow, i. e., $\|S(t, \cdot)\|$ exists for $t \leq 0$ until $\|S(t; \cdot)\|$ goes to infinity. However, small reflectivities are possible and physically relevant.

We reformulate (2.1)-(2.3) to exploit its particular structure. The space dependent subsystem is linear in ψ and p :

$$\partial_t \begin{pmatrix} \psi \\ p \end{pmatrix} = H(n) \begin{pmatrix} \psi \\ p \end{pmatrix}. \quad (3.2)$$

The linear operator

$$H(n) = \begin{pmatrix} \sigma \partial_z + \beta(n) - i\kappa \sigma_c & \rho(n) \\ \Gamma & (i\Omega_r(n) - \Gamma) \end{pmatrix} \quad (3.3)$$

acts from

$$Y := \{(\psi, p) \in \mathbb{H}^1([0, L]; \mathbb{C}^2) \times \mathbb{L}^2([0, L]; \mathbb{C}^2) : \psi \text{ satisfying (3.1)}\}$$

into $X = \mathbb{L}^2([0, L]; \mathbb{C}^4)$. $H(n)$ generates a C_0 semigroup $T_n(t)$ acting in X . Its coefficients κ , Γ and (for each $n \in \mathbb{R}^{m_a}$) $\beta(n)$, $\Omega_r(n)$ and $\rho(n)$ are linear operators in $\mathbb{L}^2([0, L]; \mathbb{C}^2)$ defined by the corresponding coefficients in (2.1), (2.2). The maps $\beta, \rho, \Omega_r : \mathbb{R}^{m_a} \rightarrow \mathcal{L}(\mathbb{L}^2([0, L]; \mathbb{C}^2))$ are smooth.

We observe that I_k and τ_k^{-1} in (2.10) are approximately two orders of magnitude smaller than 1 (see. Table A.1). Hence, we can introduce a small parameter ε such that (2.11) reads:

$$\frac{d}{dt} n_k = f_k(n_k, x) = \varepsilon F_k(n_k) - P g_k(n_k)[x, x] \quad (3.4)$$

for $x \in X$ where the coefficients in F_k are of order 1. Although ε is not directly accessible, we treat it as a parameter and consider the limit $\varepsilon \rightarrow 0$ while keeping F_k fixed. The parameter ε is a singular perturbation parameter for system (3.2), (3.4): For $\varepsilon = 0$, the set $\mathcal{E} = \{(x, n) \in X \times \mathbb{R}^{m_a} : x = 0\}$ consists of equilibria of (3.2), (3.4). \mathcal{E} is referred to as the *slow manifold*. Simultaneously, \mathcal{E} is invariant for $\varepsilon > 0$ and the slow motion on \mathcal{E} is defined by $\frac{d}{dt}n_k = \varepsilon F_k(n_k)$. The slow variable is n . Since the semiflow $S(t; (x, n))$ induced by system (3.2), (3.4) is smooth with respect to (x, n) , we can linearize system (3.2), (3.4) for $\varepsilon = 0$ at each point $(0, n) \in \mathcal{E}$:

$$\begin{aligned} \partial_t x &= H(n)x \\ \frac{d}{dt}N &= 0. \end{aligned} \tag{3.5}$$

Hence, the spectral properties of the operator $H(n)$ determine whether x decays or grows exponentially near $(0, n) \in \mathcal{E}$.

In section 3.2, we investigate $H(n)$ and study its spectrum and the growth properties of its C_0 semigroup $T_n(t)$. In section 3.3, we focus on the dynamics near compact subsets of \mathcal{E} where a part of the spectrum of $H(n)$ is on the imaginary axis (near *critical* n). We apply the results of singular perturbation theory [19] to find an exponentially attracting invariant manifold in the environment of these subsets.

Along with (3.2), (3.4), it is convenient to introduce ε as a dummy variable and consider the extended system where (3.2), (3.4) are augmented by the equation

$$\frac{d}{dt}\varepsilon = 0. \tag{3.6}$$

3.2 Spectral Properties of $H(n)$

At first, we consider the fast subsystem (3.2) treating n as a parameter. We drop the corresponding argument in this section. As (3.2) is linear, we have to investigate the spectrum of H and how it is related to the C_0 semigroup $T(t)$ generated by H . See Figure 3.1 for a sample computation.

Define the set of complex “resonance frequencies”

$$\mathcal{W} = \{c \in \mathbb{C} : c = i\Omega_{r,k} - \Gamma_k \text{ for at least one } k \in \{1 \dots m\}\} \subset \mathbb{C}$$

and the complexified “gain curve” $\chi : \mathbb{C} \setminus \mathcal{W} \rightarrow \mathcal{L}(\mathbb{L}^2([0, L]; \mathbb{C}^2))$ (see appendix A for explanation and [50], [39] for details). For each $\lambda \in \mathbb{C} \setminus \mathcal{W}$, $\chi(\lambda)$ is a linear operator defined by

$$\chi(\lambda) = \frac{\rho\Gamma}{\lambda - i\Omega_r + \Gamma} \in \mathcal{L}(\mathbb{L}^2([0, L]; \mathbb{C}^2)).$$

For $\lambda \in \mathbb{C} \setminus \mathcal{W}$, the following relation follows from (3.3): λ is in the resolvent set of H if and only if the boundary value problem

$$(\sigma\partial_z + \beta - i\kappa\sigma_c + \chi(\lambda) - \lambda)\varphi = 0 \quad \text{with b. c.} \tag{3.1} \tag{3.7}$$

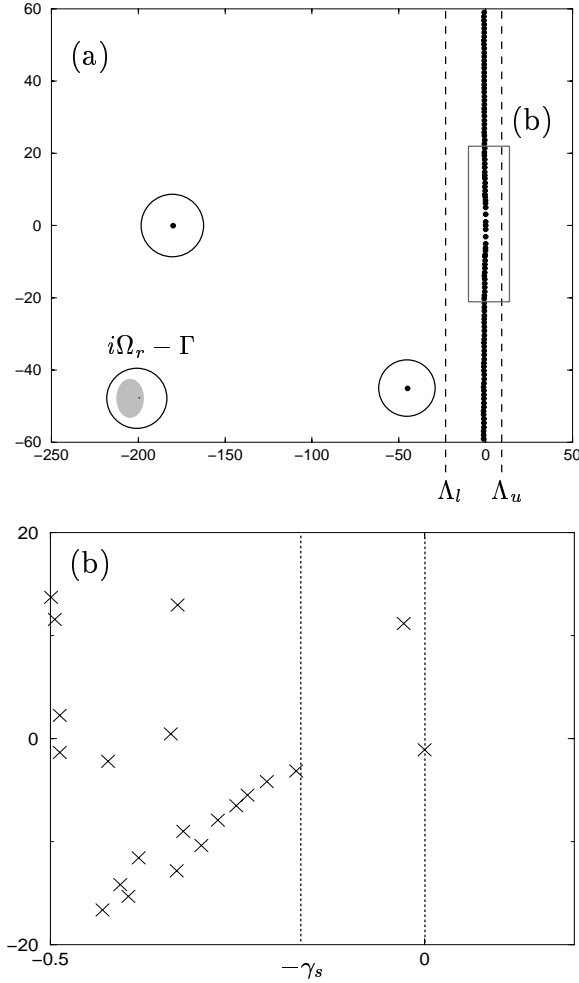


Figure 3.1: Spectrum of H : (a) global view and (b) magnified view. The black circles in (a) are the boundaries of the balls defined in (3.15), and (3.16). All other eigenvalues of H are situated within the strip $[\Lambda_l, \Lambda_u]$. The shadowing around $i\Omega_r - \Gamma$ indicates a sequence of eigenvalues (not actually computed) accumulating to $i\Omega_r - \Gamma$. The magnified view (b) shows a typical situation for $\kappa > 0$. Here two eigenvalues of $H(n)$ are close to the imaginary axis.

has only the trivial solution $\varphi = 0$ in $\mathbb{H}^1([0, L]; \mathbb{C}^2)$. The transfer matrix corresponding to (3.7) is

$$T_k(z, \lambda) = \frac{e^{-\gamma_k z}}{2\gamma_k} \begin{pmatrix} \gamma_k + \mu_k + e^{2\gamma_k z}(\gamma_k - \mu_k) & i\kappa_k(1 - e^{2\gamma_k z}) \\ -i\kappa_k(1 - e^{2\gamma_k z}) & \gamma_k - \mu_k + e^{2\gamma_k z}(\gamma_k + \mu_k) \end{pmatrix} \quad (3.8)$$

for $z \in S_k$ where $\mu_k = \lambda - \chi_k(\lambda) - \beta_k$ and $\gamma_k = \sqrt{\mu_k^2 + \kappa_k^2}$ (see [6], [20], [36] for

details). Hence, the function

$$h(\lambda) = (r_L \quad -1) T(L, 0; \lambda) \begin{pmatrix} r_0 \\ 1 \end{pmatrix} = (r_L \quad -1) \prod_{k=m}^1 T_k(l_k; \lambda) \begin{pmatrix} r_0 \\ 1 \end{pmatrix} \quad (3.9)$$

defined in $\mathbb{C} \setminus \mathcal{W}$ is the characteristic function of H : Its roots are the eigenvalues of H and $\{\lambda \in \mathbb{C} \setminus \mathcal{W} : h(\lambda) \neq 0\}$ is the resolvent set. Consequently, all $\lambda \in \mathbb{C} \setminus \mathcal{W}$ are either eigenvalues or resolvent points of H , i. e., there is no essential (continuous or residual) spectrum in $\mathbb{C} \setminus \mathcal{W}$. We note that $\text{Re } \mathcal{W} \ll -1$.

The following lemma provides an upper bound for the real parts of the eigenvalues. Moreover, we derive a result about the spatial shape of an eigenvector corresponding to an eigenvalue of H with nonnegative real part.

Lemma 3.1 *Let $\lambda \in \mathbb{C} \setminus \mathcal{W}$ be in the point spectrum of H . Then, λ is geometrically simple. Denote its corresponding scaled eigenvector by (ψ, p) . Then, $\|\psi\| \geq 1/2$, and the following estimates hold:*

$$\text{Re } \lambda \leq \Lambda_u := \max_{k=1 \dots m} \frac{\Gamma_k \cdot (\text{Re } \beta_k + 4\rho_k)}{\Gamma_k - 4\rho_k}. \quad (3.10)$$

If $\text{Re } \lambda \geq 0$,

$$\max_{k=1 \dots m} l_k g_k \left[\begin{pmatrix} \psi \\ p \end{pmatrix}, \begin{pmatrix} \psi \\ p \end{pmatrix} \right] + \text{Re } d_k \|\psi\|_k^2 \geq 0. \quad (3.11)$$

Proof: Let (ψ, p) be an eigenvector associated to λ . Then, ψ is a multiple of $T(z, 0; \lambda) \begin{pmatrix} r_0 \\ 1 \end{pmatrix}$, and $p = \Gamma\psi/(\lambda - i\Omega_r + \Gamma)$. Thus, λ is geometrically simple and $\|\psi\| \geq \|p(z)\|$ (hence, $\|\psi\| \geq 1/2$). Partial integration of the eigenvalue equation (3.7) and its complex conjugate equation yields:

$$2 \text{Re } \lambda \leq 2 \max_{k=1 \dots m} (\text{Re } \beta_k + \text{Re } \chi_k(\lambda)). \quad (3.12)$$

For $\text{Re } \lambda > -\Gamma_k/2$, we get $\text{Re } \chi_k(\lambda) \leq 4\rho_k + 4\rho_k/\Gamma_k \text{Re } \lambda$. For realistic parameter values, we have $\Lambda_u > -\Gamma_k/2$ and $4\rho_k/\Gamma_k < 1$ for all k implying (3.10). Estimate (3.11) follows immediately from (3.12), the definition (2.9) of the hermitian form g_k , and $p = \Gamma\psi/(\lambda - i\Omega_r + \Gamma)$. \square

Next, we show how to split the spectrum of H into two parts for realistic parameter values and in particular for small r_0, r_L (for possible ranges of parameters see Table A.1). Figure 3.1 visualizes this splitting.

Lemma 3.2 *Let us introduce $\delta_1 = |r_0|^2/(|r_0| + |\kappa_1|)$, $\delta_m = |r_L|^2/(|r_L| + |\kappa_m|)$ and $\varrho_k = \sqrt{\rho_k \Gamma_k}$. We denote by \mathcal{S} the strip $\{\lambda \in \mathbb{C} : \text{Re } \lambda \in [\Lambda_l, \Lambda_u]\} \subset \mathbb{C}$ where Λ_l is the minimum of the quantities*

$$\min \left\{ (2l_k)^{-1} \log[\delta_k/3], -|\kappa_k| \right\} - |\kappa_k| + \text{Re } \beta_k - \varrho_k \text{ for } k = 1 \text{ and } m, \quad (3.13)$$

$$\min \left\{ -m|\kappa_k|, \frac{-\log(m+1)}{2l_k} - |\kappa_k| \right\} + \text{Re } \beta_k - \varrho_k \text{ for } k = 2 \dots m-1. \quad (3.14)$$

Then, $\lambda \in \mathbb{C} \setminus \mathcal{W}$ is in the resolvent set of H if $\lambda \notin \mathcal{S}$ and

$$\lambda \notin B_{R_0} \left(\beta_1 - \frac{i}{2} \kappa_1 (r_0^{-1} + r_0) \right) \cup B_{R_L} \left(\beta_m - \frac{i}{2} \kappa_m (r_L^{-1} + r_L) \right) \quad (3.15)$$

$$\lambda \notin B_{\varrho_k} (i\Omega_{r,k} - \Gamma_k) \quad (3.16)$$

where $R_0 = \varrho_1 + 1$ and $R_L = \varrho_m + 1$.

Proof: Relation (3.16) leads to $|\chi_k(\lambda)| < \varrho_k$. Thus, we can rewrite the condition that λ is less than (3.13)–(3.15) as conditions for μ_k :

$$\operatorname{Re} \mu_k < \min \{ (2l_k)^{-1} \log[\delta_k/3] - |\kappa_k|, -2|\kappa_k| \} \text{ for } k = 1 \text{ and } m, \quad (3.17)$$

$$\operatorname{Re} \mu_k < \min \{ -m|\kappa_k|, -(2l_k)^{-1} \log(m+1) - |\kappa_k| \} \text{ for } k = 2 \dots m-1 \quad (3.18)$$

$$\mu_1 \notin B_1 \left(-\frac{i}{2} \kappa_1 (r_0^{-1} + r_0) \right) \quad (3.19)$$

$$\mu_m \notin B_1 \left(-\frac{i}{2} \kappa_m (r_L^{-1} + r_L) \right). \quad (3.20)$$

We have to prove that $h(\lambda) \neq 0$ for λ satisfying (3.17)–(3.20). To this purpose, we define the functions $r_1, r_m : \mathbb{C} \rightarrow \mathbb{C}$ implicitly by the linear equations

$$(1, -r_1(\lambda)) \cdot T_1^1(l_1, \lambda) \begin{pmatrix} r_0 \\ 1 \end{pmatrix}, \quad (1, -r_m(\lambda)) \cdot T_m^1(l_m, \lambda) \begin{pmatrix} r_L \\ 1 \end{pmatrix}. \quad (3.21)$$

Firstly, we prove that (3.17) and (3.19) lead to $|r_1(\lambda)| > 1$. We choose for γ_k in (3.8) that branch of the square root which has negative real part. Hence, the function $\mu \rightarrow \sqrt{\mu^2 + \kappa_1^2}$ is properly defined in $\mathbb{C}_- := \{ \zeta \in \mathbb{C} : \operatorname{Re} \zeta < -2|\kappa_1| \}$ and continuous. Condition (3.17) implies $\operatorname{Re} \gamma_1 < \operatorname{Re} \mu_1 + |\kappa_1|$, and $|\gamma_1 + \mu_1| > 3|\kappa_1|$. From (3.21) and (3.8) we obtain that $|r_1(\lambda)| > 1$ if

$$\left| r_0 + \frac{i\kappa_1}{\gamma_1 + \mu_1} + e^{2\gamma_1 l_1} \left[\frac{\kappa_1^2 r_0}{(\gamma_1 + \mu_1)^2} - \frac{i\kappa_1}{\gamma_1 + \mu_1} \right] \right| > \left| \frac{-i r_0 \kappa_1}{\gamma_1 + \mu_1} + \frac{\kappa_1^2}{(\gamma_1 + \mu_1)^2} + e^{2\gamma_1 l_1} \left[\frac{i\kappa_1 r_0}{\gamma_1 + \mu_1} + 1 \right] \right|. \quad (3.22)$$

Estimating $|\kappa_1/(\gamma_1 + \mu_1)| < 1/3$, $|r_0| < 1$, and separating the terms with $e^{2\gamma_1 l_1}$, (3.22) follows from

$$\left| r_0 + \frac{i\kappa_1}{\gamma_1 + \mu_1} \right| > 3 \cdot |e^{2\gamma_1 l_1}|. \quad (3.23)$$

Condition (3.17) ensures that the right-hand-side of (3.23) is less than δ_1 . Then, the function $z : \mu \rightarrow \mu + \sqrt{\mu^2 + \kappa_1^2}$ is properly defined in \mathbb{C}_- , maps \mathbb{C}_- into itself and its inverse has a Lipschitz constant < 1 . Therefore, (3.19) leads to $\gamma_1 + \mu_1 \notin B_1(-i\kappa_1 r_0^{-1})$, hence, the left-hand-side of (3.23) is larger than δ_1 . Consequently,

(3.17) and (3.19) lead to $|r_1(\lambda)| > 1$. Drawing the same conclusions for section S_m and r_L from (3.17) and (3.20), we obtain $|r_m(\lambda)| > 1$.

The characteristic function $h(\lambda)$ can be expressed by $r_1(\lambda)$ and $r_m(\lambda)$ as follows:

$$h(\lambda) = (r_m(\lambda), -1) \prod_{k=m-1}^2 T_k(l_k, \lambda) \begin{pmatrix} r_1(\lambda) \\ 1 \end{pmatrix} = 0.$$

Condition (3.18) implies

$$|[T_k(l_k, \lambda)]_{11}| > m \cdot \max \{ |[T_k(l_k, \lambda)]_{12}|, |[T_k(l_k, \lambda)]_{21}|, |[T_k(l_k, \lambda)]_{22}| \}$$

for each $k \in \{2, \dots, m-1\}$. This ensures $|M_{11}| > 3 \max\{|M_{12}|, |M_{21}|, |M_{22}|\}$ for the product matrix $M = \prod_{k=m-1}^2 T_k(l_k, \lambda)$. Consequently, $h(\lambda) \neq 0$. \square

We can omit condition (3.14) if there are less than 3 sections. If all $\kappa_k = 0$ for $k = \{2 \dots m-1\}$, we can replace (3.14) by $\operatorname{Re} \lambda < \operatorname{Re} \beta_k - \varrho_k$ for $k = 2 \dots m-1$.

Note that the lower bound of the strip \mathcal{S} constructed in Lemma 3.2 is logarithmic in $|r_0|$ and $|r_L|$ instead of $\sim |r_0|^{-1}, |r_L|^{-1}$ and has a moderate magnitude even for small r_0, r_L . Thus, the strip \mathcal{S} and the balls in (3.16) are separated for realistic parameter values (see Fig. 3.1). This allows to construct spectral projections onto H -invariant closed subspaces.

In order to simplify the notations in the next theorem we assume:

(H) The balls of (3.15) do not intersect with the balls of (3.16).

Theorem 3.3 lists the spectral properties of H under Assumption (H) and shows that the growth properties of $T(t)$ are determined by the eigenvalues of the non-selfadjoint operator H at least in the dominant H -invariant subspace.

Theorem 3.3 (Spectral properties of H) *Assume (H). There exists a X -automorphism J with the following properties:*

$X_P = J(\{0\} \times \mathbb{L}^2([0, L]; \mathbb{C}^2))$ and $X_E = J(\mathbb{L}^2([0, L]; \mathbb{C}^2) \times \{0\})$ are closed H -invariant subspaces. $H_P = H|_{X_P}$ is a bounded operator. For any $\gamma_P < \min_{k=1 \dots m} \Gamma_k - \varrho_k$ there exists a constant M_P such that $T_P(t) = T(t)|_{X_P}$ is bounded by

$$\|T_P(t)\| \leq M_P e^{-\gamma_P t}. \quad (3.24)$$

The spectrum of $H_E = H|_{X_E}$ is a countable set of geometrically simple eigenvalues λ_j ($j \in \mathbb{Z}$) of finite algebraic multiplicity. All but finitely many λ_j are algebraically simple. Defining

$$\xi_j := \frac{1}{L} \left(\sum_{k=1}^m \beta_k l_k - \frac{1}{2} \log(r_0 r_L) + j\pi i \right), \quad (3.25)$$

we can number the sequence λ_j in a way such that

$$\lambda_j - \xi_j = O(|j|^{-1}) \quad \text{for } |j| \rightarrow \infty, \quad (3.26)$$

counting algebraically multiple eigenvalues λ_j repeatedly. There exists a set of generalized eigenvectors $b_j = (\varphi_j, p_j)$ corresponding to λ_j such that $\{J^{-1}b_j\}$ is an orthonormal basis of $\mathbb{L}^2([0, L]; \mathbb{C}^2) \times \{0\}$.

Proof: We introduce the parametric family of operators

$$H_\theta = \begin{pmatrix} \sigma\partial_z + \beta - i\kappa\sigma_c & \theta\rho \\ \theta\Gamma & (i\Omega_r - \Gamma) \end{pmatrix}$$

for $\theta \in [0, 1]$. The domain of H_θ is Y for all $\theta \in [0, 1]$. All H_θ are generators of C_0 semigroups $T_\theta(t) : X \rightarrow X$. The semigroups $T_\theta(t)$ depend continuously on θ for bounded intervals of t . The characteristic functions $h_\theta(\lambda)$ are defined in $\mathbb{C} \setminus \mathcal{W}$ and have the form (3.9) for all θ where $\mu_k = \lambda - \theta^2\chi_k(\lambda) - \beta_k$ in (3.8). Moreover, we can choose the strip \mathcal{S} and the balls in (3.15) and (3.16) independent of $\theta \in [0, 1]$. Thus, the intersection \mathcal{R} of the resolvent sets of all H_θ is nonempty and the resolvents $(\lambda Id - H_\theta)^{-1} : X \rightarrow X$ depend continuously on θ uniformly for compact subsets \mathcal{R} . Let γ be a closed rectifiable curve within \mathcal{R} around the balls $B_{\rho_k}(i\Omega_{r,k} - \Gamma_k)$ ($k = 1 \dots m$). Define the θ -dependent spectral projection

$$P_\theta x = \frac{1}{2\pi i} \oint_\gamma (\lambda Id - H_\theta)^{-1} x d\lambda \quad (3.27)$$

splitting X into the H_θ -invariant closed subspaces

$$X_{-, \theta} = \text{rg } P_\theta \quad (3.28)$$

$$X_{+, \theta} = \text{ker } P_\theta \quad (3.29)$$

and set $X_P = X_{-,1}$ and $X_E = X_{+,1}$. Then, H_0 is decoupled. We have:

- $X_{-,0} = \{0\} \times \mathbb{L}^2([0, L]; \mathbb{C}^2)$ and $H_{-,0} := H_0|_{X_{-,0}} = i\Omega_r - \Gamma$. Hence, $\text{spec } H_{-,0} = \mathcal{W}$ and $H_{-,0}$ is bounded.
- $X_{+,0} = \mathbb{L}^2([0, L]; \mathbb{C}^2) \times \{0\}$ and $H_{+,0} := H_0|_{X_{+,0}} = \sigma\partial_z + \beta - i\kappa$ defined in $\{\psi \in \mathbb{H}^1([0, L]; \mathbb{C}^2) : \psi \text{ satisfying (3.1)}\}$. [20], [36], [37] have shown:

$\text{spec } H_{+,0}$ is a countable set of geometrically simple eigenvalues $\lambda_{0,j}$ of finite algebraic multiplicity. All but finitely many $\lambda_{0,j}$ are algebraically simple. For $|j| \rightarrow \infty$, $\lambda_{0,j} - \xi_j = O(|j|^{-1})$ counting algebraically multiple $\lambda_{0,j}$ repeatedly. There exists a set of generalized eigenvectors $\varphi_{0,j} = Le_j$ associated to $\lambda_{0,j}$ such that L is a \mathbb{L}^2 -automorphism and $\{e_j\}$ is an orthonormal basis of $\mathbb{L}^2([0, L]; \mathbb{C}^2)$.

Hence, all assertions of the theorem are valid at the point $\theta = 0$ for the X -automorphism $\begin{pmatrix} L & 0 \\ 0 & Id \end{pmatrix}$. We have to confirm that they are preserved along the path to $\theta = 1$.

The projections P_θ and $Q_\theta = Id - P_\theta$ are continuous in θ . Define a sufficiently fine mesh $\{\theta_l : l = 0 \dots l_{\max}, \theta_0 = 0, \theta_{l_{\max}} = 1\}$ on $[0, 1]$ such that $\|P_{\theta_l} - P_{\theta_{l-1}}\| < 1$ for all $l \in \{1 \dots l_{\max}\}$. Then, $J_l = Q_{\theta_{l-1}} + P_{\theta_l}$ is an automorphism in X . The concatenation $J_P = \prod_{l=l_{\max}}^1 J_l$ maps $\text{rg } P_0 = \{0\} \times \mathbb{L}^2([0, L]; \mathbb{C}^2)$ onto X_P . H_P is a bounded operator since its spectrum is in the interior of γ . We define

$$Jx = J_P x \quad \text{for } x \in \{0\} \times \mathbb{L}^2([0, L]; \mathbb{C}^2). \quad (3.30)$$

Moreover, the resolvent of H_θ is a compact perturbation of the map $(\psi, p) \rightarrow (0, (\lambda - i\Omega_r + \Gamma)^{-1}p)$. Thus, P_θ is a compact perturbation of $\begin{pmatrix} 0 & 0 \\ 0 & Id \end{pmatrix}$, and the X -automorphism J_P is a compact perturbation of Id .

The spectrum of H_P is discrete outside of \mathcal{W} , it is located inside of γ and can accumulate only in points of \mathcal{W} . Consequently, the growth of $T_P(t) = \exp(H_P t)$ in X_P is bounded according to (3.24).

The spectrum of H_E is situated within the set \mathcal{C} : the union of the strip \mathcal{S} and the balls (3.15). Hence, it is a countable set of eigenvalues λ_j which are the roots of $h = h_1$ within \mathcal{C} . Therefore, the λ_j have finite algebraic multiplicity. If (φ, p) is an eigenvector associated to λ_j , then φ is a multiple of $T(z, 0; \lambda) \begin{pmatrix} r_0 \\ 1 \end{pmatrix}$. Thus, all eigenvalues are geometrically simple. Define

$$\tilde{h}(\lambda) = r_0 r_L e^{-2L\lambda + 2\sum_{k=1}^m \beta_k l_k} - 1.$$

The values ξ_j ($j \in \mathbb{Z}$) are the simple roots of \tilde{h} which is π/L -periodic in $\text{Im } \lambda$. Asymptotically, we have

$$h_\theta(\lambda) - \tilde{h}(\lambda) = O(|\text{Im } \lambda|^{-1}) \text{ for } |\text{Im } \lambda| \rightarrow \infty \text{ and } \lambda \in \mathcal{C}$$

uniformly for all $\theta \in [0, 1]$. Hence, $h_\theta(\lambda) - h_0(\lambda) = O(|\text{Im } \lambda|^{-1})$ for all θ . This leads to the one-to-one correspondence of the roots of h_θ and h_0 within \mathcal{C} and the convergence asserted in (3.26) since no root crosses the boundary of \mathcal{C} for varying θ and h_θ is analytic in \mathcal{C} .

Last, we define how J maps $\mathbb{L}^2([0, L]; \mathbb{C}^2) \times \{0\}$ onto X_E . The one-to-one correspondence between the eigenvalues $\lambda_{0,j}$ and λ_j in \mathcal{C} results in a one-to-one correspondence between the sets of generalized eigenvectors $\{(\varphi_{0,j}, 0)\}$ on one hand, and $b_j = (\varphi_j, p_j)$ on the other hand. All $\lambda_{0,j}$ and λ_j with large imaginary part are simple eigenvalues. For sufficiently large $|j|$, we have $\varphi_j = T(z, 0; \lambda) \begin{pmatrix} r_0 \\ 1 \end{pmatrix}$ implying the asymptotics

$$\|\varphi_j - \varphi_{0,j}\| = O(|\text{Im } \lambda_j|^{-1}) = O(|j|^{-1}) \text{ for } |j| \rightarrow \infty$$

in the \mathbb{L}^2 -norm. Consequently,

$$\|b_j - (\varphi_{0,j}, 0)\| = O(|j|^{-1}) \text{ for } |j| \rightarrow \infty. \quad (3.31)$$

The set $\{b_j\}$ is ω -linearly independent and satisfies

$$\sum_{j \in \mathbb{Z}} \|b_j - (\varphi_{0,j}, 0)\|^2 < \infty.$$

Therefore, there exists a X -automorphism J_E mapping each $(\varphi_{0,j}, 0)$ onto b_j of the form $J_E = Id - K$ where K is a compact linear operator [27].

We define

$$Jx = J_E(Lx_1, 0) \quad \text{for } x = (x_1, 0) \in \mathbb{L}^2([0, L]; \mathbb{C}^2) \times \{0\}. \quad (3.32)$$

(3.30) and (3.32) define a linear map of Fredholm index 0 from X into X . It is injective from $\{0\} \times \mathbb{L}^2([0, L]; \mathbb{C}^2)$ onto X_P and it maps $\mathbb{L}^2([0, L]; \mathbb{C}^2) \times \{0\}$ into X_E . Since J_E is injective and $X_E \cap X_P = \{0\}$, J is injective. Hence J is an X -automorphism. \square

Remarks

- If Assumption (H) is not valid, we can choose the curve γ around the balls $B_{\varrho_k}(i\Omega_{r,k} - \Gamma_k)$ ($k = 1 \dots m$) and the balls (3.15). This leads to the same statements as in Theorem 3.3 but with a slightly different decomposition $X = X_P \oplus X_E$: There exists a decomposition $\mathbb{L}^2([0, L]; \mathbb{C}^2) = U \oplus V$ ($\dim V < \infty$) such that the X -automorphism J maps a subspace $U \times \{0\}$ onto X_E and $V \times \mathbb{L}^2([0, L]; \mathbb{C}^2)$ onto X_P . Moreover, $\gamma_P = \min_{k=1 \dots m}(\Gamma_k) - \varrho_1 - \varrho_m - 2$.
- A remark about the structure of X_P and H_P : Let $\delta > 0$. There exists a decomposition

$$X_P = X_{P,f} \oplus \bigoplus_{\omega \in \mathcal{W}} X_\omega$$

where $X_{P,f}$ is spanned by generalized eigenvectors of H_P ($\dim X_{P,f} < \infty$) and the spectral radii of $(H + \omega Id)|_{X_\omega}$ are less than δ for each $\omega \in \mathcal{W}$.

- The number $\text{Re } \xi_0$ is the asymptotic growth rate approached by the real parts of the eigenvalues λ of H for $\text{Im } \lambda \rightarrow \infty$.

Corollary 3.4 *Let $\gamma > \text{Re } \xi_0$. Then, X can be decomposed into two $T(t)$ -invariant subspaces*

$$X = X_+ \oplus X_-$$

where X_+ is at most finite-dimensional and spanned by the generalized eigenvectors associated to the eigenvalues of H in the right half-plane $\{\lambda \in \mathbb{C} : \text{Re } \lambda \geq \gamma\}$. The restriction of $T(t)$ to X_- is bounded according to

$$\|T(t)|_{X_-}\| \leq M_\eta e^{\eta t} \quad \text{for } t \geq 0 \quad (3.33)$$

for any $\eta \in (\sup [\text{Re spec } (H|_{X_-})], \gamma)$ and any norm which is equivalent to the X -norm.

Remarks

- The growth rate η does not depend on the particular norm chosen for the inequality (3.33) (as long as it is equivalent to the X -norm) but M_η does. We have to choose a norm such that the magnitude of εM_η is small for realistic values of the singular perturbation parameter ε . The generalized eigenvectors b_j of H (see Theorem 3.3) induce an appropriate norm in the H -invariant subspace X_E . The original \mathbb{L}^2 -norm gives a constant M_η of order $\sqrt{|r_0 r_L|}^{-1}$ which can be very large.
- The eigenvalues of H can be computed numerically by solving the complex equation $h(\lambda) = 0$. The eigenvalues of H_E form the sequence ξ_j for $\kappa = 0$, $\rho = 0$ (see Theorem 3.3). We obtain the roots of the actual characteristic function h by following along the parameter path $\theta \kappa$, $\theta \rho$ for $\theta \in [0, 1]$.
- The simple eigenvectors corresponding to the eigenvalues of H are usually referred to as the (longitudinal) *modes* of the laser.

3.3 Existence and Properties of the Finite-dimensional Center-unstable Manifold

The *off-state* $x = 0$, $n_k = I_k \tau_k$ is an equilibrium of system (3.2), (3.4) for $\varepsilon \neq 0$. It is located in \mathcal{E} and asymptotically stable if all $I_k \tau_k$ are small due to the results of section 3.2. However, we are not interested in the behavior of the semiflow $S(t; \cdot)$ in the vicinity of the off-state but near the *on-states*. System (3.2), (3.4) has a rotational symmetry. That is, if $(x(t), n(t))$ is a solution, then $(e^{i\varphi} x(t), n(t))$ is also a solution for every $\varphi \in [0, 2\pi)$. Thus, we have the following class of rotating-wave solutions:

Definition 3.5 *The solution $(x(t), n(t))$ of (3.2), (3.4) is an on-state if $n(t) = n_0$ is constant in time and $x(t, z) = e^{i\omega t} x_0(z)$ where $x_0 \in Y \subset X$ is referred to as the amplitude and $\omega \in \mathbb{R}$ as the frequency of the on-state.*

$(e^{i\omega t} x_0(z), n_0)$ is an on-state if $i\omega$ is an eigenvalue of $H(n_0)$, x_0 is a multiple of the corresponding scaled eigenvector (ψ, p) and if there exists a $S > 0$ such that

$$\varepsilon F_k(n_{0,k}) = S^2 P g_k(n_{0,k})[(\psi, p), (\psi, p)] \quad \text{for all } k \in \mathcal{A}.$$

See Lemma 3.1 for the necessary spectral properties of H . Lemma 3.1 shows also that $g_k(n_{0,k})[(\psi, p), (\psi, p)] > 0$ for at least one k . Therefore, the variation of the parameter ε affects the on-states $(e^{i\omega t} x_0(z), n_0)$ only by scaling the amplitude $S = \|x_0\|$. The frequency ω , the geometric shape (ψ, p) and n_0 do not depend on ε .

The scaling factor P in the carrier density equation (3.4) determines the typical scale of $\|x_0\|$. By choosing $P = 1$, we ensure that all on-states have an amplitude of order $O(\sqrt{\varepsilon})$.

Subsequently, we are interested in the dynamics near the on-states. Hence, we may restrict our analysis to solutions $(x(t), n(t))$ whose amplitude $\|x\|$ does not exceed the amplitude of the on-states significantly

$$\|x(t)\| \leq C\sqrt{\varepsilon} \quad \text{for some fixed } C \text{ and all } t \geq 0. \quad (3.34)$$

That is, we focus on the dynamics of system (3.2), (3.4) near \mathcal{E} . We should remark that large-amplitude oscillations will not be detected due to this restriction.

We will now introduce some notation and formulate the conditions which are necessary to apply the results of invariant manifold theory formulated in [10], [11], [19], [47], [49].

The results of section 3.2 show that all eigenvalues of $H(n)$ are in the left half-plane if $n_k \leq 1$ for all $k \in \mathcal{A}$. Then, $T_n(t)$ decays in the whole space X . However, for larger n_k a finite number of eigenvalues must cross the imaginary axis. This allows for the following considerations. Let $\mathcal{K} \subset \mathbb{R}^{m_a}$ be a compact set with the following properties:

(H1) \mathcal{K} is simple, i. e., either a single point or homeomorphic to a closed ball.

(H2) $\text{spec } H(n)$ can be split into two parts for all $n \in \mathcal{K}$:

$$\begin{aligned} \text{spec } H(n) &= \sigma_{cu}(n) \cup \sigma_s(n) \quad \text{where} \\ \text{Re } \sigma_{cu}(n) &\geq 0 \\ \text{Re } \sigma_s(n) &< -\gamma_s \end{aligned}$$

and the number q of elements of $\sigma_{cu}(n)$ counted according to their algebraic multiplicity is positive and finite. Moreover, $\gamma_s > 0$ is independent of $n \in \mathcal{K}$.

Consequently, q is also independent of $n \in \mathcal{K}$. Furthermore, (H1) and (H2) and the results of section 3.2 imply that there exists an open neighborhood U of \mathcal{K} which is diffeomorphic to an open ball in \mathbb{R}^{m_a} such that:

- $\text{spec } H(n)$ can be split into $\sigma_{cu}(n)$ and $\sigma_s(n)$ for all $n \in U$ such that $\text{Re } \sigma_s(n) < -\gamma_s$ and $\text{Re } \sigma_{cu}(n) > -\gamma_s$.
- There exists a decomposition of X into $H(n)$ -invariant subspaces

$$X = X_s(n) \oplus X_{cu}(n)$$

associated to $\sigma_{cu}(n)$ and $\sigma_s(n)$ depending smoothly on n for all $n \in U$. The complex dimension of X_{cu} is q .

We introduce the according spectral projections for $H(n)$ by $P_{cu}(n)$ and $P_s(n)$. P_{cu} and P_s depend smoothly on n . The spectra of the restrictions of $H(n)$ satisfy

$$\begin{aligned} \text{Re}(\text{spec } H(n)|_{X_{cu}}) &> -\gamma_s \\ \text{Re}(\text{spec } H(n)|_{X_s}) &< -\gamma_s \end{aligned}$$

for all $n \in U$. Let $B(n) : \mathbb{C}^q \rightarrow X_{cu}$ be a smooth basis of X_{cu} introducing \mathbb{C}^q -coordinates in X_{cu} .

Corollary 3.4 ensures that the semigroup $T_n(t)$ generated by $H(n)$ restricted to $X_s(n)$ has a decay rate γ_s which is uniform for all $n \in U$:

$$\|T_n(t)x\| \leq M_s e^{-\gamma_s t} \|x\| \quad \text{for all } n \in U, x \in X_s(n), t \geq 0.$$

We introduce coordinates $x = B(n)x_{cu} + x_s$ decomposing X using the projections P_{cu} and P_s . That is, x_{cu} represents the *critical-unstable* part $P_{cu}x \in X_{cu}$ in the basis B , and x_s is the *stable* part $P_s x$. Then, a decomposition of (3.2), (3.4) by P_{cu} and P_s implies that $x_{cu} \in \mathbb{C}^q$, $x_s \in X_s \subset X$, and $n \in \mathbb{R}^{m_a}$ satisfy the system

$$\frac{d}{dt} x_{cu} = g_{cu}(x_{cu}, x_s, n, \varepsilon) \tag{3.35}$$

$$= A_{cu}(n)x_{cu} + a_{11}(x_{cu}, x_s, n, \varepsilon)x_{cu} + a_{12}(x_{cu}, x_s, n, \varepsilon)x_s$$

$$\frac{d}{dt} x_s = g_s(x_{cu}, x_s, n, \varepsilon) \tag{3.36}$$

$$= A_s(n)x_s + a_{21}(x_{cu}, x_s, n, \varepsilon)x_{cu} + a_{22}(x_{cu}, x_s, n, \varepsilon)x_s$$

$$\frac{d}{dt} n = f(x_{cu}, x_s, n, \varepsilon) \tag{3.37}$$

where $A_{cu}, a_{11} : \mathbb{C}^q \rightarrow \mathbb{C}^q$, $a_{12} : X \rightarrow \mathbb{C}^q$, $a_{21} : \mathbb{C}^q \rightarrow X$, $a_{22} : X \rightarrow X$, $A_s : Y \rightarrow X$ are linear operators defined by

$$\begin{aligned} A_{cu}(n) &= B^{-1}HP_{cu}B & A_s(n) &= HP_s - 2\gamma_s P_{cu} \\ a_{11}(x_{cu}, x_s, n, \varepsilon) &= -B^{-1}P_{cu}\partial_n Bf & a_{12}(x_{cu}, x_s, n, \varepsilon) &= B^{-1}\partial_n P_{cu}fP_s \\ a_{21}(x_{cu}, x_s, n, \varepsilon) &= -P_s\partial_n Bf & a_{22}(x_{cu}, x_s, n, \varepsilon) &= -P_{cu}\partial_n P_{cu}fP_s \\ f_k(x_{cu}, x_s, n, \varepsilon) &= \varepsilon F_k(n_k) - P g_k(n_k)[Bx_{cu} + x_s, Bx_{cu} + x_s] \text{ for } k \in \mathcal{A}. \end{aligned}$$

We introduced the term $-2\gamma_s P_{cu}x_s$ which is 0 for $x_s \in X_s$ artificially in (3.36). System (3.35)–(3.37) couples an ordinary differential equation in \mathbb{R}^{m_a} , an ordinary differential equation in \mathbb{C}^q , and an evolution equation in X . The semiflow induced by (3.35)–(3.37) is properly defined as long as $n(t)$ stays in the neighborhood U of \mathcal{K} . It has the invariant set $\mathcal{S} = \{(x_{cu}, x_s, n) \in \mathbb{C}^q \times X \times \mathbb{R}^{m_a} : x_s \in X_s(n)\}$ due to

$$\frac{d}{dt}(P_{cu}x_s) = (\partial_n P_{cu}f - 2\gamma_s Id)(P_{cu}x_s). \quad (3.38)$$

and is equivalent to $S(t, \cdot)$ in \mathcal{S} . The right-hand-sides of (3.35)–(3.37) satisfy for all $n \in U$:

$$\begin{aligned} g_{cu}(0, 0, n, 0) &= 0 & \partial_n g_{cu}(0, 0, n, 0) &= 0 \\ g_s(0, 0, n, 0) &= 0 & \partial_n g_s(0, 0, n, 0) &= 0 \\ f(0, 0, n, 0) &= 0 & \partial_n f(0, 0, n, 0) &= 0 \end{aligned}$$

The linearization (3.5) of $S(t, \cdot)$ reads in the coordinates $(x_{cu}, x_s, n, \varepsilon)$ as follows (at $x_{cu} = 0$, $x_s = 0$, $n \in U$ and $\varepsilon = 0$):

$$\begin{aligned} \frac{d}{dt}x_{cu} &= A_{cu}(n)x_{cu} \\ \frac{d}{dt}x_s &= A_s(n)x_s \\ \frac{d}{dt}n &= 0. \end{aligned} \quad (3.39)$$

The operators A_{cu} and A_s are the restrictions of $H(n)$ onto its invariant subspaces X_{cu} and X_s . Hence, the assertion (H2) about the spectrum of H ensures that $\text{Re}(\text{spec } A_{cu}(n)) \geq 0$ and the C_0 semigroup generated by $A_s(n)$ decays with the rate γ_s in X for all $n \in \mathcal{K}$.

Exploiting that $S(t; \cdot)$ is locally a flow, we define:

Definition 3.6 *A manifold \mathcal{M} is called S -invariant relative to the bounded open set \mathcal{N} if for any $m \in \mathcal{M} \cap \mathcal{N}$ we have $S(t; m) \in \mathcal{M}$ for all $t \in \mathbb{R}$ satisfying $S(t; m) \in \mathcal{N}$.*

The existence theorems for normally hyperbolic invariant manifolds stated in [10], [11], [19], [49], [47] apply to the particular situation presented in this section:

Theorem 3.7 *Assume (H1), (H2). Let $k > 0$ be an integer number. Let U' be a sufficiently small open neighborhood of \mathcal{K} and the numbers $r_{cu} > 0$, $r_s > 0$, $\varepsilon_0 > 0$ be sufficiently small. Then, there exists a manifold \mathcal{C}_{cu} with the following properties:*

1. \mathcal{C}_{cu} can be represented as the graph of a C^k function $x_s = \xi(x_{cu}, n, \varepsilon)$ in $D(\xi) = \{(x_{cu}, n, \varepsilon) : \|x_{cu}\| < r_{cu}, n \in U', \varepsilon \in [0, \varepsilon_0]\}$.
2. \mathcal{C}_{cu} is S -invariant relative to the open bounded set $\mathcal{N} = \{(x_{cu}, x_s, n) : \|x_{cu}\| < r_{cu}, \|x_s\| < r_s, n \in U'\}$ if $\varepsilon < \varepsilon_0$.
3. Let $u \in \mathcal{N}$ be such that $S(t; u) \in \mathcal{N}$ for all $t \geq 0$. Then, there exists a $u_c \in \mathcal{C}_{cu}$ such that $\|S(t; u) - S(t; u_c)\|$ decays exponentially.
4. $\xi(x_{cu}, n, \varepsilon) \in X_s(n) \cap Y$ for all $(x_{cu}, n, \varepsilon) \in D(\xi)$, the flow on \mathcal{C}_{cu} is C^1 in time, and is governed by

$$\begin{aligned} \frac{d}{dt}x_{cu} &= A_{cu}(n)x_{cu} + a_{11}(x_{cu}, \xi, n, \varepsilon)x_{cu} + a_{12}(x_{cu}, \xi, n, \varepsilon)\xi \\ \frac{d}{dt}n &= f(x_{cu}, \xi(x_{cu}, n, \varepsilon), n, \varepsilon). \end{aligned} \tag{3.40}$$

5. For $k \geq 3$, ξ can be expanded to

$$\xi(x_{cu}, n, \varepsilon) = (O(\|x_{cu}\|^2) + O(\varepsilon))x_{cu}. \tag{3.41}$$

Proof:

Invariance and Representation

The statements 1–3 are a direct consequence of the results of [10], [11] except for the higher order $k > 1$ of smoothness for ξ . Indeed, the situation is much simpler than in [10], [11] since X is a Hilbert space, and the coordinates for the unperturbed invariant manifold are global and known explicitly.

Firstly, we append the dummy equation (3.6) to (3.35)–(3.37) and (3.39) and extend the semiflow $S(t; \cdot)$ accordingly. Let S_0 be the semiflow induced by (3.39), (3.6). Then, $S(t_1; \cdot)$ is a C^1 small perturbation of $S_0(t_1; \cdot)$ for any finite t_1 . $S_0(t; \cdot)$ has the finite-dimensional normally hyperbolic invariant manifold $\mathcal{C}_0 = \{(x_{cu}, x_s, n, \varepsilon) : x_s = 0, n \in U\}$ (see appendix B for the precise definition of normal hyperbolicity; its conditions are satisfied due to $\text{Re spec } A_s(n) < -\gamma_s < \text{Re spec } A_{cu}(n)$ for all $n \in U$ in (3.39)).

We choose an open bounded set $\tilde{\mathcal{N}} = \{(x_{cu}, x_s, n, \varepsilon) : \|x_{cu}\| < r_{cu}, \|x_s\| < r_s, n \in U' \subseteq U, |\varepsilon| < \varepsilon_0\}$ and modify the right-hand-side of (3.39), (3.6) for $u \notin \mathcal{N}$ such that \mathcal{C}_0 becomes compact. We can do so smoothly since X is a Hilbert space. If we choose $\tilde{\mathcal{N}}$ sufficiently small, the perturbation $S_0 \rightarrow S$ gets sufficiently small. According to [10] (see appendix B), \mathcal{C}_0 persists under the perturbation $S_0 \rightarrow S$. Denote the perturbed manifold by $\tilde{\mathcal{C}}_{cu}$. We can represent $\tilde{\mathcal{C}}_{cu}$ as a graph $x_s = \xi(x_{cu}, n, \varepsilon)$ in $\tilde{\mathcal{N}}$ since it is a C^1 small perturbation of \mathcal{C}_0 . The same graph ξ is also the representation of the manifold \mathcal{C}_{cu} claimed in the theorem. \mathcal{N} is the corresponding restriction of $\tilde{\mathcal{N}}$.

Stability

Moreover, $\tilde{\mathcal{C}}_{cu}$ has a center-stable manifold \mathcal{C}_{cs} in a sufficiently small r_s -neighborhood of $\tilde{\mathcal{C}}_{cu}$ (according to [10], see appendix B). \mathcal{C}_{cs} is characterized as the set of all u which

stay in the neighborhood of $\tilde{\mathcal{C}}_{cu}$ for all $t \geq 0$. According to [11], \mathcal{C}_{cs} is decomposed into an invariant family of foliations (stable fibers) (see appendix B). This implies statement 3.

Higher Orders of Smoothness

The only open question is the C^k smoothness of $\tilde{\mathcal{C}}_{cu}$ for $k \geq 2$. The unperturbed manifold \mathcal{C}_0 is C^∞ . Then, we may use exactly the procedure outlined in [49] to find the higher order derivatives of ξ inductively (since X is a Hilbert space, $\tilde{\mathcal{C}}_{cu}$ is compact and finite-dimensional, and we have a global coordinate representation). The domain of definition for ξ shrinks for increasing k .

Flow on \mathcal{C}_{cu}

Due to (3.38), we have $P_s(n)x_s = 0$ if $(x_{cu}, x_s, n, \varepsilon) \in \mathcal{C}_{cu}$, i. e., $x_s = \xi(x_{cu}, n, \varepsilon)$ in \mathcal{N} . Hence, $\xi(x_{cu}, n, \varepsilon) \in X_s(n)$ for all $(x_{cu}, n, \varepsilon) \in D(\xi)$. The solutions in \mathcal{C}_{cu} have the form

$$(x(t), n(t)) = (B(n(t))x_{cu}(t) + \xi(x_{cu}(t), n(t), \varepsilon), n(t))$$

where x_{cu} and n satisfy the system

$$\begin{aligned} \frac{d}{dt}x_{cu} &= g_{cu}(x_{cu}, \xi(x_{cu}, n, \varepsilon), n, \varepsilon) \\ &= A_{cu}(n)x_{cu} + a_{11}(x_{cu}, \xi, n, \varepsilon)x_{cu} + a_{12}(x_{cu}, \xi, n, \varepsilon)\xi \\ \frac{d}{dt}n &= f(x_{cu}, \xi(x_{cu}, n, \varepsilon), n, \varepsilon). \end{aligned}$$

Since $\xi \in C^1$ with respect to its arguments, $\frac{d}{dt}\xi(x_{cu}(t), n(t), \varepsilon)$ exists and is continuous. Hence, all solutions in \mathcal{C}_{cu} are classical solutions in the sense of Definition 2.1, and $\xi(x_{cu}, n, \varepsilon) \in Y = D(H(n)) = D(A_s(n))$.

Expansion of ξ

The slow manifold $\mathcal{E} = \{(x, n) \in X \times \mathbb{R}^{m_a} : x = 0\}$ is invariant (and still slow) even for $\varepsilon > 0$. Hence, it is a subset of \mathcal{C}_{cu} , i. e., $\xi(0, n, \varepsilon) = 0$ for all n and ε . Since $\xi \in C^1$, we can write ξ as

$$\xi(x_{cu}, n, \varepsilon) = \nu(x_{cu}, n, \varepsilon)x_{cu} \tag{3.42}$$

where $\nu(x_{cu}, n, \varepsilon) = \int_0^1 \partial_{x_{cu}}\xi(sx_{cu}, n, \varepsilon)ds$ is bounded and continuous in $D(\xi)$. Furthermore, we obtain

$$A_s\xi + a_{21}x_{cu} + a_{22}\xi = \partial_{x_{cu}}\xi \cdot (A_{cu}x_{cu} + a_{11}x_{cu} + a_{12}\xi) + \partial_n\xi f \tag{3.43}$$

since $\mathcal{C}_{cu} = \{(x_{cu}, x_s, n) \in \mathcal{N} : x_s = \xi(x_{cu}, n, \varepsilon)\}$ is invariant with respect to $S(t, \cdot)$ (note that $\xi \in Y = D(A_s(n))$). Assume that ξ is sufficiently smooth. Then, we can insert (3.42) into (3.43) and differentiate with respect to x_{cu} in the point $x_{cu} = 0, \varepsilon = 0$. We obtain $A_s(n)\nu(0, n, 0) = \nu(0, n, 0)A_{cu}(n)$. Hence, $\nu(0, n, 0) = 0$. Differentiating (3.43) twice with respect to x_{cu} in $x_{cu} = 0, \varepsilon = 0$, we compute $A_s(n)\partial_{x_{cu}}\nu(0, n, 0) = 2\partial_{x_{cu}}\nu(0, n, 0)A_{cu}(n)$. Hence, $\partial_{x_{cu}}\nu(0, n, 0) = 0$ and we can expand

$$\begin{aligned} \nu(x_{cu}, n, \varepsilon) &= O(\|x_{cu}\|^2) + O(\varepsilon) \\ \xi(x_{cu}, n, \varepsilon) &= (O(\|x_{cu}\|^2) + O(\varepsilon))x_{cu} \end{aligned}$$

if ξ is sufficiently smooth. □

Remarks

- If a solution of (3.2), (3.4) stays in \mathcal{N} for all $t \geq 0$, its long-time behavior can be approximated by a trajectory on \mathcal{C}_{cu} due to the exponential attractivity of \mathcal{C}_{cu} . Thus, it is sufficient to study the flow of the finite-dimensional system (3.40).
- If $A_{cu}(n)$ has a strictly positive eigenvalue for all $n \in U'$, one component of x_{cu} will increase exponentially. Hence, most trajectories of (3.40) leave $D(\xi)$ directly. Consequently, we choose the set $\mathcal{K} \in \mathbb{R}^{m_a}$ typically such that $\text{Re } \sigma_{cu} = 0$ (see condition (H2)). That means, e. g., \mathcal{K} is generically an isolated point n_0 (the *threshold carrier density*) if $m_a = 1$. Then, the manifold \mathcal{C}_{cu} is a local center manifold according to [14], [47], and U' is a small neighborhood of n_0 . If $m_a = 2$, \mathcal{K} is either a piece of a curve where one eigenvalue of $H(n)$ is on the imaginary axis and all other eigenvalues have negative real part, or it is an intersection point of two of these curves.
- The rotational symmetry of the system is reflected in ξ by

$$e^{i\varphi} \xi(x_{cu}, n, \varepsilon) = \xi(e^{i\varphi} x_{cu}, n, \varepsilon)$$

for all $\varphi \in [0, 2\pi)$. Thus, (3.40) is symmetric with respect to rotation of x_{cu} : if $(x_{cu}(t), n(t))$ is a solution of (3.40) then, $(e^{i\varphi} x_{cu}(t), n(t))$ is also a solution for all $\varphi \in [0, 2\pi)$.

Mode approximation Consider solutions of the system (3.2), (3.4), (3.6) in the cone $\|x\| \leq C\sqrt{\varepsilon}$ according to (3.34). Within this cone, we can scale up x to order $O(1)$ by setting the scaling factor P in the carrier density equation (3.4) to ε :

$$\begin{aligned} P_{\text{new}} &= \varepsilon & x_{cu, \text{new}} &= x_{cu, \text{old}} / \sqrt{\varepsilon} \\ x_{\text{new}} &= x_{\text{old}} / \sqrt{\varepsilon} & \xi_{\text{new}}(x_{cu, \text{new}}, n, \varepsilon) &= \nu(\sqrt{\varepsilon} x_{cu, \text{new}}, n, \varepsilon) x_{cu, \text{new}}. \end{aligned}$$

This scaling changes the carrier density equation to

$$\frac{d}{dt} n_k = \varepsilon f_k(n_k, x) = \varepsilon (F_k(n_k) - g_k(n_k)[x, x]). \quad (3.44)$$

The system (3.40) for the flow on \mathcal{C}_{cu} changes to:

$$\begin{aligned} \frac{d}{dt} x_{cu} &= A_{cu}(n)x_{cu} + \varepsilon a_{11}(x_{cu}, \xi, n)x_{cu} + \varepsilon a_{12}(x_{cu}, \xi, n)\xi \\ \frac{d}{dt} n &= \varepsilon f(x_{cu}, \xi(x_{cu}, n, \varepsilon), n) \end{aligned} \quad (3.45)$$

where $A_{cu}, a_{11} : \mathbb{C}^q \rightarrow \mathbb{C}^q$, $a_{12} : X \rightarrow \mathbb{C}^q$ are linear operators defined by

$$\begin{aligned} A_{cu}(n) &= B^{-1} H P_{cu} B & a_{11}(x_{cu}, \xi, n) &= -B^{-1} P_{cu} \partial_n B f \\ & & a_{12}(x_{cu}, \xi, n) &= B^{-1} \partial_n P_{cu} f P_s \end{aligned}$$

$$f_k(x_{cu}, \xi, n) = F_k(n_k) - g_k(n_k)[Bx_{cu} + \xi, Bx_{cu} + \xi] \text{ for } k \in \mathcal{A}.$$

Moreover, ξ changes such that its expansion (3.41) reads

$$\xi(x_{cu}, n, \varepsilon) = \varepsilon \nu(x_{cu}, n, \varepsilon) x_{cu} \quad (3.46)$$

where $\nu \in C^1$ if ξ is sufficiently smooth. Inserting (3.46) into system (3.45), we obtain that the expression $\nu(x_{cu}, n, \varepsilon) x_{cu}$ enters the system only with a factor ε^2 in front of it. Hence, replacing ξ by 0 is a regular small perturbation of (3.45), i. e., it is of order $O(\varepsilon^2)$ in the C^1 -norm. Moreover, the perturbation preserves the rotational symmetry of system (3.45). The approximate system is called *mode approximation* and reads

$$\frac{d}{dt}x = A_{cu}(n)x + \varepsilon a_{11}(x, n)x \quad (3.47)$$

$$\frac{d}{dt}n = \varepsilon f(x, n) \quad (3.48)$$

where $x \in \mathbb{C}^q$, and the matrices $A_{cu}(n), a_{11}(x, n) : \mathbb{C}^q \rightarrow \mathbb{C}^q$ are defined by

$$\begin{aligned} A_{cu}(n) &= B^{-1}(n)H(n)P_{cu}(n)B(n) \\ a_{11}(x, n) &= -B^{-1}(n)P_{cu}(n)\partial_n B(n)f(x, n) \\ f_k(x, n) &= F_k(n_k) - g_k(n_k)[B(n)x, B(n)x] \text{ for } k \in \mathcal{A}. \end{aligned}$$

The matrix A_{cu} is a representation of $H(n)$ restricted to its critical subspace $X_{cu}(n)$ in some basis $B(n)$. The matrix A_{cu} depends on the particular choice of the basis $B(n)$ but its spectrum coincides with the critical spectrum of $H(n)$. The term $\varepsilon a_{11}x$ appears since the space X_{cu} depends on time t .

Any normally hyperbolic invariant manifold (e. g. fixed point, periodic orbit, invariant torus) which is present in the dynamics of (3.47), (3.48) persists under the perturbation ξ . Hence, it is also present in system (3.45) describing the flow on the invariant manifold \mathcal{C}_{cu} and in the semiflow of the complete system (3.2), (3.4). Furthermore, its hyperbolicity and the exponential attractivity of \mathcal{C}_{cu} ensure its continuous dependence on small parameter perturbations.

4 Bifurcation Analysis of the Mode Approximations

The mode approximations derived in the previous chapter allow for detailed studies of their long-time behavior since they are low-dimensional ordinary differential equations. Several analytic and computational results have been obtained previously about the existence regions of *self-pulsations* ([6], [9], [44], [51]) and its synchronization properties [8] using the single-mode approximation (see section 4.1).

The particular form of system (3.47), (3.48) depends on the set \mathcal{K} of critical carrier densities n chosen in the construction of the center-unstable manifold \mathcal{C}_{cu} and its properties (H1)–(H3). Practically, only few constellations for \mathcal{K} are of interest and have been observed during numerical simulations of the PDE ([35], [50]). We focus on situations where the number of unstable eigenvalues of A_{cu} is 0. Hence, \mathcal{C}_{cu} is in fact an exponentially attracting center manifold. Moreover, we restrict our interest to cases where the number q of critical eigenvalues of H is less or equal to 2. The case $q = 2$ is treated in the limit of two critical eigenvalues with very different frequencies. Furthermore, multi-section-lasers are currently designed such that they consist of at most three sections and typically one but at most two of them active. Thus, we restrict to the cases where the number of sections $m = 3$ and only one equation for n_1 ($\mathcal{A} = \{1\}$) is present.

We obtain the coefficients of (3.47), (3.48) in the following manner:

We compute the critical eigenvalues numerically by continuing the roots λ_j of the characteristic function $h(\lambda)$ with respect to n (see section 3.2). If $\lambda \neq i\Omega_{r,k} - \Gamma_k$ for $k \in \{1 \dots m\}$, the corresponding eigenvector $x_j = (\psi_j, p_j)$ and the adjoint eigenvector $x_j^\dagger = (\psi_j^\dagger, p_j^\dagger)$ have the form (see [8], [51] for the adjoint)

$$\begin{pmatrix} \psi_j \\ p_j \end{pmatrix} = \begin{pmatrix} T(z, 0; \lambda_j) \begin{pmatrix} r_0 \\ 1 \end{pmatrix} \\ \frac{\Gamma}{\lambda_j - i\Omega_r + \Gamma} T(z, 0; \lambda_j) \begin{pmatrix} r_0 \\ 1 \end{pmatrix} \end{pmatrix} \quad \begin{pmatrix} \psi_j^\dagger \\ p_j^\dagger \end{pmatrix} = \begin{pmatrix} \begin{pmatrix} \bar{\psi}_{j,2} \\ \bar{\psi}_{j,1} \end{pmatrix} \\ \frac{\rho}{\Gamma} \begin{pmatrix} \bar{p}_{j,2} \\ \bar{p}_{j,1} \end{pmatrix} \end{pmatrix}. \quad (4.1)$$

We do not consider the degenerate case where a critical eigenvalue has algebraic multiplicity ≥ 2 . Hence, λ_j , x_j and x_j^\dagger depend smoothly on n . Moreover, we can scale x_j such that

$$(x_j^\dagger, x_j) = 1 \quad (4.2)$$

for all n under consideration. Then, we can choose (x_j^\dagger, \cdot) for the components of the spectral projector $B^{-1}P_{cu}$ in (3.47), (3.48) using the eigenbasis of $H|_{\mathcal{C}_{cu}}$ for B . Hence, $A_{cu}(n)$ is a diagonal matrix with $\lambda_j(n)$ in the diagonal. Subsequently, we refer to the components of B (which are eigenvectors of H) and x_{cu} as *modes* of H .

4.1 The Single Mode Case

Firstly, we consider a multi-section laser with one active section ($n = n_1 \in \mathbb{R}$) in the generic case where a single eigenvalue λ of $H(n)$ is on the imaginary axis ($q = 1$). Thus, the set \mathcal{K} of critical carrier densities consists of a single point

$n_0 > 1$. The mode approximation is valid in the vicinity of this point n_0 . We introduce $N = (n - n_0)/(n_0 - 1)$. The term a_{11} in (3.47) vanishes if we choose the corresponding eigenvector (ψ, p) according to (4.2). Moreover, we can decouple the phase of the complex x in (3.47) due to the rotational symmetry of the system. Hence, we have to analyse a two-dimensional system for $S = |x|^2$ and N which reads as follows:

$$\dot{S} = G(N)S \quad (4.3)$$

$$\dot{N} = \varepsilon (I - N - (1 + N)R(N)S) \quad (4.4)$$

where the coefficient functions are defined by

$$G(N) = 2 \operatorname{Re} \lambda(N) \quad (4.5)$$

$$(1 + N)R(N) = [g(N) - \rho(N) + \operatorname{Re}(\chi(N, \lambda(N)))] \|\psi(N)\|_1^2 \quad (4.6)$$

and the current is adjusted to

$$I = (I_1 - n_0)/(n_0 - 1)$$

Here, the definition for R exploits that the right-hand-side of (4.6) is zero at $N = -1$ (corresponding to $n = 1$). Moreover, we know that $G(0) = 0$. If λ crosses the imaginary axis transversally at $n = n_0$, we have $G'(0) > 0$. For typical parameter situations, the functions G and R look like depicted in Figure 4.1. The long-time behavior of (4.3), (4.4) has been investigated numerically by [44] using the models

$$G(N) = \alpha N \quad (4.7)$$

$$R(N) = 1 + \frac{AW^2}{(N - N_r)^2 + W^2} \quad (4.8)$$

for G and R where N_r represents the position of the peak in R visible in figure 4.1, A its height, and W its half width at half maximum. The bifurcation diagram of (4.3), (4.4) with respect to the primary bifurcation parameter N_r is reported in [44]. It shows a family of periodic orbits with a fold (see also Fig. 4.2). The stable branch of this type of periodic orbits is usually referred to as (single mode) *self-pulsations*. The motion is actually quasiperiodic taking the rotational velocity $\operatorname{Im} \lambda$ into account.

We pointed out in chapter 3 that the mode approximation is only valid within a bounded region of S . Hence, we have to perform a perturbation analysis for small ε to check if the amplitude of the periodic orbits of (4.3), (4.4) remains finite for $\varepsilon \rightarrow 0$. Besides, the perturbation analysis results in approximations for the Hopf points and the locations of the self-pulsations.

To this end, we transform (4.3), (4.4) into a small perturbation of a conservative

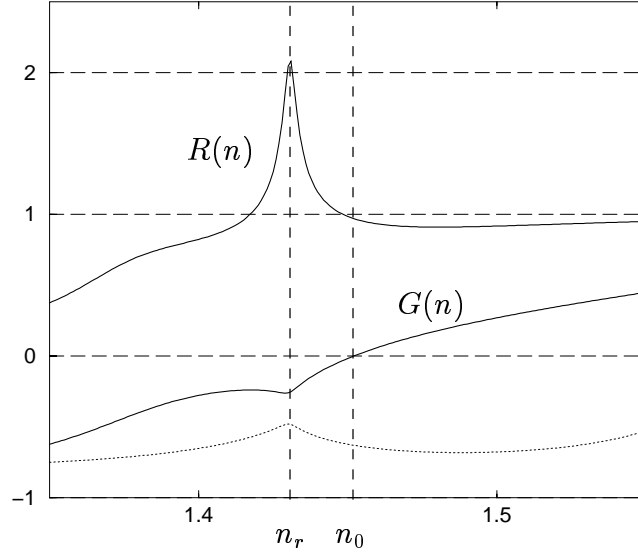


Figure 4.1: Typical shape of G and R with respect to the unscaled variable n . The position n_r and the height of the peak in R relative to the zero of G are the mathematical parameters determining the dynamics of system (4.3), (4.4) [44]. The dotted line is the function G for the eigenvalue nearest to λ . The models (4.7) and (4.8) fit the depicted functions with $N_r = -0.05$, $A = 1$, $W = 0.007$, $\alpha = 4$ (or $y_r = -0.83$, $w = 2$ for $\delta = 0.06$, $\varepsilon = 1/300$ in the rescaled system (4.10), (4.11), respectively).

oscillator: We introduce the scaled parameters and coefficient functions

$$\begin{aligned}
 \delta &= \sqrt{\varepsilon I / \alpha} & R(y, \delta, y_r) &= 1 + \frac{\delta^2 A w^2}{(y - y_r)^2 + \delta^2 w^2} \\
 y_r &= N_r / \delta & & & & (4.9) \\
 w &= W / \delta^2 & r(y, \delta, y_r) &= \frac{R(y, \delta, y_r)}{R(0, \delta, y_r)}
 \end{aligned}$$

the new state space variables

$$x = \log S - \log \left[\frac{I}{R(0, \delta, y_r)} \right] \quad y = N / \delta,$$

and introduce a new time $t_{\text{new}} = \sqrt{\alpha I \varepsilon} t_{\text{old}}$. The transformed system reads

$$\dot{x} = y \quad (4.10)$$

$$\dot{y} = 1 - \delta / I \cdot y - (1 + \delta y) r(y, \delta, y_r) \exp(x) \quad (4.11)$$

where $\delta = O(\sqrt{\varepsilon})$ is small. This scaling treats N and some of the original quantities as naturally small, i. e. $N = O(\sqrt{\varepsilon})$, $N_r = O(\sqrt{\varepsilon})$, and W even $O(\varepsilon)$. Other parameters (I and A) are considered as positive and of order 1. System (4.10), (4.11) is equivalent to (4.3), (4.4) in the invariant half-plane $\{S > 0\}$. The transformed

system (4.10), (4.11) has exactly one equilibrium $x = y = 0$. Changing y_r , a pair of complex eigenvalues of its linearization at 0 crosses the imaginary axis transversally at $y_{r,\pm}$ satisfying $\partial_{y_r} r(0, \delta, y_r) = -\delta(1 + I^{-1})$ which amounts to [44]

$$\frac{y_{r,\pm}}{\delta w} = -\frac{\delta^2 w(1 + I^{-1})}{2A} \left[\left(\frac{y_{r,\pm}}{\delta w} \right)^2 + 1 \right] \left[\left(\frac{y_{r,\pm}}{\delta w} \right)^2 + 1 + A \right]. \quad (4.12)$$

For fixed $I > 0$, $A > 0$ and $w > 0$, this equation has exactly two solutions $y_{r,+}$ and $y_{r,-}$ if the factor μ in front of the right-hand-side is small. These Hopf points can be approximated by

$$y_{r,-} \approx -\left(\frac{2\delta A w^2}{1 + I^{-1}} \right)^{\frac{1}{3}}, \quad y_{r,+} \approx -\delta^3 w^2 (1 + I^{-1}) \frac{1 + A}{2A}$$

by dropping terms of order $\mu^{2/3}$ (for $y_{r,-}$) or μ^2 (for $y_{r,+}$), respectively.

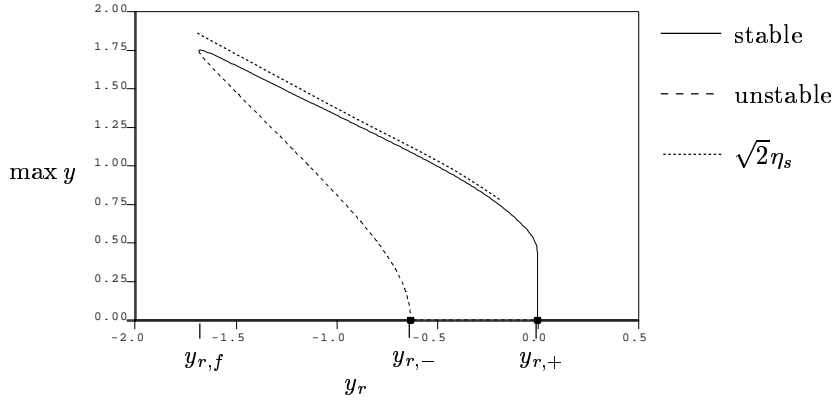


Figure 4.2: Bifurcation diagram for the scaled single mode approximation (4.10), (4.11). The parameters are as indicated in the caption of figure 4.1, and $I = 2$. The picture shows the two Hopf points $y_{r,\pm}$ and the family of periodic orbits with a fold at $y_{r,f}$. We report $\max y$ of the stable and unstable periodic orbits and of the critical energy level η_s of the conservative oscillator.

An important aspect is how the amplitude of the self-pulsations changes for $\delta \rightarrow 0$. As the mode approximation is only valid within a bounded region of x (or S in (4.3), respectively), we have to verify that the amplitudes of the self-pulsations remain bounded for $\delta \rightarrow 0$.

Consider system (4.10), (4.11) as a perturbation of the conservative oscillator $\ddot{x} = 1 - e^x$ (see [33] for references about the close to conservative nature of single mode models). The conserved quantity along the periodic orbits of the conservative oscillator is

$$E(x, y) = y^2/2 + e^x - x - 1.$$

$E(x, y) > 0$ if $(x, y) \neq 0$, $E(0, 0) = 0$, E is strictly monotone in $x^2 + y^2$ and $E \rightarrow \infty$ for $x^2 + y^2 \rightarrow \infty$. This allows us to introduce polar coordinates:

$$\begin{aligned} \eta(x, y) &= \sqrt{E(x, y)} = \sqrt{y^2/2 + e^x - x - 1} \\ \varphi(x, y) &= \text{angle between } (x, y) \in \mathbb{R}^2 \setminus \{0\} \text{ and the ray } \{x = 0, y \leq 0\}. \end{aligned} \quad (4.13)$$

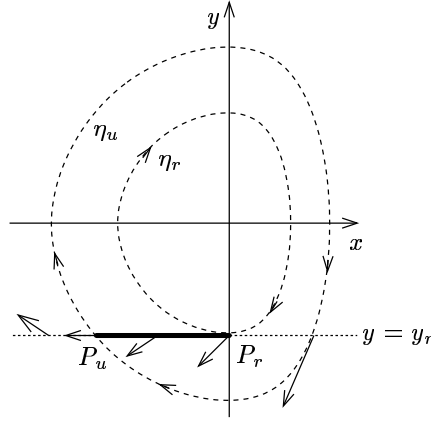


Figure 4.3: Sketch of single mode system in the limit $\delta \rightarrow 0$. System (4.10), (4.11) is discontinuous at the dotted line $y = y_r$ and it is in a sliding mode along the lower side of the thick part of the line between $P_r = (0, y_r)$ and $P_u = (-\log(1 + A), y_r)$. For $y \neq y_r$ the vector field points along the level lines $\eta = \text{const}$.

Then, $\dot{\varphi}$ is uniformly positive for bounded η . Furthermore, let us introduce the numbers

$$\begin{aligned} \eta_r &= y_r / \sqrt{2} \\ \eta_u &= \sqrt{\eta_r^2 + \frac{1}{1+A} + \log(1+A) - 1}. \end{aligned} \quad (4.14)$$

The right-hand-side of system (4.10), (4.11) is a $O(\delta)$ -perturbation of $(y, 1 - e^x)$ (the right-hand-side of $\ddot{x} = 1 - e^x$) except in the vicinity of the line $y = y_r$. In the limit $\delta \rightarrow 0$, (4.10), (4.11) is discontinuous at $y = y_r$ and equal to $\ddot{x} = 1 - e^x$ outside of this line (see Fig. 4.3). The region $x \in (-\log(1 + A), 0)$ on the line $y = y_r$ plays a special role since the sign of $\dot{y} = 1 - (1 + A)e^x$ opposes the sign of $\dot{y} = 1 - e^x$. The level line $\eta = \eta_r$ touches the line $y = y_r$ at the right end $(x = 0, y = y_r)$ of this region. The level line η_u crosses $y = y_r$ at the left end $(x = -\log(1 + A), y = y_r)$ of this region. The following Lemma 4.1 claims that the discontinuity at $y = y_r$ acts as a small perturbation if $x \notin [-\log(1 + A), 0]$.

Lemma 4.1 *Let x_* have a positive non-small distance from $[-\log(1 + A), 0]$ and $y_* = y_r$. Let $A > 0$, $w > 0$, $y_r < 0$ be of order $O(1)$. Denote the trajectory of system (4.10), (4.11) through (x_*, y_*) by $(x(t), y(t))$ and the trajectory of $\ddot{x} = 1 - e^x$ through (x_*, y_*) by $(x_0(t), y_0(t))$. Let the time interval $[-T, T]$ be sufficiently small such that $y_0(t) - y_r$ is only small in the vicinity of $t = 0$. Then, $|x_0(t) - x(t)|$, $|y_0(t) - y(t)|$ are of order $O(\delta)$ for $t \in [-T, T]$.*

Proof: We have to compute the difference between $(x(t), y(t))$ and $(x_0(t), y_0(t))$ only in the vicinity of $t = 0$. Since $x(t) - x_0(t) = \int_0^t (y(s) - y_0(s)) ds$, it is sufficient to prove that $|y_0(t) - y(t)| = O(\delta)$ for t in some interval around 0. Let $\eta_*^2 = y_r^2/2 + e^{x_*} - x_* - 1$. The trajectory (x_0, y_0) has the form $y_0(x_0) = -\sqrt{2} \sqrt{\eta_*^2 - e_0^x + x_0 + 1}$. Since \dot{x} is

uniformly negative for y near y_r , we can parametrize the trajectory $(x(t), y(t))$ also with respect to x . We have

$$\begin{aligned} \frac{1}{2}(y(x)^2 - y_0(x)^2) &= \int_{x_*}^x y(\xi) \frac{dy(\xi)}{d\xi} - y_0(\xi) \frac{dy_0(\xi)}{d\xi} d\xi \\ &= - \int_{x_*}^x \frac{A\delta^2 w^2}{(y(\xi) - y_r)^2 + \delta^2 w^2} d\xi + O(\delta). \end{aligned} \quad (4.15)$$

The quantity $\partial y(x)/\partial x$ is uniformly positive in the vicinity of (x_*, y_*) if $x_* > c_u > 0$, and it is uniformly negative if $x_* < c_l < -\log(1 + A)$. Hence, we can estimate the term $(y(\xi) - y_r)^2$ from below by $a(x - x_*)^2$ where $a > 0$. Then, the integral in the right-hand-side of (4.15) is of order $O(\delta)$. \square

According to numerical observations, the stable periodic orbits of system (4.10), (4.11) are only small in a very small parameter region near $y_{r,+}$ (see Fig. 4.2). On the other hand, the conservative oscillator $\ddot{x} = 1 - e^x$ is not harmonic far away from 0. Hence, we should not consider the self-pulsations as small perturbations of harmonic oscillations expanding them near the Hopf points. Rather, we search for a level line η_s of the conservative oscillator where the stable limit cycles branch from at $\delta = 0$.

The following Theorem 4.2 proves the existence of this level line η_s and, hence, the boundedness of the self-pulsations for $\delta \rightarrow 0$. Furthermore, its proof provides a formula for η_s which can be used for a zero-order approximation of the self-pulsations.

Theorem 4.2 *Let $R > 0$ be sufficiently large, $\delta_0 > 0$ be sufficiently small, and $y_r < 0$, $A > 0$, $J > 0$, $w > 0$ be of order $O(1)$. Then,*

1. *system (4.10), (4.11) has a first return map $r_\delta(\eta) = \eta + g(\eta)$ to the ray $\mathcal{R} = \{\varphi = 0\}$, such that the interval $[0, R]$ is forward invariant for r_δ for all $\delta \in (0, \delta_0)$.*
2. *$|g(\eta)|$ is of order $O(\delta)$ in any compact subset \mathcal{C} of $(0, \eta_r) \cup (\eta_u, \infty)$.*
3. *There exists exactly one level line η_s of $\eta(x, y)$ within $B_R(0)$ such that an isolated parametric family of stable limit cycles branches from η_s for $\delta \in (0, \delta_0)$.*

Proof: Since $\dot{\varphi}$ is uniformly positive for bounded η , the system (4.10), (4.11) induces a first return map to the ray $\mathcal{R} = \{\varphi = 0\}$. We denote this first return map by $r_\delta : \eta \in [0, \infty) \rightarrow [0, \infty)$. r_δ is smooth for $\delta > 0$. It converges uniformly in each compact subset of $[0, \infty) \setminus \{\eta_r\}$ to

$$r_0(\eta) = \begin{cases} \eta & \text{for } \eta \in \mathcal{H}_c := [0, \eta_r) \cup (\eta_u, \infty) \\ \eta_u & \text{for } \eta \in (\eta_r, \eta_u] =: \mathcal{H}_f \end{cases}$$

for $\delta \rightarrow 0$. We have to study the effect of the perturbation by δ only where r_0 is critical i. e. in \mathcal{H}_c . Let $\xi : \mathbb{R} \rightarrow \mathbb{R}$ be a monotone increasing function defined by

the equation $\xi(x)^2 = e^x - x - 1$. ξ is a diffeomorphism on \mathbb{R} with $\xi(0) = 0$ and an inverse function $\tilde{x}(\xi)$ defined by

$$\xi^2 = e^{\tilde{x}(\xi)} - \tilde{x}(\xi) - 1. \quad (4.16)$$

Let $\mathcal{C} \subset \mathcal{H}_c$ be compact, and $\eta \in \mathcal{C}$. For $\eta \in \mathcal{C}$ we may formally expand

$$r_\delta(\eta) = \eta + \delta \left. \frac{\partial}{\partial \delta} r_\delta(\eta) \right|_{\delta=0} + o(\delta).$$

Hence, if $\left. \frac{\partial}{\partial \delta} r_\delta(\eta) \right|_{\delta=0}$ exists and changes its sign from $+$ to $-$ at η , the fixed point $r_0(\eta) = \eta$ will persist for $\delta > 0$ and be stable and uniformly isolated for small δ . Consider

$$(r_\delta(\eta) - \eta)/\delta = \delta^{-1} \left[\sqrt{E(x(T(\eta, \delta)), y(T(\eta, \delta)))} - \sqrt{E(x(0), y(0))} \right]$$

for $\eta \in \mathcal{C}$ where $T(\eta, \delta)$ is the time for the first return to \mathcal{R} , and $(x(t), y(t))$ is the trajectory inducing $r_\delta(\eta)$. The trajectory $(x(t), y(t))$ is a $O(\delta)$ -perturbation of the periodic solution of the conservative oscillator along the level line η according to Lemma 4.1. We have

$$\begin{aligned} (r_\delta(\eta) - \eta)/\delta &= \\ &= \delta^{-1} \int_0^{T(\eta, \delta)} \frac{d}{dt} \sqrt{E(x(t), y(t))} dt \\ &= \underbrace{- \int_0^{T(\eta, \delta)} \frac{1}{2\eta} \left(\frac{y^2}{I} + y^2 e^x \right) dt}_{S_1(\eta, \delta)} - \underbrace{\int_0^{T(\eta, \delta)} \frac{1}{2\eta} \frac{\delta A w^2 y e^x}{(y - y_r)^2 + \delta^2 w^2} dt}_{S_2(\eta, \delta)} + O(\delta) \end{aligned}$$

The $O(\delta)$ is uniform for $\eta \in \mathcal{C}$. Hence, $g(\eta) = r_\delta(\eta) - \eta$ is of order δ in \mathcal{C} . The first part S_1 is negative. For $\eta \in \mathcal{C}$, it can be approximated up to order $O(\delta)$ by replacing $(x(t), y(t))$ by the periodic orbit of the conservative oscillator:

$$S_1(\eta, \delta) = -\frac{2\sqrt{2}}{\eta} (I^{-1} + 1) \int_{-\eta}^{\eta} \sqrt{\eta^2 - \xi^2} \frac{\xi}{\xi^2 + \tilde{x}(\xi)} d\xi + O(\delta) \quad (4.17)$$

Concerning S_2 , we consider $\eta \in \mathcal{C} \cap (0, \eta_r)$ firstly. The term S_2 is of order $O(\delta)$ if $\eta \in \mathcal{C} \cap (0, \eta_r)$. Therefore, $r_\delta(\eta) < \eta$ for $\eta \in \mathcal{C} \cap (0, \eta_r)$ and sufficiently small δ . Thus, there is no fixed point of r_δ in $\mathcal{C} \cap (0, \eta_r)$. However, there must be an unstable fixed point in $(0, \eta_r] \setminus \mathcal{C}$ for sufficiently small $\delta > 0$ since r_δ is smooth in η for $\delta > 0$ and $\lim_{\eta \searrow \eta_r} r_0(\eta) = \eta_u > \eta_r$. Consequently, a family of unstable fixed points of r_δ branches from η_r . This implies that there is no isolated stable family of fixed points of r_δ in $(0, \eta_r]$.

Consider $\eta \in \mathcal{C} \cap (\eta_u, \infty)$ now. Then, $\dot{y} \neq 0$ at $y = y_r$ for sufficiently small δ . Hence, we can substitute dt by dy/\dot{y} near $y = y_r$. Let $(x(t_-), y_r)$, and $(x(t_+), y_r)$ be the

crossing points of the trajectory $(x(t), y(t))$ with $\{y = y_r\}$ ($x(t_-) < 0, x(t_+) > 0$). We expand S_2 with respect to δ to obtain

$$S_2(\eta, \delta) = \frac{\pi A w y_r}{2} \left[\frac{e^{x(t_-)}}{\eta(t_-) \sqrt{(1 - e^{x(t_-)})(1 - (1 + A)e^{x(t_-)})}} + \frac{e^{x(t_+)}}{\eta(t_+) \sqrt{(e^{x(t_+)} - 1)((1 + A)e^{x(t_+)} - 1)}} \right] + O(\delta). \quad (4.18)$$

The values $x(t_{\pm})$ and $\eta(t_{\pm})$ may be replaced by the corresponding values for the periodic orbit of the conservative oscillator:

$$x(t_{\pm}) = \tilde{x} \left(\pm \sqrt{\eta^2 - y_r^2/2} \right) + O(\delta) \text{ and } \eta(t_{\pm}) = \eta + O(\delta).$$

The term $S_1(\eta, 0)$ is zero at $\eta = 0$ and decreases monotone and super-linearly for $\eta \rightarrow \infty$ whereas $S_2(\eta, 0)$ is a monotone increasing function with $\lim_{\eta \searrow \eta_u} S_2(\eta, 0) = -\infty$ and $\lim_{\eta \rightarrow \infty} S_2(\eta, 0) = 0$. Thus, $S_1(\eta, 0) - S_2(\eta, 0)$ has exactly one root η_c in (η_u, ∞) . The sign change at η_c is from $+$ to $-$. This situation persists for $S_1(\eta, \delta) - S_2(\eta, \delta)$. Consequently, there exists exactly one stable fixed point $\eta_c(\delta) \geq \eta_u$ of r_δ for sufficiently small δ with $\eta_c(\delta) \rightarrow \eta_c$ for $\delta \rightarrow 0$. \square

The statement of Theorem 4.2 in terms of the original system (4.3), (4.4) is:

Corollary 4.3 *For $\varepsilon \rightarrow 0$, there exists a family of uniformly bounded stable limit cycles if $N_r < 0$ and the scaling of the parameters is $N_r = O(\sqrt{\varepsilon})$, $A = O(1)$ and $W = O(\varepsilon)$.*

The following corollary is also an immediate consequence of Lemma 4.1 and the argumentation in the proof of Theorem 4.2:

Corollary 4.4 *Let $(x(t; \eta), y(t; \eta))$ be the trajectory for system (4.10), (4.11) inducing the return map $r_\delta(\eta)$ ($t \in [0, T(\eta, \delta)]$), i. e., $x(0; \eta) = x(T(\eta, \delta); \eta) = 0$, $y(0) = -\sqrt{2}\eta$). Denote the corresponding trajectory of the conservative oscillator $\ddot{x} = 1 - e^x$ by $(x_0(t; \eta), y_0(t; \eta))$. Let η be in a compact subset of $(0, \infty) \setminus [\eta_r, \eta_u]$. Then, the distance $\|(x(t; \eta), y(t; \eta)) - (x_0(t; \eta), y_0(t; \eta))\|$ is of order $O(\delta)$ for all $t \in [0, T(\eta, \delta)]$. The same holds for the time of the first return: $T(\eta, \delta) = T(\eta, 0) + O(\delta)$.*

Remarks

Location of the Fold Periodic Orbit There is always an unstable limit cycle near the level line $\eta_r = -y_r/\sqrt{2}$ for sufficiently small δ . However, the physically relevant parameters do not reflect this asymptotical behavior yet. Typically, the Hopf point $y_{r,-}$ is of order $O(1)$ for realistic δ . Since the unstable periodic orbits are located near $\eta < \eta_r$ and the self-pulsations branch from level lines $\eta > \eta_r$, the location of the fold of periodic orbits in phase space must be in the vicinity of the level line η_r . We can exploit this fact to obtain a crude heuristic approximation of the fold in the parameter space. We insert the orbit of $\ddot{x} = 1 - e^x$ along η_r for

$(x(t), y(t))$ into the term $S_2(\eta, \delta)$. Because S_2 is of order δ except in the vicinity of $(x = 0, y = y_r)$, we only evaluate it around that point and substitute dt by dx/y :

$$S_2(\eta_r, \delta) = -\frac{1}{2\eta_r} \int_{-c}^c \frac{\delta A w^2 e^x}{(y(x) - y_r)^2 + \delta^2 w^2} dx + O(\delta)$$

where $y(x) = \sqrt{2} \sqrt{\eta_r^2 - e^x + x + 1}$ and $c > 0$ of order $O(1)$. We expand this expression with respect to δ and obtain

$$S_2(\eta_r, \delta) = -\frac{\sqrt{2}\pi}{2} \frac{A\sqrt{w}}{\sqrt{-y_r}} \cdot \delta^{-1/2} + O(\sqrt{\delta}).$$

We equate the leading term of $S_2(\eta_r, \delta)$ with $S_1(\eta_r, 0)$ to get an approximation of the location of the fold in parameter space:

$$S_1(y_r/\sqrt{2}, 0) = -\frac{\sqrt{2}\pi}{2} \frac{A\sqrt{w}}{\sqrt{-y_r}} \cdot \delta^{-1/2} \quad (4.19)$$

However, this approximation is only heuristic, since we do not know a priori whether the fold periodic orbit is sufficiently close to the orbit of $\ddot{x} = 1 - e^x$ along η_r to have the same expansion. We plot the approximate fold location for a sample parameter setting in the (A, y_r) -plane and compare it to the numerical solution in Fig. 4.6.

The Corresponding Averaged Equation The proof of Theorem 4.2 approximates the first return map $r(\eta)$ for $\eta \in \mathcal{H}_c$ to find a periodic orbit and to show its stability. Alternatively, we could employ first-order averaging. This would be only formally correct since $\dot{\eta}/\dot{\varphi}$ does not have a uniform Lipschitz constant with respect to (φ, η) for $\delta \rightarrow 0$. However, the consideration of the return map in Theorem 4.2 has proved that the averaged equation

$$\dot{\eta} = \frac{1}{2\pi} g(\eta) \quad (4.20)$$

approximates the first return-map for small δ if η is in compact subsets of \mathcal{H}_c (i. e., $g(\eta)$ is of order $o(1)$). For $\eta > \eta_u$, we may use the approximation $g(\eta) = \delta(S_1(\eta, 0) - S_2(\eta, 0))$.

Location of the Self-Pulsation The critical level line η_s is a zero-order approximation for the location of the stable limit cycle if $y_r = O(1)$. For simplicity, we can replace the integral in S_1 by its Taylor expansion [33] when solving $S_1(\eta, 0) - S_2(\eta, 0) = 0$:

$$S_1(\eta, 0) = - (I^{-1} + 1) \left(\pi\eta + \frac{\pi}{24}\eta^3 \right)$$

which is very accurate within the interval $[0, 4]$. The third order term is important since η is typically far away from 0. Then, the approximate equation for $S_1(\eta, 0) = S_2(\eta, 0)$ reads

$$-\frac{I^{-1} + 1}{A w y_r} \left(2\eta^2 + \frac{1}{12}\eta^4 \right) = \frac{\left(1 - \frac{A}{e^{-x_r^-} - 1} \right)^{-\frac{1}{2}}}{e^{-x_r^-} - 1} + \frac{\left(1 + \frac{A}{1 - e^{-x_r^+}} \right)^{-\frac{1}{2}}}{1 - e^{-x_r^+}} \quad (4.21)$$

where $x_r^\pm = \tilde{x} \left(\pm \sqrt{\eta^2 - y_r^2/2} \right)$. This equation is easy to solve for I or w with a given η^2 . Figure 4.2 compares the extrema of the level lines computed with (4.21) to extrema of the actual periodic orbits.

4.2 Two modes with different frequencies

Next, we consider a laser with one active section ($n = n_1 \in \mathbb{R}$) in the vicinity of the situation where two eigenvalues $\lambda_1(n)$ and $\lambda_2(n)$ of $H(n)$ cross the imaginary axis transversally at the same n_0 . This case is observed frequently in numerical computations using the full system (3.2), (3.4) [35], [50] even though it seems to be non-generic at first sight. The reason is the following: A laser consisting of a single DFB-section (i. e. $m = m_a = 1$, $\kappa \neq 0$) with zero facet reflectivities ($r_0 = r_L = 0$) is symmetric with respect to reflection. Thus, if $H(n)$ has the eigenvalue $\lambda + i \operatorname{Im} \beta$, it has also the eigenvalue $\bar{\lambda} + i \operatorname{Im} \beta$. Typically, a pair of eigenvalues becomes critical having the frequencies $\operatorname{Im} \lambda_{1,2} \approx \operatorname{Im} \beta_1 \pm \kappa_1$. The frequency region $(\operatorname{Im} \beta_1 - \kappa_1, \operatorname{Im} \beta_1 + \kappa_1)$ is usually referred to as the *stopband* of the active section. Hence, a solitary section typically supports modes at both ends of the stopband. This situation is slightly perturbed by the passive sections and the nonzero facet reflectivity preferring one of the two ends of the stopband. However, this preference is usually small and may change for varying parameters (see Fig. 3.1 b for a typical situation).

4.2.1 Motivation

For motivation, we present a result of numerical long-time computations for system (3.2), (3.4) in Fig. 4.4 which has been obtained by [7] and [50].

The geometric configuration for Figure 4.4 is the following: We have two DFB sections S_1 and S_3 (i. e. $\kappa_1, \kappa_3 \neq 0$) and a phase tuning section S_2 ($\kappa_2 = 0$). S_1 is active, S_3 acts as a reflector. The parameter $p = -2l_2 \operatorname{Im} d_2$ adjusts the phase of the feedback from S_3 . Hence, p influences the behavior only modulo 2π .

Within this period, the authors of [7] choose a fine mesh, start the simulation, and wait until the system “settles” to some final state. The approximate limits $\limsup_{t \rightarrow \infty} |\psi(t, 0)|^2$ and $\liminf_{t \rightarrow \infty} |\psi(t, 0)|^2$ are reported in Figure 4.4 A. Then, they advance p to the next mesh point starting the computations from the previously reported final state. The mesh is traversed in forward and in backward direction in order to detect coexisting final states. If there are coexisting final states, the arrows in Figure 4.4 A indicate how p was being changed. In this manner, the pseudo bifurcation diagram of Figure 4.4 A is obtained which reports only stable limiting states.

If $\limsup_{t \rightarrow \infty} |\psi(t, 0)|^2 \neq \liminf_{t \rightarrow \infty} |\psi(t, 0)|^2$, the time profile of $|\psi(t, 0)|^2$ is supposed to be (roughly) periodic. It is shown in Figure 4.4 C for these cases. For orientation, we draw the root curves $\{(n, p) : \lambda_j(n, p) = 0\}$ of the dominating eigenvalues of H in Figure 4.4 B. The dashed/solid profile of the lines indicates that λ_1 (solid) is at the low end of the stopband (i. e. $\operatorname{Im} \lambda_1 \approx \operatorname{Im} \beta_1 - \kappa_1$) whereas λ_2 and λ_2 (dashed) are at the high end of the stopband (i. e. $\operatorname{Im} \lambda_2, \operatorname{Im} \lambda_2 \approx \operatorname{Im} \beta_1 + \kappa_1$). We observe the following scenarios of interaction between modes at different ends of the stopband in Fig. 4.4:

- (T1) There is no interaction visible at all if each of the modes has an on-state which is stable in the sense of the single mode model. For $p < p_0$, the on-state

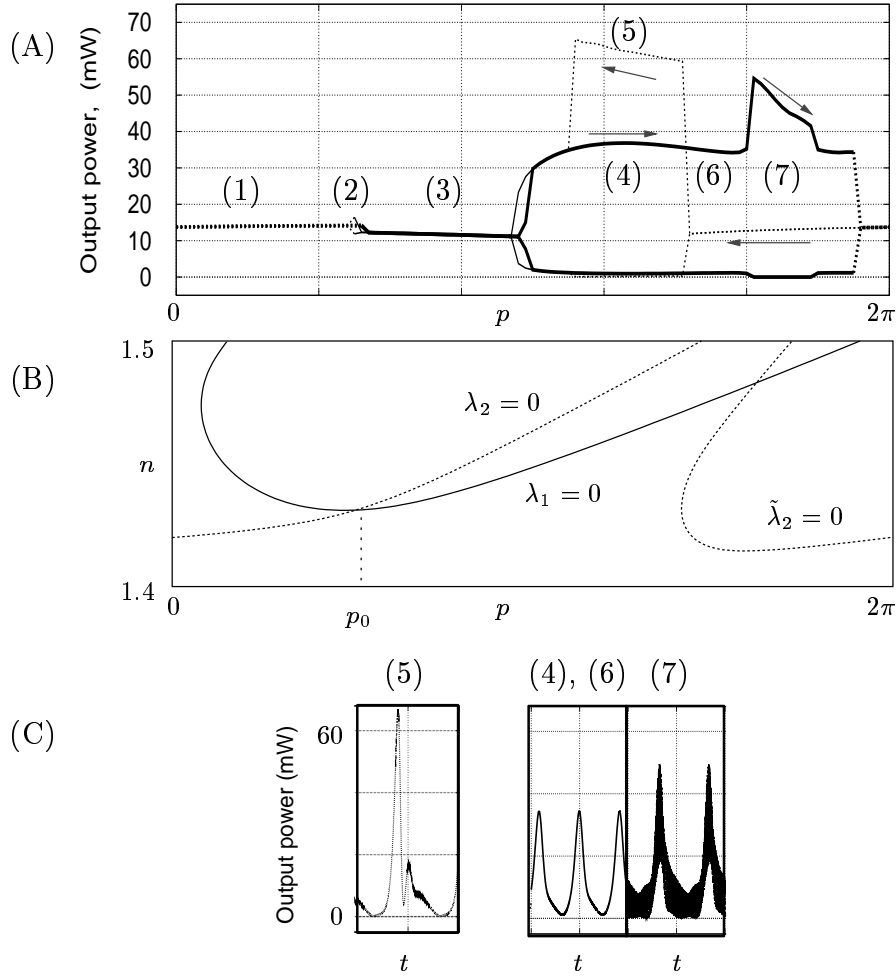


Figure 4.4: Pseudo bifurcation diagram for 3-section laser from [7], [50]: In Figure (A), $\limsup_{t \rightarrow \infty} |\psi(t, 0)|^2$ and $\liminf_{t \rightarrow \infty} |\psi(t, 0)|^2$ are plotted over a fine mesh in one period of the parameter $p = -2l_2 \text{Im } d_2$. The arrows indicate the direction the mesh is traversed. Figure (B) shows the root curves $\{(n, p) : \lambda_j(n, p) = 0\}$ for the dominant eigenvalues of $H(n)$. In (C), we plot the time profile over one period of $\psi(t, 0)$ for the non-stationary scenarios in Figure (A). See text of section 4.2 for details. Device configuration: $n = n_1$ ($\mathcal{A} = \{1\}$), $\kappa_1 = \kappa_3 \neq 0$, $\kappa_2 = 0$.

corresponding to λ_2 is stable, and the on-state corresponding to λ_1 is unstable (scenario (1) in Fig. 4.4 A). The situation is vice versa if $p > p_0$ (scenario (3)). Near $p = p_0$, the transition between the two on-states is extremely slow in time but sharp in the parameter space (scenario (2)).

- (T2) The behavior changes if at least one of the modes has a self-pulsation in the sense of the single mode model. There is a parameter region where the self-pulsation corresponding to λ_1 is stable and coexists with the stable on-state corresponding to $\tilde{\lambda}_2$ (scenario (6)) or with a stable self-pulsation corresponding to λ_2 ((4) and (5)).

(T3) In region (7), a regime is stable where modes from both ends of the stopband contribute. The time profile of the solution (7) shows that the frequency of the self-pulsation is overlapped with another very large frequency. This large frequency is approximately $\text{Im } \lambda_1 - \text{Im } \lambda_2$.

The large frequency difference between the dominant eigenvalues $\text{Im } \lambda_1 - \text{Im } \lambda_2$ is a characteristic feature for the situations described above. We exploit this characteristic in the following paragraphs by considering the first order averaged equations instead of the full two mode system. This approach has the advantage that we can use the knowledge about the bifurcation diagram of the single mode case. Nevertheless, it predicts and explains the scenarios (T1)–(T3) accurately.

4.2.2 Derivation of the Averaged Two Mode Equation

System (3.47), (3.48) reads

$$\begin{aligned}\dot{x}_1 &= \lambda_1(n)x_1 + \varepsilon\Delta_1(n)f(n, x_1, x_2)x_2 \\ \dot{x}_2 &= \lambda_2(n)x_2 + \varepsilon\Delta_2(n)f(n, x_1, x_2)x_1 \\ \dot{n} &= \varepsilon f(n, x_1, x_2)\end{aligned}\tag{4.22}$$

where (omitting the section index 1 and the n -dependence of some coefficients)

$$\begin{aligned}\Delta_1(n) &= \frac{1}{\lambda_2 - \lambda_1} \left[\partial_n \beta + \frac{\partial_n \rho \Gamma + i \partial_n \Omega_r \chi(\lambda_1)}{\lambda_2 - i \Omega_r + \Gamma} \right] (\psi_1^\dagger, \psi_2)_1 \\ \Delta_2(n) &= \frac{1}{\lambda_1 - \lambda_2} \left[\partial_n \beta + \frac{\partial_n \rho \Gamma + i \partial_n \Omega_r \chi(\lambda_2)}{\lambda_1 - i \Omega_r + \Gamma} \right] (\psi_2^\dagger, \psi_1)_1 \\ f(n, x_1, x_2) &= I - n - (n - 1) [R_1(n)|x_1|^2 + R_2(n)|x_2|^2 + \\ &\quad + \text{Re}(R_{12}(n)\bar{x}_1 x_2)] \\ (n - 1)R_1(n) &= (g(n) - \rho(n) + \text{Re } \chi(\lambda_1(n))) \|\psi_1\|^2 \\ (n - 1)R_2(n) &= (g(n) - \rho(n) + \text{Re } \chi(\lambda_2(n))) \|\psi_2\|^2 \\ (n - 1)R_{12}(n) &= \left[2(g(n) - \rho(n)) + \overline{\chi(\lambda_1(n))} + \overline{\chi(\lambda_2(n))} \right] (\psi_1, \psi_2)_1.\end{aligned}$$

The two amplitudes x_1 and x_2 and the coefficients λ_j , Δ_j and R_{12} are complex quantities.

We rescale system (4.22) in a similar way as in section 4.1: Let $\text{Re } \lambda_1(n_1) = 0$, $\text{Re } \lambda_1'(n_1) > 0$, and $\text{Im } \lambda_1(n) < \text{Im } \lambda_2(n)$ for all n under consideration. We introduce

$$\begin{aligned}I_{\text{new}} &= \frac{I_{\text{old}} - n_1}{n_1 - 1} & \delta &= \sqrt{\frac{I\varepsilon}{2\lambda_1'(n_1)}} \\ t_{\text{new}} &= \sqrt{2\lambda_1'(n_1)I\varepsilon}t_{\text{old}} & G_j(y) &= 2\delta^{-1} \text{Re } \lambda_j((n_1 - 1)\delta y + n_1) \\ y &= \delta^{-1} \frac{n - n_1}{n_1 - 1} & R_{j,\text{new}}(y) &= R_{j,\text{old}}((n_1 - 1)\delta y + n_1) \\ \varphi_j(0) &= 0 & \dot{\varphi}_j &= -\delta^{-1} \text{Im } \lambda_j((n_1 - 1)\delta y + n_1) \\ \xi_j &= x_j e^{i\varphi_j} / I & \Delta_{j,\text{new}}(y) &= \Delta_{j,\text{old}}((n_1 - 1)\delta y + n_1)\end{aligned}\tag{4.23}$$

for $j = 1, 2$. Denoting $\tau = \varphi_1 - \varphi_2$, the rescaled system reads

$$\dot{\xi}_1 = \frac{1}{2}G_1(y)\xi_1 + \delta\Delta_1(y)f(y, \xi_1, \xi_2, \tau)e^{i\tau}\xi_2 \quad (4.24)$$

$$\dot{\xi}_2 = \frac{1}{2}G_2(y)\xi_2 + \delta\Delta_2(y)f(y, \xi_1, \xi_2, \tau)e^{-i\tau}\xi_1 \quad (4.25)$$

$$\begin{aligned} \dot{y} &= f(y, \xi_1, \xi_2, \tau) \\ &= 1 - \delta/I \cdot y - (1 + \delta y) [R_1(y)|\xi_1|^2 + R_2(y)|\xi_2|^2 + \\ &\quad + \operatorname{Re}(R_{12}(y)\bar{\xi}_1\xi_2e^{i-\tau})] \end{aligned} \quad (4.26)$$

$$\dot{\tau} = \delta^{-1}(\operatorname{Im} \lambda_2 - \operatorname{Im} \lambda_1). \quad (4.27)$$

Introduction of time $\tau = \varphi_1 - \varphi_2$ transforms system (4.24)–(4.26) into a standard form $\dot{x} = \varepsilon g(x, t)$ where a small $\varepsilon \approx (\operatorname{Im} \lambda_2 - \operatorname{Im} \lambda_1)^{-1}\delta$ is put in front of the right-hand-side and g is 2π -periodic. The term $e^{i(\varphi_2 - \varphi_1)}$ changes to $e^{-i\tau}$. The corresponding first order averaged equation reads (with respect to time t , dropping terms of order $(\operatorname{Im} \lambda_2 - \operatorname{Im} \lambda_1)^{-1}\delta$)

$$\dot{s}_1 = G_1(y)s_1 \quad (4.28)$$

$$\dot{s}_2 = G_2(y)s_2 \quad (4.29)$$

$$\dot{y} = 1 - \delta/I \cdot y - (1 + \delta y) [R_1(y)s_1 + R_2(y)s_2] \quad (4.30)$$

$$\arg \xi_j \equiv \text{const} \quad \text{for } j = 1, 2 \quad (4.31)$$

in polar coordinates ($s_j = |\xi_j|^2$). Equation (4.31) is decoupled from system (4.28)–(4.30). Hence, we can continue our analysis using subsystem (4.28)–(4.30).

We note that the functions R_j and G_j have the same meaning for their respective mode as G and $R(\cdot, \delta, y_r)$ in the single mode case.

The functions G_j are the effective gain functions of their corresponding modes. The function G_1 has the root 0, and $G'_1(0) = 1$. Moreover, we assume that $G'_2(0)$ is positive, not small and without loss of generality $G'_2(0) \leq 1$. Then, we can introduce $\alpha = G'_2(0)^{-1} \geq 1$ and rescale $s_{2,\text{new}} = s_{2,\text{old}}^\alpha$. This scaling changes $G'_2(0)$ to 1 and equation (4.30) to

$$\dot{y} = 1 - \delta/I \cdot y - (1 + \delta y) [R_1(y)s_1 + R_2(y)s_2^\alpha]. \quad (4.32)$$

We take (4.31) into account only to interpret the long-time behavior of the averaged system in terms of the original quantities. The following Lemma 4.5 summarizes how standard averaging theory [21], [38] allows to lift results for (s_1, s_2, y) back to (x_1, x_2, n) .

Lemma 4.5 *Denote the minimum of $(\operatorname{Im} \lambda_1(y) - \operatorname{Im} \lambda_2(y))/\delta$ by μ^{-1} . Let $(\xi_1, \xi_2, y) : \mathcal{M} \rightarrow \mathbb{C}^2 \times \mathbb{R}$ be a normally hyperbolic invariant manifold of system (4.28)–(4.31). Let the flow on \mathcal{M} be governed by $\dot{m} = F(m)$. Then, there exists a normally hyperbolic invariant manifold of system (4.22) which is the transformation of a small perturbation $(\tilde{\xi}_1, \tilde{\xi}_2, \tilde{y}) : \mathcal{M} \times S^1 \rightarrow \mathbb{C}^2 \times \mathbb{R}$ of (ξ_1, ξ_2, y) of order $O(\mu)$ in the following sense:*

$$\begin{aligned} |\tilde{\xi}_j(m, \varphi) - \xi_j(m)| &= O(\mu) \\ |\tilde{y}(m, \varphi) - y(m)| &= O(\mu) \end{aligned}$$

for $j = 1, 2$, all $m \in \mathcal{M}$, and $\varphi \in S^1$. Moreover, $(m, \varphi) \in \mathcal{M} \times S^1$ satisfy the equations

$$\begin{aligned}\dot{m} &= F(m) + F_1(m, \varphi) \\ \dot{\varphi} &= -\delta^{-1}(\operatorname{Im} \lambda_2(\tilde{y}(m, \varphi)) - \operatorname{Im} \lambda_1(\tilde{y}(m, \varphi)))\end{aligned}$$

where F_1 is of order $O(\mu)$. We obtain x_j and n by setting $\varphi(0) = 0$ and

$$\begin{aligned}x_j(t) &= \tilde{\xi}_j(t)e^{-i\varphi_j(t)} \\ n(t) &= (n_1 - 1)\delta\tilde{y}(t) + n_1 \\ \varphi_j(t) &= \int_0^t -\delta^{-1} \operatorname{Im} \lambda_j(\tilde{y}(s)) ds.\end{aligned}$$

Proof: We imbed the non-averaged system (4.24)–(4.27) into a $\mathbb{C}^2 \times \mathbb{R} \times S^1$ -system by leaving the initial condition on $\varphi_2 - \varphi_1$ free in S^1 . The extended system has the form

$$\begin{aligned}\dot{u} &= f(u, \varphi) \\ \dot{\varphi} &= \mu^{-1}g(u)\end{aligned}\tag{4.33}$$

where $u \in \mathbb{C}^2 \times \mathbb{R}$, $\varphi = \varphi_1 - \varphi_2 \in S^1$ (f is 2π -periodic in φ), and g is uniformly positive and of order 1. Let $\tilde{f}(u)$ be the average of f with respect to φ : $\tilde{f}(u) = (2\pi)^{-1} \int_{S^1} f(u, \varphi) d\varphi$. After a near-identity change of coordinates $u = v + \mu w(v, \varphi)$, we have

$$\begin{aligned}\dot{v} &= \tilde{f}(v) + \mu f_1(v, \varphi) \\ \dot{\varphi} &= \mu^{-1}g(v + \mu w(v, \varphi))\end{aligned}\tag{4.34}$$

where

$$\begin{aligned}w &= g(v)^{-1} \int_0^\varphi f(v, \theta) d\theta - \tilde{f}(v) \\ f_1 &= [Id + \mu \partial_1 w(v, \varphi)]^{-1} \left[\frac{f(v + \mu w(v, \varphi), \varphi) - f(v, \varphi)}{\mu} - \partial_1 w(v, \varphi) \tilde{f}(v) \right].\end{aligned}$$

Hence, $f_1 \in C^1$ is of order $O(1)$. (4.34) is a regular perturbation of order $O(\mu)$ of the averaged system

$$\begin{aligned}\dot{v} &= \tilde{f}(v) \\ \dot{\varphi} &= \mu^{-1}g(v + \mu w(v, \varphi)).\end{aligned}\tag{4.35}$$

Consequently, if \mathcal{M} is a normally hyperbolic invariant manifold of $\dot{v} = \tilde{f}(v)$, $\mathcal{M} \times S^1$ is a normally hyperbolic invariant manifold of (4.35). This manifold persists under the regular perturbation f_1 implying the existence of a normally hyperbolic invariant manifold $\tilde{\mathcal{M}}$ of (4.33) after transforming back from v to u . At the end, we choose those trajectories where φ starts at 0. The manifold $\tilde{\mathcal{M}}$ is a small perturbation of \mathcal{M} as a graph, and the flow on $\tilde{\mathcal{M}}$ is a regular perturbation of the flow on \mathcal{M} . \square

Lemma 4.5 implies:

- A hyperbolic equilibrium ($s_1 \neq 0, s_2 = 0, y = \text{const}$) of (4.28)–(4.30) is a small perturbation of the periodic orbit ($x_1 = \sqrt{s_1}e^{i\theta_1 - i\varphi_1(t)}, x_2 = 0, n = \text{const}$). We have to take into account the particular structure of f_1 and w in (4.34) to obtain that the perturbation is actually 0 in this case.
- A hyperbolic equilibrium ($s_1 \neq 0, s_2 \neq 0, y = \text{const}$) is a normally hyperbolic invariant 2-torus close to

$$(x_1 = \sqrt{s_1}e^{i\theta_1 - i\varphi_1(t)}, x_2 = \sqrt{s_2}e^{i\theta_2 - i\varphi_2(t)}, n = \text{const}).$$

This type of solutions is referred to as *pulsations of mode beating type*.

- A single-mode self-pulsation ($s_1(t), s_2 = 0, y(t)$) is a normally hyperbolic invariant 2-torus close to

$$(x_1 = \sqrt{s_1(t)}e^{i\theta_1 - i\varphi_1(t)}, x_2 = 0, n(t)).$$

- A hyperbolic periodic orbit ($s_1(t), s_2(t), y(t)$) is a normally hyperbolic invariant 3-torus close to

$$(x_1 = \sqrt{s_1(t)}e^{i\theta_1 - i\varphi_1(t)}, x_2 = \sqrt{s_2(t)}e^{i\theta_2 - i\varphi_2(t)}, n(t)).$$

Remark: The definition of normal hyperbolicity of an invariant manifold imposes conditions on the rates of attraction and expansion normal to the manifold (see appendix B). These rates have to be large compared to the μ discussed in Lemma 4.5. Since the averaged system (4.28)–(4.30) will turn out to be singularly perturbed, this imposes a restriction on the smallness of the singular perturbation parameter.

4.2.3 Dynamics in the Vicinity of the On-states

We note that system (4.28), (4.29), (4.32) has two invariant planes: $\mathcal{S}_1 = \{s_2 = 0\}$ and $\mathcal{S}_2 = \{s_1 = 0\}$. Between the invariant planes, the ratio $r = s_1/(s_2 + s_1)$ satisfies the differential equation

$$\dot{r} = (G_1(y) - G_2(y))(r - r^2). \quad (4.36)$$

We can introduce the new variable $x = \log(s_1 + s_2)$ and rewrite the equations (4.28), (4.32):

$$\dot{x} = (rG_1(y) + (1 - r)G_2(y)) \quad (4.37)$$

$$\dot{y} = 1 - \frac{\delta}{I}y - (1 + \delta y)(rR_1(y)e^x + (1 - r)^\alpha R_2(y)e^{\alpha x}). \quad (4.38)$$

System (4.36), (4.37), (4.38) is equivalent to (4.28), (4.29), (4.32) in the invariant subspace $\{s_1 + s_2 > 0\}$ ($s_1 = re^x, s_2 = (1 - r)^\alpha e^{\alpha x}$). The invariant planes are now $\mathcal{S}_1 = \{r = 1\}$ and $\mathcal{S}_2 = \{r = 0\}$.

Since $G_1'(0) = G_2'(0) = 1$, the long-time behavior of r is determined by $G_2(0)$ if y is near 0 for all times i. e. if the on-states

$$\begin{aligned} O_1 &= (x = -\log R_1(0), y = 0, r = 1) \in \mathcal{S}_1 \\ O_2 &= \left(x = \frac{1}{\alpha} \log \left(\frac{1 - \delta/I \cdot y_0}{(1 + \delta y_0) R_2(y_0)} \right), y = y_0, r = 0 \right) \in \mathcal{S}_2 \end{aligned} \quad (4.39)$$

are stable with respect to x and y . In (4.39), y_0 is the root of G_2 near 0 which is approximately $-G_2(0)$ if $G_2(0)$ is small. Hence, we may use y_0 as a control parameter instead of $G_2(0)$.

The linearization of the right-hand-side of system (4.28), (4.29), (4.32) at O_1 possesses the eigenvalue $G_2(0)$ corresponding to the eigenvector v_1 transversal to \mathcal{S}_1 . At O_2 , the linearization has the eigenvalue $G_1(y_0)$ corresponding to the eigenvector v_2 transversal to \mathcal{S}_2 .

The following Theorem 4.6 shows the dynamics in the vicinity of $y \approx 0$ for y_0 of order $o(\delta)$ if O_1 and O_2 are stable within their plane:

Theorem 4.6 *Let the equilibria O_1 and O_2 be asymptotically stable with respect to x and y i. e. within their corresponding invariant plane \mathcal{S}_1 and \mathcal{S}_2 , respectively. Then, for sufficiently small y_0 there exists an exponentially attracting heteroclinic between O_1 and O_2 which is tangent to v_1 at O_1 and tangent to v_2 at O_2 . The zero-order approximation for the motion of r on the heteroclinic is*

$$r(t) = \frac{1}{1 + e^{-y_0 t} r(0)}. \quad (4.40)$$

Proof: The assumptions on the functions G_1 and G_2 imply that

$$G_1(y) - G_2(y) = y_0 + O(y^2) \quad (4.41)$$

for small y_0 and y . Hence, we can consider system (4.36), (4.37), (4.38) as a small perturbation of the case $G_1 = G_2$ in the vicinity of $y = 0$ for small y_0 . For $G_1 = G_2$ we obtain a line of equilibria $\mathcal{E} = \{(x, y, r) : y = 0, 1 = rR_1(0)e^x + (1 - r)^\alpha R_2(0)e^{\alpha x}, r \in [0, 1]\}$. The variable r is constant in time. Each of these equilibria has the asymptotic decay rate

$$\theta_r = \frac{1}{2} (\delta + \delta/I + r^\alpha R_1'(0)e^x + (1 - r)^\alpha R_2'(0)e^{\alpha x})$$

normal to \mathcal{E} . We assume that θ_0 and θ_1 are positive. Hence, θ_r is positive and has a uniform distance from 0 for all $r \in [0, 1]$.

Consequently, (4.36), (4.37), (4.38) is a singular perturbation of the situation $G_1 = G_2$. The slow manifold \mathcal{E} is uniformly exponentially attractive, compact and over-flowing invariant. Thus, it persists under the small perturbation $G_1 - G_2$. Denote the unique center manifold of the perturbed system (which is (4.36), (4.37), (4.38)) by $\tilde{\mathcal{E}}$. Since $\tilde{\mathcal{E}}$ is one-dimensional, it is a trajectory. It contains both equilibria O_1 and O_2 and is tangent to v_1 at O_1 and v_2 at O_2 since it is a center manifold. The zero-order approximation for the flow on $\tilde{\mathcal{E}}$ is (4.36). Inserting (4.41) and dropping $O(y^2)$, we obtain $\dot{r} = y_0(r - r^2)$. (4.40) is the explicit solution of this zero-order approximation. \square

Remarks

- If we assume the parameters in R_j to be of similar magnitude as in section 4.1 (i. e. $A_j = O(1)$, $y_{r,j} = O(1)$, $w = O(1)$), the asymptotic transversal decay rate θ_r is of order $O(\delta)$. Hence, the admissible magnitude for the perturbation y_0 is only $o(\delta)$ for the application of Theorem 4.6.
- There exists a heteroclinic similar to $\tilde{\mathcal{E}}$ of Theorem 4.6 if both equilibria O_1 and O_2 are exponentially unstable within their invariant plane. However, $\tilde{\mathcal{E}}$ is exponentially repelling in this case.
- The situation changes if the equilibria O_1 and O_2 have different asymptotic stability, say O_1 is unstable and O_2 is stable. The family of transversal flows (4.37), (4.38) undergoes a Hopf bifurcation for some $r \in (0, 1)$. In general, the heteroclinic connection between O_1 and O_2 is split near this Hopf point. We study this situation in the next section.
- Formula (4.40) is globally valid (i. e. for all $y \in \mathbb{R}$) if the functions G_j are affine:

$$\begin{aligned} G_1(y) &= y \\ G_2(y) &= y - y_0. \end{aligned}$$

This implies trivial dynamics between \mathcal{S}_1 and \mathcal{S}_2 : Either \mathcal{S}_1 or \mathcal{S}_2 is globally attracting depending on the sign of y_0 . The other plane is globally repelling, respectively.

- Interpretation of the results in terms of the original (non-averaged) quantities of system (4.22): The family of equilibria \mathcal{E} at $y_0 = 0$ corresponds to a family of invariant 2-tori with the radius pair s_1 and s_2 and the rotational velocities $\text{Im } \lambda_1(n_1)$ and $\text{Im } \lambda_2(n_1)$. However, these tori are not normally hyperbolic. Hence, we only know that the formerly stable on-state O_1 undergoes an almost vertical torus bifurcation leaving O_1 unstable if y_0 approaches 0 from above. Virtually at the same parameter value $y_0 = 0$, the formerly unstable on-state O_2 gains stability through a vertical torus bifurcation. Near the torus bifurcation parameter the transition between the two modes is very slow. This scenario agrees precisely with the behavior observed in the simulations of system (3.2), (3.4). It corresponds to scenario (T1) of section 4.2.1 and proves that stable pulsations of mode beating type do not occur between two modes with very different frequencies if we have only one active section. The first-order averaged model (4.36)–(4.38) is not able to resolve what happens in the tiny parameter region near $y_0 = 0$ ($y_0 = O(\mu)$, see Lemma 4.5).

4.2.4 Interaction Between a Self-pulsating Mode and an On-state — Bifurcation Study for a Simple Model of G_1 and G_2

In this section, we present a simple mechanism for mode interaction between two modes with different frequencies explaining the phenomena (T2) and (T3) shown in

section 4.2.1. We concluded in the previous section that we have trivial dynamics between \mathcal{S}_1 and \mathcal{S}_2 if y is always near 0, or if $G_1(y) - G_2(y)$ does not have any sign changes. Hence, the mechanism for the mode interaction presented in section 4.2.1 must be the interplay between sign changes of $G_1(y) - G_2(y)$ for different y and a self-pulsation within at least one of the invariant planes \mathcal{S}_1 and \mathcal{S}_2 .

We pointed out in section 4.2.3 that system (4.36), (4.37), (4.38) is a singular perturbation of the situation $G_1 = G_2$. In order to keep the presentation concise, we consider the following simplified parameter situation:

Firstly, assume that there is a stable self-pulsation within \mathcal{S}_1 and a stable equilibrium O_2 within \mathcal{S}_2 . We introduce the nonlinearity in $G_1(y) - G_2(y)$ by a y^2 -term in G_2 . The coefficient in front of y^2 is typically of order δ after rescaling (4.23). Thus, we introduce the parameters μ and γ and consider

$$\begin{aligned} G_1(y) &= y \\ G_2(y) &= y - \delta (\mu + \gamma y^2). \end{aligned}$$

We study the parameter points (μ, γ) in the vicinity of $\mu = \gamma = 0$. Secondly, we set $\alpha = 1$, $R_2(y) = 1$ and drop the index 1 of R_1 to reduce the consideration of the fast subsystem exactly to the single-mode case studied in section 4.1. Moreover, let the parameters of R_1 be of similar magnitude as in section 4.1, i. e., $A = O(1)$, $y_r = O(1)$ ($y_r < y_{r,+}$), $w = O(1)$. We shift x to $x_{\text{new}} = x_{\text{old}} + \log R(0, r)$. This modifies (4.37) such that the system under consideration reads

$$\dot{x} = y - \delta(1 - r) (\mu + \gamma y^2) \varrho(r) \quad (4.42)$$

$$\dot{y} = 1 - \delta/I y - (1 + \delta y) \frac{R(y, r)}{R(0, r)} e^x. \quad (4.43)$$

$$\dot{r} = \delta(\mu + \gamma y^2)(r - r^2) \quad (4.44)$$

where

$$\begin{aligned} R(y, r) &= 1 + \frac{rA\delta^2 w^2}{(y - y_r)^2 + \delta^2 w^2} \\ \varrho(r) &= 1 - r \partial_r R(0, r) / R(0, r). \end{aligned}$$

System (4.42)–(4.44) is singularly perturbed. Its slow variable is the ratio r . In the singular limit $\mu = \gamma = 0$, the phase space \mathbb{R}^3 is foliated by the planes $r = \text{const}$. The fast subsystem

$$\dot{x} = y \quad (4.45)$$

$$\dot{y} = 1 - \frac{\delta}{I} y - (1 + \delta y) \frac{R(y, r)}{R(0, r)} e^x. \quad (4.46)$$

is the single mode equation described in section 4.1 in each slice r . The variable r acts as a parameter in the singular limit and changes the amplitude rA of the Lorentzian curve R . We have shown in section 4.1 that the attraction rate of limit cycles or equilibria of (4.45), (4.46) is of order δ . Thus, if μ and γ are small, the variable r is slow compared to this attraction rate.

For $\mu\gamma > 0$, we have trivial dynamics between \mathcal{S}_1 and \mathcal{S}_2 since \dot{r} has always the same sign as μ in this case. We consider the case $\mu\gamma \leq 0$ in the next sections.

4.2.5 Geometric Shape of the Slow Manifold

Let $\mu = \gamma = 0$. Then, r is constant in time. There is a family \mathcal{E} of equilibria ($x = 0, y = 0$) of the fast subsystem (4.45), (4.46) parametrized by r . This family

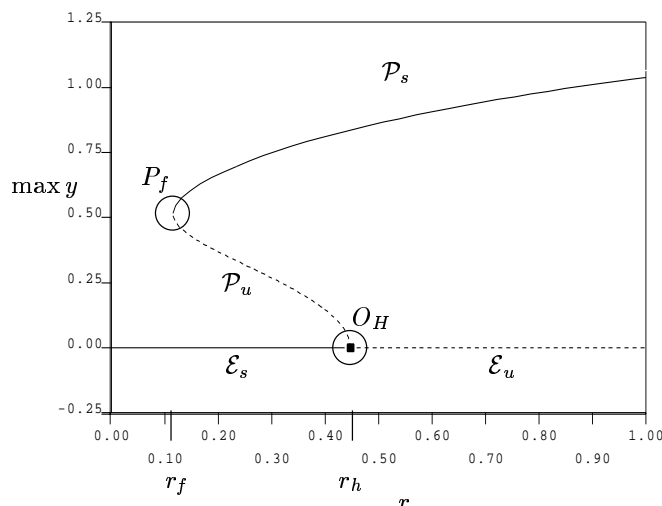


Figure 4.5: Stable and unstable parts of the slow manifold. The relation between η and $\max y$ is: $\max y = \sqrt{2}\eta$. We denote the fold periodic orbit by P_f . It appears at r_f . The Hopf point is denoted by O_H . The parameter values in (4.45), (4.46) are: $y_r = -0.5$, $A = 1$, $\delta = 0.06$, $w = 2$, $I = 2$.

undergoes a Hopf bifurcation if $y_r \in (y_{r,-}, y_{r,+})$. The Hopf parameter value is (according to (4.12))

$$r_h = -\frac{1}{A} \frac{(y_r^2 + w^2\delta^2)^2(1 + I^{-1})}{w^2\delta((1 + I^{-1})\delta(y_r^2 + w^2\delta^2) + 2y_r)} = \frac{-y_r^3}{2\delta A w^2} (1 + I^{-1}) + O(\delta). \quad (4.47)$$

\mathcal{E} is split into a family of stable equilibria \mathcal{E}_s and unstable equilibria \mathcal{E}_u at r_h if $r_h \in (0, 1)$. Moreover, a branch \mathcal{P} of periodic orbits of (4.45), (4.46) emerges at $O_H = (x = 0, y = 0, r = r_h)$. The self-pulsation in \mathcal{S}_1 is the other end of the branch \mathcal{P} . We show a numerically computed example of \mathcal{P} in Fig. 4.5. In this case, the Hopf bifurcation is unstable (subcritical) and the periodic branch has a fold P_f at $r = r_f$. This fold splits the branch \mathcal{P} into an unstable part \mathcal{P}_u and a stable part \mathcal{P}_s . Using the definition (4.13), φ , η and r are cylindrical coordinates in the phase space of system (4.42)–(4.44).

Furthermore, the analysis of section 4.1 has shown that the trajectories of the fast subsystem (4.45), (4.46) are small perturbations of the level lines $\eta = \text{const}$ on time-scales of order $O(1)$ in at least the following two constellations:

- (C1) rA is sufficiently small. Then, (4.45), (4.46) is a small perturbation of the weakly damped oscillator $\ddot{x} = 1 - \delta/I\dot{x} - (1 + \delta\dot{x})e^x$. Hence, all trajectories of (4.45), (4.46) are perturbations of order $\max\{rA, \delta\}$ of the level lines $\eta = \text{const}$. The fold point r_f is of order $\sqrt{\delta}$ according to (4.19).

(C2) η has a positive distance from $[\eta_r, \eta_u(r)]$ (see (4.14) where A has to be replaced by rA). Within this region, Corollary 4.4 applies such that the trajectories of (4.45), (4.46) are perturbations of order $O(\delta)$ of the level lines $\eta = \text{const}$.

We exploit the proximity of the trajectories to level lines of η and the time-scale difference between $\dot{\varphi}$ and $\dot{\eta}$ to perform one more averaging step to eliminate the rotation along φ in section 4.2.6. If (C1) and (C2) are violated (rA of order $O(1)$ and η in a small environment of $[\eta_r, \eta_u(r)]$), η may increase more rapidly ($\dot{\eta}$ may be of order $O(1)$ and strictly positive).

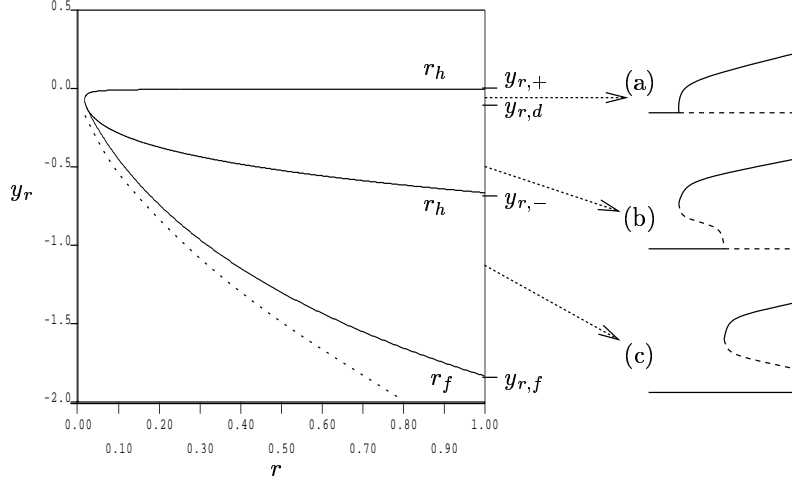


Figure 4.6: Continuation of r_h and r_f with respect to y_r . The Hopf line r_h is given by (4.47). The dotted line is the asymptotic approximation of the fold line according to equation (4.19). The values $y_{r,\pm}$ are the Hopf parameters of the single-mode system in \mathcal{S}_1 , $y_{r,f}$ is its fold parameter. For $y_r = y_{r,d}$, the Hopf point r_h becomes degenerate. The sketches beside the bifurcation diagram show how the families \mathcal{E} and \mathcal{P} look like for (a) $y_r \in (y_{r,d}, y_{r,+})$, (b) $y_r \in (y_{r,-}, y_{r,d})$, (c) $y_r \in (y_{r,f}, y_{r,-})$. Fig. 4.5 corresponds to case (b). The parameters A , w , δ and I are as in Fig. 4.5

In order to obtain all possible constellations for \mathcal{E} and \mathcal{P} , we continue the Hopf parameter value r_h (using (4.47)) and the fold parameter value r_f (numerically, or using (4.19)) with respect to y_r . The bifurcation diagram Figure 4.6 was reported in [44] for the unscaled single-mode system (4.3), (4.4).

Fig. 4.6 shows three possible generic constellations:

- (a) For $y_r \in (y_{r,d}, y_{r,+})$, the Hopf bifurcation at r_h is stable (supercritical) and the entire family of periodic orbits is stable ($\mathcal{P} = \mathcal{P}_s$).
- (b) For $y_r \in (y_{r,-}, y_{r,d})$, the Hopf bifurcation at r_h is unstable (subcritical) and the family of periodic orbits \mathcal{P} has a fold at r_f splitting it into a stable part \mathcal{P}_s and an unstable part \mathcal{P}_u .
- (c) For $y_r \in (y_{r,f}, y_{r,-})$, \mathcal{E} and \mathcal{P} are not connected anymore. The complete line of equilibria \mathcal{E} is stable such that Theorem 4.6 applies locally around \mathcal{E} . The

family of periodic orbits is split by a fold at r_f into a stable part \mathcal{P}_s and an unstable part \mathcal{P}_u .

At $y_r = y_{r,d}$, the first Lyapunov coefficient at the Hopf point r_h vanishes such that we have a generalized Hopf bifurcation (Bautin bifurcation) at this point. We observe that the family of fold periodic orbits emerges there.

4.2.6 Averaging of the Rotation in the Fast Subsystem

We perform another averaging step within the fast subsystem to reduce the dimension of the system once more to a two-dimensional system. This allows for an easy study of the bifurcation scenarios because the objects become much simpler (i. e., periodic solutions become fixed points, invariant tori become periodic solutions). Thereafter, we have to investigate how the results obtained from the analysis of the averaged system persist under the fast periodic perturbation.

Let us introduce the new variable $z = \log(r/(1-r)) \in (-\infty, \infty)$ ($r(z) = e^z/(1+e^z)$). Then, z satisfies the differential equation

$$\dot{z} = \delta(\mu + \gamma y^2). \quad (4.48)$$

The variables z and r are equivalent between the invariant planes \mathcal{S}_1 and \mathcal{S}_2 . In z, x, y , the phase space of system (4.42), (4.43), (4.48) is the whole \mathbb{R}^3 , and the variables z, η and φ are cylindrical coordinates in \mathbb{R}^3 . The limit $r \rightarrow 1$ corresponds to $z \rightarrow \infty$, and $r \rightarrow 0$ corresponds to $z \rightarrow -\infty$. We define the Hopf point of the fast subsystem $z_h = \log(r_h/(1-r_h))$, and the fold point $z_f = \log(r_f/(1-r_f))$, respectively (see Fig. 4.5).

System (4.42), (4.43), (4.48) induces a first-return map $(\tilde{z}(z, \eta), \tilde{\eta}(z, \eta))$ to the half-plane $\{\varphi = 0\}$ for $\eta \geq \eta_l > 0$. In the following Lemma 4.7, we exploit that η and φ operate on different time scales and write an approximate equation for the first-return map. Beforehand, we introduce the following functions:

Let $T(\eta)$ be the period of the periodic orbit of the conservative oscillator $\ddot{x} = 1 - e^x$ along the level line η ($\eta^2 = (\dot{x})^2/2 + e^x - x - 1$). Let $Y^2(\eta)$ be the integral of $(\dot{x})^2$ along this orbit. For simpler calculations, we can approximate T and Y^2 by their Taylor series:

$$\begin{aligned} T(\eta) &= 2\pi + \frac{\pi}{6}\eta^2 + \frac{\pi}{240}\eta^4 + \dots \\ Y^2(\eta) &= 2\pi\eta^2 + \frac{\pi}{12}\eta^4 + \dots \end{aligned} \quad (4.49)$$

Let $\tilde{\eta}_1(r, \eta) = \eta + g(r, \eta)$ be the first return map of the single mode system (4.45), (4.46) with r as parameter. Then, we have $g(r, 0) = 0$. Moreover, we have obtained an approximation of order $O(\delta^2)$ of g in section 4.1:

$$\begin{aligned} \frac{g(r, \eta)}{\delta} &= -(I^{-1} + 1) \frac{Y^2(\eta)}{2\eta} \\ &\quad - \frac{\pi r A \omega y_r}{2\eta} \left[\frac{\left[1 - \frac{rA}{e^{-x_r^-} - 1}\right]^{-\frac{1}{2}}}{e^{-x_r^-} - 1} + \frac{\left[1 + \frac{rA}{1 - e^{-x_r^+}}\right]^{-\frac{1}{2}}}{1 - e^{-x_r^+}} \right] + O(\delta) \end{aligned} \quad (4.50)$$

where $x_r^\pm = \tilde{x} \left(\pm \sqrt{\eta^2 - y_r^2/2} \right)$ and \tilde{x} is defined by (4.16). However, this approximation is valid only if the difference $\eta - \eta_u(r)$ is greater than 0 and of order $O(1)$ ($\eta_u^2(r) = y_r^2 + (1 + rA)^{-1} + \log(1 + rA) - 1$, see (4.14)).

Now, we can approximate the first-return map of system (4.42), (4.43), (4.48) to the half-plane $\{\varphi = 0\}$ for $\eta \geq \eta_l > 0$ with the help of the functions T , Y^2 and g :

Lemma 4.7 *Let $\eta \geq \eta_l > 0$ and z satisfy one of the following two conditions:*

1. $r(z)A$ is of order $o(1)$.
2. η has a positive distance of order $O(1)$ from $[\eta_r, \eta_u(r(z))]$.

Let $h = \sqrt{\mu^2 + \gamma^2}$ and δ be sufficiently small. In case 1, define $\tilde{\delta} = \max\{\delta, r(z)A\}$, and, in case 2, let $\tilde{\delta} = \delta$. Then, we can approximate the first-return map of system (4.42), (4.43), (4.48) to the half-plane $\{\varphi = 0, \eta \geq \eta_l\}$ by

$$\tilde{z}(z, \eta) = z + \delta(\mu T(\eta) + \gamma Y^2(\eta)) + O(h\delta\tilde{\delta}) \quad (4.51)$$

$$\tilde{\eta}(z, \eta) = \eta + g(r(z), \eta) + O(h\delta). \quad (4.52)$$

Proof: Let $(z(t), \eta(t), \varphi(t))$ be the trajectory starting at $(z = z_*, \eta = \eta_* \geq \eta_l, \varphi = 0)$ and $T(z_*, \eta_*, \delta, \mu, \gamma)$ the time for the first return. Denote the trajectory in the singular limit $\mu = \gamma = 0$ starting at the same point by $(z_*, \eta_1(t), \varphi_1(t))$ and its first-return time by $T(z_*, \eta_*, \delta, 0, 0)$, and the periodic orbit of $\ddot{x} = 1 - e^x$ along the level line η_* by $\varphi_0(t)$. We use the triangle inequality for these trajectories to prove (4.51), (4.52).

According to section 4.2.5, we have $\eta_1(t) - \eta_* = O(\tilde{\delta})$, $\varphi_1(t) - \varphi_0(t) = O(\tilde{\delta})$ and $T(z_*, \eta_*, \delta, 0, 0) - T(\eta_*) = O(\tilde{\delta})$ if η_* satisfies condition 1 or 2. Moreover, the right-hand-side of (4.42), (4.43) is Lipschitz continuous with respect to r , and, hence, z (uniformly with respect to δ and h). Thus, we get $\eta(t) - \eta_1(t) = O(h\delta)$, $\varphi(t) - \varphi_1(t) = O(h\delta)$ and $T(z_*, \eta_*, \delta, \mu, \gamma) - T(z_*, \eta_*, \delta, 0, 0) = O(h\delta)$ since \dot{z} is of order $O(h\delta)$. This implies (4.52), $\eta(t) - \eta_* = O(\tilde{\delta})$ and $\varphi(t) - \varphi_0(t) = O(\tilde{\delta})$. Since $y(\eta, \varphi)$ is Lipschitz continuous with respect to its arguments, the first return map \tilde{z} is

$$\begin{aligned} \tilde{z}(z_*, \eta_*) &= \int_0^{T(z_*, \eta_*, \delta, \mu, \gamma)} \delta(\mu + \gamma y^2(\eta(t), \varphi(t))) dt \\ &= \int_0^{T(\eta_*)} \delta(\mu + \gamma y^2(\eta_*, \varphi_0(t))) dt + O(h\delta\tilde{\delta}). \end{aligned}$$

□

Lemma 4.7 implies for the variable r the first-return map

$$\tilde{r}(r, \eta) = r + (\delta(\mu T(\eta) + \gamma Y^2(\eta) + O(h\delta\tilde{\delta}))r(1 - r). \quad (4.53)$$

Moreover, we observe that the first-order averaged equations for z and η

$$\dot{z} = \frac{\delta}{2\pi}(\mu T(\eta) + \gamma Y^2(\eta)) \quad (4.54)$$

$$\dot{\eta} = \frac{1}{2\pi}g(r(z), \eta) \quad (4.55)$$

have asymptotically (up to order $O(\tilde{\delta})$) the return map (4.51), (4.52) within the region where the conditions 1 and 2 of Lemma 4.7 are satisfied. Hence, within this region we can consider the averaged equations (4.54), (4.55) instead of the first-return map.

The averaged equation for r reads (according to (4.54))

$$\dot{r} = \frac{\delta}{2\pi}(\mu T(\eta) + \gamma Y^2(\eta))r(1 - r). \quad (4.56)$$

4.2.7 Discussion of the Two-dimensional System

We are now in the position to analyse the averaged system (4.55), (4.56) (or (4.54)) completely. We distinguish several cases depending on the geometric shape of the root curve of $g(r, \eta)$. This root curve coincides with the families of equilibria and periodic orbits of the fast subsystem shown in Fig. 4.5 for a particular set of parameters. Hence, the curve $\{(r, \eta) : g(r, \eta) = 0\}$ is depicted in Fig. 4.5, and we have outlined in Fig. 4.6 how the shape of this curve may look like in principle. Since we do not know the complete curve analytically, our bifurcation analysis is in part only qualitative. The curve $g(r, \eta) = 0$ has several branches (denoted by $\mathcal{P}_{u,s}$ and $\mathcal{E}_{u,s}$ in Fig. 4.5). We refer to the stability of these branches according to the stability of the corresponding fixed point or periodic orbit in the fast subsystem.

Invariant Lines System (4.55), (4.56) has the invariant lines $\eta = 0$, $r = 1$ and $r = 0$ (the planes \mathcal{S}_1 and \mathcal{S}_2 in system (4.42), (4.43), (4.44)). The direction of motion is described correctly along $\eta = 0$ according to Theorem 4.6. The stability is also described correctly if we are not in the vicinity of r_h . Generally, we have perturbed invariant curves $\tilde{\mathcal{E}}_s$ (for $r < r_h$) and $\tilde{\mathcal{E}}_u$ (for $r > r_h$) in the vicinity of $\eta = 0$ which are split near r_h in system (4.42)–(4.44).

The motion near the invariant lines $r = 0$, $r = 1$ is described correctly, since the approximation error for the motion of r is of order $O(h\delta\tilde{\delta}) \cdot r(1 - r)$ (see (4.53)).

Transition of Stability from or to Single-mode Planes — Parametric Families of Equilibria System (4.55), (4.56) has the equilibria $O_1 = (r = 1, \eta = 0)$ and $O_2 = (r = 0, \eta = 0)$. If $\mu > 0$, O_1 is stable along the line $\eta = 0$, and O_2 is unstable along $\eta = 0$ (vice versa if $\mu < 0$). O_2 is stable along $r = 0$, and O_1 is unstable along $r = 1$ if $y_r > y_{r,-}$ and stable if $y_r < y_{r,-}$ (see Fig. 4.6). Moreover, we have a fixed point $P_1 = (r = 1, \eta = \eta_s)$ corresponding to the self-pulsation in \mathcal{S}_1 where the stable branch of the root curve $g(r, \eta) = 0$ intersects the line $r = 1$ (i. e. $g(1, \eta_s) = 0$). P_1 is stable along $r = 1$. The stability transversal to $r = 1$ is

determined by the linearization of (4.56). We obtain the following corollaries using that $\partial_r g(r, \eta) > 0$ for all $r \in [0, 1]$ and $\partial_\eta g(r, \eta) < 0$ for (r, η) in the vicinity of P_1 :

Corollary 4.8 *Consider μ and γ within a sufficiently small ball of radius h around $(0, 0)$ in the parameter plane of (μ, γ) . A line \mathcal{T} of transcritical bifurcations through $(0, 0)$ tangent to $\{\mu T(\eta_s) + \gamma Y^2(\eta_s) = 0\}$ is the stability boundary for P_1 . For $\mu > 0$, $\gamma < 0$, P_1 passes its stability to a fixed point P_r with $r < 1$ which becomes stable. For $\mu < 0$, $\gamma > 0$, P_1 passes its instability to a fixed point P_r with $r < 1$ which becomes unstable and separates the stable equilibrium O_2 and the stable fixed point P_1 .*

The stability follows immediately from the linear stability analysis at the fixed points P_1 and P_r , respectively.

Moreover, we can exploit that $Y^2(\eta)/T(\eta)$ is monotone increasing and that the equation $g(r, \eta) = 0$ is uniquely solvable w. r. t. r for all $\eta \in (0, \eta_s)$ to obtain:

Corollary 4.9 *Let μ and γ be within a sufficiently small ball of radius h around $(0, 0)$ in the parameter plane of (μ, γ) .*

- (1) *Assume that the root curve of g connects P_1 and the invariant line $\eta = 0$. Then, for each pair (μ, γ) with $-\mu/\gamma \in (0, Y^2(\eta_s)/T(\eta_s))$, we have exactly one fixed point P with $r \in (0, 1)$ and $\eta \in (0, \eta_s)$.*
- (2) *Assume that the root curve of g connects P_1 and another fixed point P'_1 at $\eta = \eta_i$ on the invariant line $r = 1$. Then, for each pair (μ, γ) with $-\mu/\gamma \in (Y^2(\eta_i)/T(\eta_i), Y^2(\eta_s)/T(\eta_s))$, we have exactly one fixed point P with $r \in (0, 1)$ and $\eta \in (\eta_i, \eta_s)$.*

Case (1) corresponds to the shapes (a) and (b) of the root curves of g shown in Fig. 4.6, case (2) corresponds to shape (c). However, Corollary 4.9 depends on our specific choice of the nonlinearity of $G_1 - G_2$. A fixed point with $r \in (0, 1)$ is hyperbolic if it is situated on the hyperbolic parts of the branches of the curve $g(r, \eta) = 0$ (i. e., not in the vicinity of the fold P_f or the branch point O_H as shown in Fig. 4.5) since η is fast compared to r there.

The transcritical bifurcation and the family of fixed points branching from P_1 persist under the periodic perturbation to system (4.42), (4.43), (4.44) since P_1 is located within the region where Lemma 4.7 applies. Indeed, Corollary 4.8 follows directly from the approximation of the first-return map (4.52), (4.53). We can use the approximation (4.50) for $g(r, \eta)$ to approximate the corresponding periodic orbits of (4.42), (4.43), (4.44).

Stability near Supercritical Hopf Point The previous paragraph has shown that fixed points of the averaged system (4.55), (4.56) with $r \in (0, 1)$ may change their stability only near the degenerate points of the curve $g(r, \eta) = 0$, i. e. near the branching point $O_H = (r = r_h, \eta = 0)$ or near the fold $P_f = (r = r_f, \eta = \eta_f)$.

Firstly, let us consider the case (a) of Fig. 4.6 and $\mu > 0$: $g(r, \eta)$ does not have a fold, its branching point corresponds to a supercritical Hopf bifurcation, and its

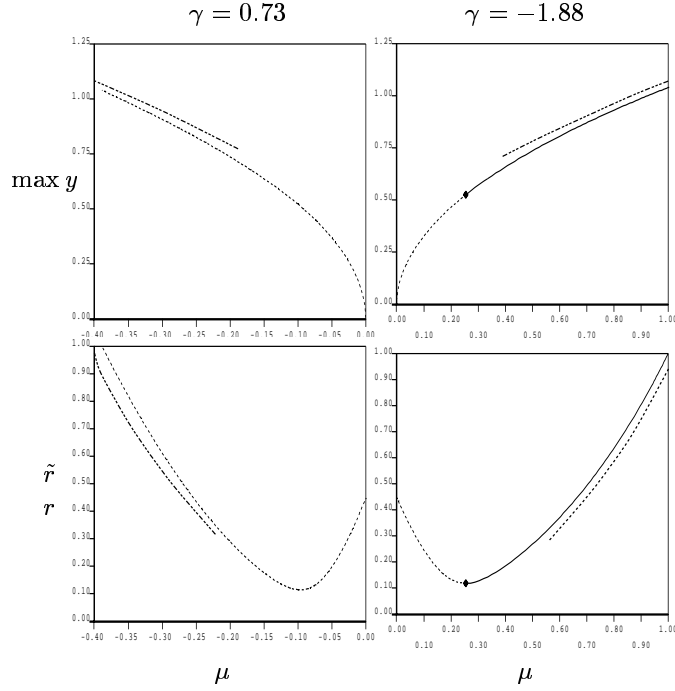


Figure 4.7: Comparison between the averaged approximations and the numerically computed periodic solutions of system (4.42)–(4.44) for varying μ between 0 and the transcritical bifurcation value for $\gamma = -1.88$ and $\gamma = 0.73$: The dotted lines correspond to the predictions solving $g(r, \eta) = 0$, $\mu T(\eta) + \gamma Y^2(\eta) = 0$ using (4.49) and (4.50). The solid and dashed lines show the numerically obtained periodic orbits of system (4.42)–(4.44) (solid means stable, dashed unstable). We show the predicted maximum of the y -component (which corresponds to $\sqrt{2}\eta$ in the solution of (4.55), (4.56)) and r . Since r is not constant in time for the numerical solutions of (4.42)–(4.44) we report $\bar{r} = \oint r$ for comparison.

entire branch is stable for $\eta > 0$. According to Corollary 4.9, we obtain a family of fixed points $P_r = (r, \eta)$ on this branch for varying ratio $-\mu/\gamma$. These fixed points are stable if η is not small, i. e., P_r is not in the vicinity of O_H .

For small η we can expand the function $g(r, \eta)$ near O_H dropping higher order terms of η :

$$g(z, \eta) = \delta\eta(z - a\eta^2)$$

where we use the coordinate z instead of r for convenience, shift z by z_h (such that $O_H = (z = 0, \eta = 0)$), and assume $a > 0$ (supercriticality). Moreover, we drop all terms of order $O(\eta^4)$ or greater in $T(\eta)$ and $Y^2(\eta)$ ending up with an approximation for the vicinity of O_H :

$$\dot{\eta} = \eta(z - a\eta^2) \quad (4.57)$$

$$\dot{z} = (\mu + (\gamma + \mu/12)\eta^2) = \mu(1 - \lambda^{-1}\eta^2) \quad (4.58)$$

introducing the parameter $\lambda = -(\gamma/\mu + 1/12)^{-1} > 0$ and changing the time-scale to $t_{\text{new}} = \delta t_{\text{old}}$. This system has an equilibrium at $P = (z = a\lambda, \eta = \sqrt{\lambda})$. The

Jacobian of (4.57), (4.58)

$$J_P = \begin{pmatrix} -2a\lambda & \sqrt{\lambda} \\ -2\mu/\sqrt{\lambda} & 0 \end{pmatrix}$$

has a pair of stable complex eigenvalues for sufficiently small λ . Their decay rate is $a\lambda$.

In the case $\mu < 0$, the fixed points on the branch $g(r, \eta) = 0$ are saddles. We can use the same asymptotic model near O_H as for the case $\mu > 0$. The determinant of the Jacobian $\det(J_P) = 2\mu$ is negative implying that the fixed points remain saddles near O_H .

Appearance of Limit Cycles near Fold Next, we consider the cases (b) and (c) outlined in Fig. 4.6 for the shape of the curve $g(r, \eta) = 0$, and $\mu > 0$. Then, the fixed point $P_r = (r, \eta)$ on the stable branch of $g(r, \eta) = 0$ is stable for decreasing $-\mu/\gamma$ (and η) until it approaches the vicinity of the fold point $P_f = (r_f, \eta_f)$. Due to Corollary 4.9 the family continues through the fold point to the unstable branch of $g(r, \eta) = 0$. For $-\mu/\gamma < Y^2(\eta_f)/T(\eta_f)$ and $\eta < \eta_f$, the fixed point is unstable in both directions. Hence, the fixed point must lose its stability in the vicinity of the fold through a Hopf bifurcation.

Again, we can expand the function g near P_f dropping higher order terms of $\eta - \eta_f$:

$$g(z, \eta) = z - b \cdot (\eta - \eta_f)^2$$

where we use again the variable z shifted by z_f (such that $P_f = (0, \eta_f)$) and assume $b > 0$ (fold turns to the right). Then, the fixed point $P = (z, \eta)$ has the form $z = b(\eta - \eta_f)^2$ where $Y^2(\eta)/T(\eta) = -\mu/\gamma$. The Jacobian in P is

$$J_P = \begin{pmatrix} -2b(\eta - \eta_f) & 1 \\ \delta(\mu T'(\eta) + \gamma(Y^2)'(\eta)) & 0 \end{pmatrix}$$

where $\mu T'(\eta) + \gamma(Y^2)'(\eta) < 0$. The eigenvalues become complex for η in a very small neighborhood of η_f (since δ is small) and change their sign at $\eta = \eta_f$ implying a Hopf bifurcation.

This situation has been studied extensively in e. g. [1] [3], [4], with special regard to the slow-fast character of the system (z is slow, η fast in our case). It is typically referred to as *singular Hopf bifurcation* since the branch of periodic solutions is almost vertical. The small-amplitude periodic solutions are called *Canard* solutions as they follow the unstable branch of $g(r, \eta) = 0$. Moreover, the stability and the position of the Canard periodic orbits is difficult to determine due to the verticality of the branch.

There is no bifurcation near the fold P_f in the case $\mu < 0$: The determinant of J_P is negative, since $\mu T'(\eta) + \gamma(Y^2)'(\eta) > 0$ for $\eta \approx \eta_f$. Hence, the family of fixed points consists of saddles along the entire curve $g(r, \eta) = 0$ (for $\eta > 0$).

The results of this paragraph imply the existence of a torus bifurcation in system (4.42), (4.43), (4.44) near P_f for $\mu > 0$. The conditions of Lemma 4.7 are satisfied

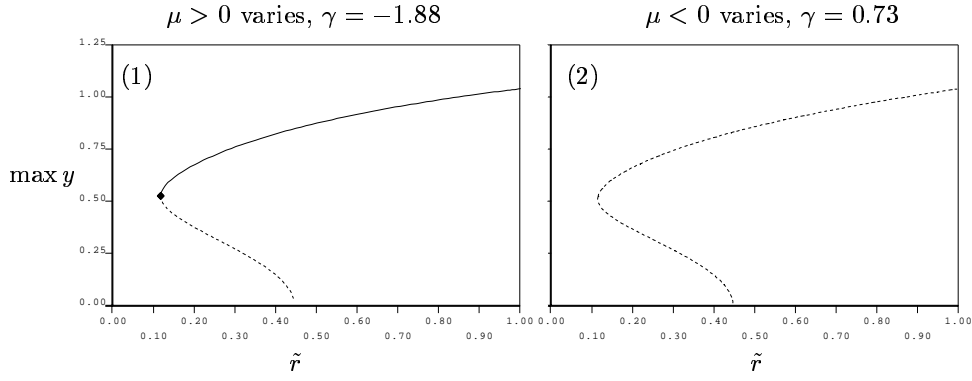


Figure 4.8: Families of periodic orbits between the invariant planes $r = 0$ and $r = 1$. The parameters are $y_r = -0.5$, $A = 1$, $I = 2$, $w = 2$, $\delta = 0.06$.

if rA is of order $o(1)$. Then, the averaged system is an approximation of order $o(1)$. We get a crude approximation of the torus bifurcation if we insert $\eta_f = \eta_r = y_r/\sqrt{2}$ for the location of the fold in phase space (as in section 4.1) and obtain $-\mu/\gamma = Y^2(y_r/\sqrt{2})/T(y_r/\sqrt{2})$. Since the Hopf bifurcation in the averaged system is nearly vertical, the torus bifurcation must be almost vertical, too. For $\mu < 0$, $\gamma > 0$, we can deduce that the family of saddle periodic orbits near $g(r, \eta) = 0$ continues through the fold.

Note that the averaged system (4.55), (4.56) can not be used to determine the behavior on the vertical branch from the torus bifurcation (neither the position in phase space nor the normal hyperbolicity of the tori). The averaged equations approximate system (4.42)–(4.44) up to order $O(\tilde{\delta})$ whereas the parameter region for the solutions of the vertical branch is exponentially small.

We computed the family of periodic orbits corresponding to fixed points along the branch $g(r, \eta) = 0$ numerically for varying $-\mu/\gamma$. The results are depicted in Fig. 4.8.

Continuation of the Families of Limit Cycles in Case (b) If the shape of the root curve of g is as depicted in Fig. 4.6 (b), system (4.42)–(4.44) coincides with the situation investigated in [23], [24]. The branch becomes a family of relaxation oscillations after its vertical part for $-\mu/\gamma \in (0, Y^2(\eta_f)/T(\eta_f))$. These relaxation oscillations pass periodically through the branch point $O_H = (r = r_h, \eta = 0)$ of $g(r, \eta)$ along the invariant line $\eta = 0$ with increasing r and through the fold point $P_f = (r_f, \eta_f)$ with decreasing r (see Fig. 4.9 sketch (2a)). The trajectory is subject to a delayed loss of stability near O_H in each period of its oscillation. There must exist corresponding oscillations in system (4.42)–(4.44) which are typically referred to as *subcritical elliptic bursting*. The passage through O_H is in fact a slow passage through a Hopf bifurcation.

For this kind of “dynamic Hopf bifurcations”, it has been shown in [31] how the location of the departure from $\eta = 0$ depends on the location of the approach to $\eta = 0$ for analytical systems. In particular, it was demonstrated (also in [5]) that

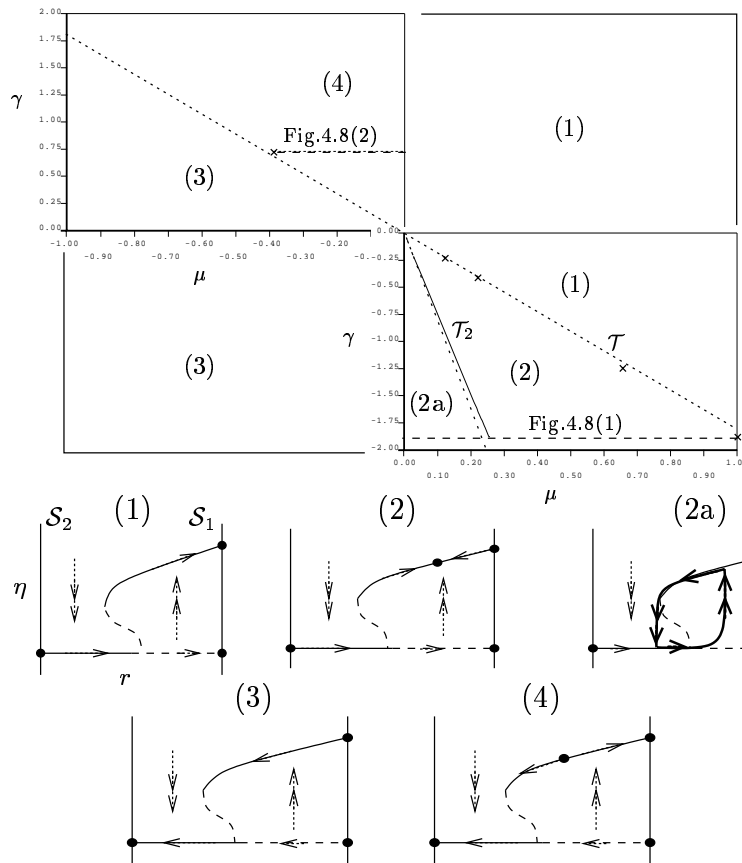


Figure 4.9: Bifurcation diagram for μ and γ for case (b) of Fig. 4.6. The crosses are the numerically computed transcritical bifurcations of the self-pulsation in S_1 . (AUTO cannot continue transcritical bifurcations.) The dotted line \mathcal{T} is the asymptotic line $\mu T(\eta_s) + \gamma Y^2(\eta_s)$ where $g(1, \eta_s) = 0$ using the approximations (4.49), (4.50). The solid line \mathcal{T}_2 is the numerically computed line of torus bifurcations. The dotted line nearby is the approximation assuming that the fold P_f is at the level $\eta_r = y_r/\sqrt{2}$, and that the torus bifurcation is at the fold. The dashed lines are the cuts through the parameter plane presented in Fig. 4.8. The sketches below the diagram depict the averaged system (4.55), (4.56) (as in Fig. 4.5). The fast motion of η is shown by double arrows and the slow drift along the curve $g(r, \eta) = 0$ as simple arrows. Sketch (2a) corresponds to the subcritical elliptic bursting.

the departure may be at a distance of order $O(1)$ from r_h (*Slow Passage Effect*). However, this effect is extremely sensitive to non-smooth perturbations [31] or noise [5], [23]. Hence, it is not reflected correctly in the averaged system where we have always a delayed loss of stability.

Consequently, the torus corresponding to the oscillation of the averaged system does not need to be a quantitatively good approximation of the bursting type solution.

A canonical model for systems like (4.42)–(4.44) and a shape of $\{g(r, \eta) = 0\}$ as in Fig. 4.6 case (b) has been derived in [23] by perturbation analysis in the vicinity of the generalized Hopf point (see Fig. 4.6). The amplitude equations of [23] have the

same structure as (4.54), (4.55). It was pointed out that this structure implies the existence of subcritical elliptic bursting which is a frequently observed phenomenon in the dynamics of neurons.

Continuation of the Families of Limit Cycles in Case (c) If the shape of the root curve of g is as depicted in Fig. 4.6 (c), the family of periodic orbits of the averaged system ends in a homoclinic bifurcation at the saddle P'_1 (corresponding to the unstable limit cycle in the invariant plane \mathcal{S}_1 of system (4.42)–(4.44)). Since, the branch is nearly vertical with respect to the parameter $-\mu/\gamma$, this homoclinic bifurcation happens immediately nearby the Hopf bifurcation.

As in case (b), the averaging approximation is not sufficiently precise to allow conclusions about the behavior of system (4.42)–(4.44) in this tiny parameter region. However, we know that the torus bifurcation exists, and that only O_1 is stable for $-\mu/\gamma$ less than the torus bifurcation value already at a very small distance.

4.2.8 Generalization and Interpretation of the Bifurcation Diagram regarding the Original Quantities

We can use the results of section 4.2.7 to explain the mechanisms behind the scenarios shown for motivation in section 4.2.1.

First, we want to mention that the procedure of the section 4.2.4–4.2.7 can be generalized to arbitrary nonlinearities of $G_1(y) - G_2(y)$ in (4.36) and to other shapes of the manifold of periodic orbits \mathcal{P} of (4.37), (4.38). If we consider the general fast subsystem (4.37), (4.38) as a small perturbation of the conservative oscillator

$$\begin{aligned}\dot{x} &= rG_1(y) + (1-r)G_2(y) \\ \dot{y} &= 1 - re^x - (1-r)e^{\alpha x}\end{aligned}$$

with the conserved quantity $\eta(r, x, y)^2$, the periodic orbits are approximately equilibria of an averaged equation $\dot{\eta} = g(r, \eta)$ similar to (4.55). For each level line η , we may define the function

$$F(\eta) = \frac{1}{2\pi} \int_0^{T(\eta)} G_1(y(\varphi(t))) - G_2(y(\varphi(t))) dt \quad (4.59)$$

which is assumed to be small compared to g . Then, we can study the general averaged system

$$\begin{aligned}\dot{\eta} &= \tilde{g}(\eta, r) \\ \dot{r} &= F(\eta)r(1-r)\end{aligned} \quad (4.60)$$

where \tilde{g} may differ slightly from g because the level lines η can depend on r . We obtain approximations for periodic orbits of the general system (4.36)–(4.38) and their stability by investigating the equilibria of (4.60). In general, we can not expect that equilibria of (4.60) are always unique (in contrast to Corollary 4.9). However, we can conclude:

Corollary 4.10 *Let μ be an arbitrary parameter, let $P_1 = (r = 1, \eta = \eta_1)$ be a self-pulsation in the invariant plane $r = 1$. P_1 undergoes a transcritical bifurcation at $\mu = \mu_0$ if $F(\eta, \mu)$ changes its sign in η_1 at $\mu = \mu_0$. P_1 gains stability if the sign-change is from $-$ to $+$. It loses stability otherwise. We have a hyperbolic fixed point $(r(\mu), \eta(\mu))$ for $r < 1$ and $\mu \approx \mu_0$ if $\partial_r \tilde{g}(1, \eta_1) \neq 0$ and $\partial_\eta F(\eta_1) \neq 0$.*

This transcritical bifurcation is the mechanism for the appearance of the scenarios (T2) and (T3) presented in section 4.2.1. The self-pulsation is actually an invariant 2-torus in the full two-mode model (4.22) as well as in the PDE system (3.2), (3.4). However, this torus is invariant with respect to rotation $x \rightarrow xe^{i\varphi}$. Hence, we may eliminate this degree of freedom and treat the self-pulsation as a periodic orbit. Then, the transcritical bifurcation of Corollary 4.8 or 4.10 is a torus bifurcation from the self-pulsation. The emerging torus (an invariant 3-torus in the original coordinates) is stable and visible in regime (T3) of section 4.2.1 and it is unstable in scenario (T2). In (T2), the unstable torus separates the stable regions such that stable on-states and self-pulsations at the different ends of the stopband (i. e., in the invariant planes $r = 0$ and $r = 1$) coexist.

The solutions of bursting type (i. e., relaxation oscillations in the averaged system (4.55), (4.56)) would correspond to invariant 4-tori if they were persistent. However, the bursting solution is known to be very sensitive to non-analytic perturbations. But the bursting behavior, i. e., the slow drift back and forth between the two ends of the stopband, must be also present in the full two-mode system (4.22) and, hence, in the PDE system (3.2), (3.4).

A Physical Interpretation of the Traveling-Wave Equations — Discussion of Typical Parameter Ranges

A.1 Physical Interpretation of the Model

System (2.1)-(2.3) is well-known as a traveling wave model describing longitudinal dynamical effects in semiconductor lasers [29], [42], [50]. Results of numerical computations have been presented in [6], [8], [9], [35], [50].

The traveling wave equations (2.1), (2.2) describe the complex optical field E in a spatially modulated waveguide:

$$E(\vec{r}, t) = E(x, y) \cdot (\psi_1(t, z)e^{i\omega_0 t - \frac{\pi}{\Lambda}z} + \psi_2(t, z)e^{i\omega_0 t + \frac{\pi}{\Lambda}z}).$$

The complex amplitudes $\psi_{1,2}(t, z)$ are the longitudinally slowly varying envelopes of E . The transversal space directions are x and y , z is the longitudinal direction, and $\vec{r} = (x, y, z)$. For periodically modulated waveguides, Λ is longitudinal modulation wavelength. The central frequency is $\omega_0/(2\pi)$, and $E(x, y)$ is the dominant transversal mode of the waveguide.

The equations (2.1), (2.2) for an uncoupled waveguide ($\kappa = 0$) and a monochromatic light-wave in forward direction $e^{i\omega t}\psi_1(z)$ lead to a spatial shape of the power $|\psi_1|^2$ according to

$$\partial_z |\psi_1(z)|^2 = (2 \operatorname{Re} \beta(z) + 2 \operatorname{Re} \chi(i\omega, z)) |\psi_1(z)|^2 \quad (\text{A.1})$$

where

$$\chi(i\omega, z) = \frac{\rho(z)\Gamma(z)}{i\omega - i\Omega_r(z) + \Gamma(z)}. \quad (\text{A.2})$$

$2 \operatorname{Re} \chi(i\omega, z)$ is a Lorentzian intended to fit the gain curve of the waveguide material (see Fig. A.1). Hence, system (2.1), (2.2) produces gain dispersion, i. e., the spatial growth rate of the wave $e^{i\omega t}\psi(z)$ depends on its frequency ω . The variable $p(t, z)$ reports the internal state of the gain filter. See [39], [50] for more details. The Lorentzian gain filter is also used by [2], [29], [32].

The equation (2.3) is a simple rate equation for the spatially averaged carrier density. It accounts for the current I , the spontaneous recombination $-n_k/\tau_k$, and the stimulated recombination.

A.2 Scaling of the Variables

In order to obtain the dimensionless quantities used in (2.1)-(2.3) and their possible ranges we have to scale the time t and the spatial variable z such that the coefficient in front of $\partial_z \psi$ is ∓ 1 . Moreover, z is scaled such that $l_1 = 1$. The carrier density n_k in the section S_k is measured in multiples of the transparency carrier density (i. e. such that $G_k(1) = 0$ for $k \in \mathcal{S}_a$). See Table A.1 for typical ranges of the quantities and [20] for further explanations.

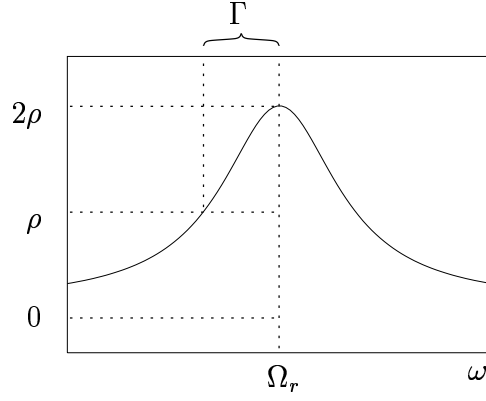


Figure A.1: Shape of the Lorentzian $2 \operatorname{Re} \chi(i\omega)$ for $\omega \in \mathbb{R}$ and visualization of its parameters (see Table A.1)

	typical range	explanation
$\psi(t, z)$	\mathbb{C}^2	optical field, forward and backward traveling wave
$i \cdot p(t, z)$	\mathbb{C}^2	nonlinear polarization for the forward and backward traveling wave
$n_k(t)$	(\underline{n}, ∞)	spatially averaged carrier density in section S_k
$\operatorname{Im} d_k$	\mathbb{R}	frequency detuning
$\operatorname{Re} d_k$	$< 0, (-10, 0)$	internal losses
$\alpha_{H,k}$	$(0, 10)$	negative of line-width enhancement factor
g_k	≈ 1	differential gain in active sections
κ_k	$(-10, 10)$	real coupling coefficients for the optical field ψ
ρ_k	$[0, 1)$	ρ_k is maximum of the gain curve
Γ_k	$O(10^2)$	half width of half maximum of the gain curve
$\Omega_{r,k}$	$O(10)$	resonance frequency
I_k	$O(10^{-2})$	current injection in section S_k
τ_k	$O(10^2)$	spontaneous lifetime for the carriers
P	$(0, \infty)$	scale of (ψ, p) (can be chosen arbitrarily)
r_0, r_L	$\mathbb{C}, r_0 , r_L < 1$	facet reflectivities
$\alpha(t)$	\mathbb{C}	optical input signal, potentially discontinuous in time

Table A.1: Ranges and explanations of the variables and coefficients appearing in (2.1)-(2.8). See also [50], [39] to inspect their relations to the originally used physical quantities and scales.

B Normally Hyperbolic Invariant Manifolds

In this appendix, we give a general definition of normal hyperbolicity applying to a general C^1 smooth manifold which is invariant with respect to some semiflow. Subsequently, we state the theorems on existence and persistence of invariant manifolds and invariant foliations for semiflows in Banach spaces as they can be found in [10], [11]. They are the basis for Theorem 3.7. However, we used the results on the persistence of normally hyperbolic invariant manifolds also in the well-known context [19], [49] of ordinary differential equations in chapter 4.

General Notation

Let X be a Banach space, and $T(t; x)$ be a C^1 semiflow on X ; that is $T(t; x)$ is continuous in t and x for $t \geq 0$, $T(t; \cdot) : X \rightarrow X$ is C^1 and $T(t+s; x) = T(t; T(s; x))$ for all $t, s \geq 0$ and $x \in X$.

Let $M \subset X$ be a C^1 connected T -invariant manifold, i. e., $T(t; M) \subset M$ for each $t \geq 0$. Denote the tangent bundle on X restricted to M by $TX|_M$ and the linearized semiflow by $DT(t) : TX \rightarrow TX$.

Definition B.1 *M is said to be normally hyperbolic, if there exists a continuous decomposition of $TX|_M$ into subbundles*

$$T|_M = X^c \oplus X^s \oplus X^u \quad \text{for } m \in M \quad (\text{B.1})$$

of closed subspaces (fibers) $X^{c,u,s}(m)$ with the following properties:

1. X_c is the tangent bundle of M .
2. The subbundles $X^{c,u,s}$ are invariant under DT , i. e.: Let $m \in M$, $m_1 = T(t; m)$ and $t \geq 0$. Then,

$$[DT(m)](t)|_{X^\alpha(m)} : X^\alpha(m) \rightarrow X^\alpha(m_1) \quad \text{for } \alpha = c, u, s$$

and $[DT(m)](t)|_{X^u(m)}$ is an isomorphism from $X^u(m)$ onto $X^u(m_1)$.

3. $X^{c,u,s}$ are distinguished by an exponential trichotomy, i. e., there exists a $\lambda < 1$ and a $t_0 \geq 0$ such that we have for all $m \in M$ and $t \geq t_0$

$$\lambda \inf_{\substack{x^u \in X^u \\ \|x^u\|=1}} \|[DT(m)](t)x^u\| > \max \{1, \|[DT(m)](t)|_{X^c(m)}\|\}$$

$$\lambda \min \{1, \inf_{\substack{x^c \in X^c \\ \|x^c\|=1}} \|[DT(m)](t)x^c\|\} > \|[DT(m)](t)|_{X^s(m)}\|$$

Remark: We may replace the Banach space X by a smooth manifold in the finite-dimensional context [19].

The main statements of [10], [11] can be summarized as follows:

Theorem B.2 (Persistence) *Suppose M is a C^1 compact connected normally hyperbolic invariant manifold with respect to $T(t; \cdot)$. Let $t_1 > 0$ be fixed and N be a fixed neighborhood of M .*

Then, there exists a $\sigma > 0$ such that if $\tilde{T}(t; x)$ is a C^1 semiflow in X which satisfies $\|\tilde{T}(t_1; \cdot) - T(t_1; \cdot)\|_{C^1(N)} < \sigma$, then \tilde{T} has a C^1 normally hyperbolic invariant manifold \tilde{M} which converges to M in the C^1 topology if $\|\tilde{T}(t_1; \cdot) - T(t_1; \cdot)\|_{C^1(N)}$ tends to 0.

Theorem B.3 (Center-stable and center-unstable manifolds)

Suppose M is a C^1 compact connected normally hyperbolic invariant manifold with respect to a C^1 semiflow $T(t; \cdot)$. Let $t_1 > t_0$ be fixed and $N(\varepsilon)$ be a sufficiently small tubular neighborhood of M .

T has unique C^1 invariant manifolds $W^{cs}(\varepsilon)$ and $W^{cu}(\varepsilon)$ in $N(\varepsilon)$ of M with the following properties:

1. $M = W^{cs}(\varepsilon) \cap W^{cu}(\varepsilon)$.
2. $W^{cs}(\varepsilon)$ and $W^{cu}(\varepsilon)$ are tangent to the center-stable vector bundle $X^c \oplus X^s$ and the center-unstable vector bundle $X^c \oplus X^u$ of M , respectively.
3. $T(t; W^{cs}(\varepsilon)) \cap N(\varepsilon) \subset W^{cs}(\varepsilon)$. $T(t; W^{cs}(\varepsilon))$ converges to M as $t \rightarrow \infty$, and

$$W^{cs}(\varepsilon) = \{x \in N(\varepsilon) : T(kt_1; x) \in N(\varepsilon) \text{ for all } k > 0.\}$$

4. $T(t_1; W^{cs}(\varepsilon)) \subset W^{cs}(\varepsilon)$;
5. $T(t_1; \cdot) : W^{cu}(\varepsilon) \cap (T(t_1; \cdot))^{-1}(W^{cu}(\varepsilon)) \rightarrow W^{cu}(\varepsilon)$ is a diffeomorphism. If we define $T(-t; \cdot)$ on $W^{cu}(\varepsilon)$ in this way, then $T(-t; W^{cu}(\varepsilon))$ converges to M as $t \rightarrow \infty$ and

$$W^{cu}(\varepsilon) = \{x \in N(\varepsilon) : \text{for all } k > 0, \text{ there exists a } y_k \in N(\varepsilon) \text{ satisfying } T(kt_1; y_k) = x\}$$

Theorem B.4 (Invariant foliations in center-stable manifold)

For small ε , there exists a unique family of C^1 submanifolds $\{W_m^{ss}(\varepsilon) : m \in M\}$ of $W^{cs}(\varepsilon)$ satisfying:

1. For each $m \in M$, $M \cap W_m^{ss}(\varepsilon) = \{m\}$, the tangent space $T_m W_m^{ss}(\varepsilon) = X_m^s$ varies continuously with respect to m on M .
2. If $m_1, m_2 \in M$ and $m_1 \neq m_2$, then $W_{m_1}^{ss}(\varepsilon) \cap W_{m_2}^{ss}(\varepsilon) = \emptyset$ and $W^{cs}(\varepsilon) = \bigcup_{m \in M} W_m^{ss}(\varepsilon)$.
3. For all $m \in M$, $T(t_1; W_m^{ss}(\varepsilon)) \subset W_{T(t_1; m)}^{ss}(\varepsilon)$.
4. For all $m \in M$ and $t > 0$, $T(t; W_m^{ss}(\varepsilon)) \cap N(\varepsilon) \subset W_{T(t; m)}^{ss}(\varepsilon)$.
5. For $x \in W_m^{ss}(\varepsilon)$ and $m \neq m_1 \in M$, we have

$$\frac{\|T(t; x) - T(t; m)\|}{\|T(t; x) - T(t; m_1)\|} \rightarrow 0 \quad \text{exponentially as } t \rightarrow +\infty.$$

6. For $x, y \in W_m^{ss}(\varepsilon)$, $\|T(t; x) - T(t; y)\| \rightarrow 0$ exponentially as $t \rightarrow \infty$.

Theorem B.5 (Invariant foliations in center-unstable manifold)

For small ε , there exists a unique family of C^1 submanifolds $\{W_m^{uu}(\varepsilon) : m \in M\}$ of $W^{cu}(\varepsilon)$ satisfying:

1. For each $m \in M$, $M \cap W_m^{uu}(\varepsilon) = \{m\}$, the tangent space $T_m W_m^{uu}(\varepsilon) = X_m^u$ varies continuously with respect to m on M .
2. If $m_1, m_2 \in M$ and $m_1 \neq m_2$, then $W_{m_1}^{uu}(\varepsilon) \cap W_{m_2}^{uu}(\varepsilon) = \emptyset$ and $W^{cu}(\varepsilon) = \bigcup_{m \in M} W_m^{uu}(\varepsilon)$.
3. For all $m \in M$, $T(t_1; \cdot) : W_m^{uu}(\varepsilon) \cap T(t_1; \cdot)^{-1} W_{T(t_1; m)}^{uu}(\varepsilon) \rightarrow W_{T(t_1; m)}^{uu}(\varepsilon)$ is a diffeomorphism.
4. For $x \in W_m^{uu}(\varepsilon)$, if $T(t; x) \in N(\varepsilon)$ for all $t \in (0, t_2)$ for some t_2 , then $T(t; x) \in W_{T(t; m)}^{uu}(\varepsilon)$ for $t \in (0, t_2)$.
5. For $x \in W_m^{uu}(\varepsilon)$ and $m \neq m_1 \in M$, we have

$$\frac{\|T(-t; x) - T(-t; m)\|}{\|T(-t; x) - T(-t; m_1)\|} \rightarrow 0 \quad \text{exponentially as } t \rightarrow +\infty.$$

6. For $x, y \in W_m^{uu}(\varepsilon)$, $\|T(-t; x) - T(-t; y)\| \rightarrow 0$ exponentially as $t \rightarrow +\infty$.

The proofs of these theorems can be found in [10], [11] under the additional assumption:

- (H) The mapping Π^α ($\alpha = c, u, s$) from $M \subset X \rightarrow \mathcal{L}(X)$ defined by $m \rightarrow \Pi_m^\alpha$ is C^1 where Π_m^α are the invariant projections associated to the decomposition (B.1).

This assumption is ensured by, e. g., $M \in C^2$. The authors of [10], [11] refer to [12] for proofs where the assumption M is C^2 can be relaxed to require only C^1 .

References

- [1] V. I. Arnold, V. S. Afrajmovich, Y. S. Ill'yashenko, L. P. Shil'nikov: Bifurcation Theory. In V. I. Arnold: Dynamical Systems V, Bifurcation and Catastrophe Theory. Springer Verlag, 1994.
- [2] E. A. Avrutin, J. H. Marsh, J. M. Arnold: Modelling of semiconductor laser structures for passive harmonic mode locking at terahertz frequencies. *Int. J. of Optoelectronics* vol. 10 No. 6 pp. 427-432, 1995.
- [3] S. M. Baer, T. Erneux: Singular Hopf Bifurcation to Relaxation Oscillations. *SIAM J. on Appl. Math.*, 46:721-730, 1986.
- [4] S. M. Baer, T. Erneux: Singular Hopf Bifurcation to Relaxation Oscillations II. *SIAM J. on Appl. Math.*, 52:1651-1664, 1992.
- [5] S. M. Baer, T. Erneux, J. Rinzel: The slow passage through a Hopf bifurcation: delay, memory effects, and resonances. *SIAM J. on Appl. Math.* 49:55-71, 1989.
- [6] U. Bandelow: Theorie longitudinaler Effekte in 1.55 μm Mehrsektions DFB-Laserdioden. PhD-thesis, Humboldt-Universität Berlin, 1994.
- [7] U. Bandelow, M. Radziunas, V. Tronciu, H.-J. Wünsche, F. Henneberger: Tailoring the dynamics of diode lasers by dispersive reflectors. *Proceedings of SPIE*, vol. 3944, pp. 536-545, 2000.
- [8] U. Bandelow, L. Recke, B. Sandstede: Frequency regions for forced locking of self-pulsating multi-section DFB lasers. *Optics Comm.* 147, pp. 212-218, 1998.
- [9] U. Bandelow, H.J. Wünsche, B. Sartorius, M. Möhrle. Dispersive self Q-switching in DFB-lasers: Theory versus experiment. *IEEE J. Selected Topics in Quantum Electronics*, Vol. 3, pp. 270-278, 1997.
- [10] P. W. Bates, K. Lu, C. Zeng: Existence and persistence of invariant manifolds for semiflows in Banach spaces. *Mem. Amer. Math. Soc.* 135, 1998
- [11] P. W. Bates, K. Lu, C. Zeng: Invariant foliations near normally hyperbolic invariant manifolds for semiflows. *Trans. Amer. Math. Soc.* 352, pp. 4641-4676, 2000.
- [12] P. W. Bates, K. Lu, C. Zeng: Invariant Manifolds and Invariant Foliations for Semiflows. book, in preparation.
- [13] P. W. Bates, C. K. R. T. Jones: Invariant Manifolds for Semilinear Partial Differential Equations. *Dynamics Reported*, Vol. 2(1989), pp. 1-38, 1989.
- [14] J. Carr: Applications of Centre Manifold Theory. Springer-Verlag, New-York, 1981.

- [15] T. Cazenave, A. Haraux: An Introduction to semilinear evolution equations. Oxford Lecture Series in Mathematics and its Applications 13, Clarendon Press, Oxford 1998.
- [16] E. J. Doedel, A. R. Champneys, T. F. Fairgrieve, Y. A. Kuznetsov, B. Sandstede, X. Wang: AUTO97, Continuation and bifurcation software for ordinary differential equations.
- [17] J. L. A. Dubbeldam, B. Krauskopf: Self-pulsation of lasers with saturable absorber: dynamics and bifurcations. *Opt. Comm.* 159:325-338, 1999.
- [18] T. Erneux, F. Rogister, A. Gavrielides, V. Kovanis: Bifurcation to mixed external cavity mode solutions for semiconductor lasers subject to external feedback. *Opt. Comm.* 183:467-477, 2000.
- [19] N. Fenichel: Geometric Singular Perturbation Theory for Ordinary Differential Equations. *Journal of Differential Equations* 31, 53-98, 1979.
- [20] S. Friese: Existenz und Stabilität von Lösungen eines Randanfangswertproblems der Halbleiterdynamik. Thesis, Humboldt-Universität Berlin, 1999.
- [21] J. Guckenheimer, P. Holmes: Nonlinear Oscillations, Dynamical Systems, and Bifurcations of Vector Fields. Springer Verlag, 1983.
- [22] D. Henry: Geometric Theory of Semilinear Parabolic Equations. Springer-Verlag, 1981.
- [23] E. M. Izhikevich: Subcritical Elliptic Bursting of Bautin Type. *SIAM J. on Appl. Math.* 60:503-535, 2000.
- [24] E. M. Izhikevich: Neural Excitability, Spiking and Bursting. *Int. J. of Bifurcation and Chaos*, 10:1171-1266, 2000.
- [25] F. Jochmann, L. Recke: Existence and uniqueness of weak solutions of an initial boundary value problem arising in laser dynamics. WIAS preprint 515, 1999.
- [26] R. Lang, K. Kobayashi: External optical feedback effects on semiconductor injection properties. *IEEE J. of Quant. El.*, Vol. 16, pp. 347-355, 1980.
- [27] T. Kato: Perturbation theory for linear operators. Springer Verlag, 1966.
- [28] Y. Kuznetsov: Elements of Applied Bifurcation Theory. Springer Verlag, 1995.
- [29] D. Marcenac: Fundamentals of laser modelling. PhD thesis, University of Cambridge, 1993
- [30] J. Mork, B. Tromborg, J. Mark: Chaos in Semiconductor Lasers with Optical Feedback: Theory and Experiment. *IEEE J. of Quant. El.*, Vol. 28, No. 1, pp. 93-108, 1992.

- [31] A. Nejshtadt: Asymptotic investigation of the loss of stability by an equilibrium as a pair of eigenvalues slowly cross the imaginary axis. *Usp. Mat. Nauk* 40:190-191, 1985
- [32] C. Z. Ning, R. A. Indik, J. V. Moloney: Effective Bloch Equations for Semiconductor Lasers and Amplifiers. *IEEE J. of Quant. El.*, Vol. 33 No. 9, pp. 1543-1550, 1997.
- [33] G. L. Oppo, A. Politi: Toda potentials in laser equations. *Z. Phys. B* 59, 111, 1985)
- [34] A. Pazy: *Semigroups of Linear Operators and Applications to Partial Differential Equations*. Applied mathematical Sciences, Springer Verlag, New York, 1983.
- [35] M. Radziunas, H.-J. Wünsche, B. Sartorius, O. Brox, D. Hoffmann, K. Schneider and D. Marcenac: Modeling Self-Pulsating DFB Lasers with Integrated Phase Tuning Section. to appear in *IEEE J. of Quantum Electronics*, 2000.
- [36] L. Recke, K.R. Schneider, V.V. Strygin: Spectral properties of coupled wave equations. *Z. angew. Math. Phys.* 50, pp. 923-933, 1999.
- [37] J. Rehberg, H.-J. Wünsche, U. Bandelow, H. Wenzel: Spectral Properties of a System Describing fast Pulsating DFB Lasers. In: *ZAMM* 77 (1997) 1, 75-77, 1997.
- [38] J. A. Sanders, F. Verhulst: *Averaging Methods in Nonlinear Dynamical Systems*. Springer Verlag, 1985.
- [39] J. Sieber, U. Bandelow, H. Wenzel, M. Wolfrum, H.-J. Wünsche: Travelling wave equations for semiconductor lasers with gain dispersion. *WIAS Preprint No. 459*, 1998.
- [40] A. A. Tager, K. Petermann: High-Frequency Oscillations and Self-Mode Locking in Short External-Cavity Laser Diodes. *IEEE J. of Quant. El.* Vol. 30, No. 7, pp. 1553-1561, 1994.
- [41] H. Triebel: *Interpolation Theory, Function Spaces, Differential Operators*. N.-Holland, Amsterdam-New-York, 1978.
- [42] B.Tromborg, H. E. Lassen, H. Olesen: Travelling Wave Analysis of Semiconductor Lasers. *IEEE J. of Quant. El.* Vol. 30, No. 5 pp. 939-956, 1994.
- [43] B. Tromborg, J. H. Osmundsen, H. Olesen: Stability Analysis for a Semiconductor Laser in an External Cavity. *IEEE J. of Quant. El.* Vol. 20, No. 9, pp. 1023-1032, 1984.
- [44] V.Z. Tronciu, H.-J. Wünsche, J. Sieber, K. Schneider, F. Henneberger: Dynamics of single mode semiconductor lasers with passive dispersive reflectors. submitted to *Optics Communications*, April 2000, accepted June.

- [45] D. Turaev: Fundamental obstacles to self-pulsations in low-intensity lasers. WIAS Preprint 629, 2000.
- [46] A. Vanderbauwhede: Centre manifolds, normal forms and elementary bifurcations. Dynamics Reported Vol. 2(1989), pp. 89-169, 1989.
- [47] A. Vanderbauwhede, G. Iooss: Center Manifold Theory in Infinite Dimensions. Dynamics Reported Vol. 1(1992), pp 125-163, 1992.
- [48] S. Wieczorek, B. Krauskopf, D. Lenstra: A unifying view of bifurcations in a semiconductor laser subject to optical injection. Opt. Comm. 172:279-295, 1999.
- [49] S. Wiggins: Normally Hyperbolic Manifolds in Dynamical Systems. Springer Verlag, 1994.
- [50] U. Bandelow, M. Wolfrum, J. Sieber, M. Radziunas: Spatio-Temporal Dynamics of Multisection DFB-lasers with Gain Dispersion. to appear in IEEE.
- [51] H. Wenzel, U. Bandelow, H.-J. Wünsche, J. Rehberg: Mechanisms of fast self pulsations in two-section DFB lasers. IEEE J. Quantum Electron. Vol. 32, No. 1, pp. 69-79, 1996.

List of Figures

2.1 Typical Geometric Configuration	5
3.1 Spectrum of $H(n)$	15
4.1 Shape of G and R	31
4.2 Primary bifurcation diagram for single mode approximation	32
4.3 Sketch of single mode system in the limit $\delta \rightarrow 0$	33
4.4 Pseudo bifurcation diagram for 3-section laser	40
4.5 Stable and unstable parts of the slow manifold	48
4.6 Continuation of r_h and r_f with respect to y_r	49
4.7 Comparison between the averaged approximations and the numerical solutions	54
4.8 Families of periodic orbits between the invariant planes	56
4.9 Bifurcation diagram for μ and γ	57
A.1 Lorentzian curve	61

List of Tables

A.1 Ranges and explanations of the variables and coefficients	61
---	----